

POLITECNICO DI MILANO

Scuola di Ingegneria Industriale e dell'Informazione

Corso di Laurea Magistrale in Ingegneria Biomedica



**CHARACTERIZATION OF HEMODYNAMIC
CONDITIONS IN TESIO AND PALINDROME
CENTRAL VENOUS CATHETER FOR
HEMODIALYSIS**

Relatore: Prof. Gabriele Dubini

Correlatori: Ing. Bogdan Ene-Iordache

Ing. Michela Bozzetto

Tesi di laurea di:

Ravasio Giovanni

Matr. 883268

Anno accademico 2018/2019

Ringraziamenti

Abstract

Dialysis is the only treatment that patients with chronic kidney disease can perform while they are waiting for the organ transplant. This treatment greatly affects patients' life because they have to go to specialized centres twice or three times a week and undergo dialysis treatment that lasts several hours (on average from four to five). The blood is withdrawn from the patient through a vascular access that is created by the nephrologist based on patient's health status, as well as vascular anatomy and quality. The vascular access of first choice is the arteriovenous fistula (AVF) that has lower risks of complications as compared to any other type of vascular access. Since AVF requires the presence of adequate native vessels and a maturation time of about 40 days, not all patients are suitable for the construction of this vascular access and the first alternative is the graft (AVG). In the case of elderly patients or those with vessels very damaged by pathological conditions, the last possibility is to insert a Central Venous Catheter (CVC).

Computational fluid dynamics (CFD) is increasingly used in the evaluation of medical devices for cardio-vascular applications. The high spatial and temporal resolution of this technique and the possibility of studying 3D models, without the expensive efforts in terms of manufacturing time of experimental set-ups, allow a reliable and accurate characterization of the blood flow field. It therefore represents a promising approach to study the effect of some hemodialysis catheter design parameters and compare the performance of different catheters in terms of flow separation and blood recirculation regions.

The main objective of the present thesis work is to set up a reliable method for the characterization of hemodynamic condition in patient-specific conditions, coupling imaging techniques and high-resolution CFD.

Key words: CVC, Palindrome, Tesio, CFD, Boundary conditions, SVC, IVC, IJV, Left anonymous vein, Right atrium, Tricuspid valve, Mesh

Sommario

La dialisi è la sola terapia che i pazienti con insufficienza renale cronica possono effettuare in attesa del trapianto di organo. Questa terapia condiziona parecchio la vita dei pazienti in quanto devono recarsi presso i centri specializzati due o tre volte la settimana e sottoporsi al trattamento dialitico che dura diverse ore (in media dalle quattro alle cinque). Il sangue viene prelevato dal paziente tramite un accesso vascolare che viene deciso in base allo stato di salute del paziente e alle condizioni dei suoi vasi sanguigni. L'accesso vascolare di prima scelta è la fistola arterovenosa (AVF) in quanto garantisce un flusso ottimale del sangue e possiede una minore percentuale di fallimento. Poiché la fistola arterovenosa richiede la presenza di vasi nativi adeguati e un tempo di maturazione di circa 40 giorni, non tutti i pazienti risultano idonei per la costruzione di questo accesso vascolare e la prima alternativa è la fistola con graft (AVG). Nel caso di pazienti anziani o con vasi molto danneggiati dalle condizioni patologiche, la terza possibilità di accesso vascolare è tramite un Catetere Venoso Centrale (CVC).

La fluidodinamica computazionale (CFD) è sempre più utilizzata nella valutazione di dispositivi medici per applicazioni cardio-vascolari. L'elevata risoluzione spaziale e temporale di questa tecnica e la possibilità di studiare modelli 3D, senza gli sforzi dispendiosi in termini di tempo di fabbricazione di set-up sperimentali, consentono una caratterizzazione affidabile e accurata del campo di flusso sanguigno. Essa rappresenta quindi un approccio promettente per studiare l'effetto di alcuni parametri di progetto del catetere per emodialisi e confrontare le prestazioni di cateteri diversi in termini di regioni di separazione del flusso e ricircolo del sangue.

L'obiettivo principale del presente lavoro di tesi è quello di impostare un metodo affidabile per la caratterizzazione delle condizioni emodinamiche in casi specifici per ogni paziente, utilizzando sia tecniche di imaging che tecniche CFD.

Parole chiave: CVC, Palindrome, Tesio, CFD, Condizioni al contorno, SVC, IVC, IJV, Vena anonima di sinistra, Atrio destro, Valvola tricuspide, Mesh

Contents

RINGRAZIAMENTI	i
ABSTRACT	iii
SOMMARIO	v
CONTENTS	vii
1. CLINICAL BACKGROUND	1
1.1. Renal failure	2
1.1.1. Etiology and classification of CKD	2
1.1.2. Epidemiology of ESRD	3
1.2. Dialysis treatment	5
1.2.1. Hemodialysis treatment	5
1.2.2. Vascular access	6
1.3. Central venous catheter	8
1.3.1. Catheterization	9
1.3.2. Insertion site	10
1.3.3. Temporary and permanent CVC	11
1.3.4. Biomaterials	12
1.3.5. Coating	12
1.3.6. Tip design	14
1.3.7. Complications	15

2. HEMODYNAICS INSIDE CVC	23
2.1. Palindrome catheter	24
2.2. Tesio catheter	29
2.3. State of the art of CFD inside CVC	33
2.4. Aim of the study	37
3. COMPUTATIONAL MESH CREATION	39
3.1. 3D model of the veins	40
3.1.1. Overview of geometry used in studied articles	40
3.1.2. Description of the geometry chosen	41
3.1.3. Reading DICOM files and selecting a Volume of Interest (VOI)	43
3.1.4. Level set segmentation	44
3.1.5. Generating the vessel wall surface with marching cubes	45
3.1.6. Surface smoothing and conversion to .stl format	46
3.1.7. Modified with Autodesk Meshmixer	47
3.2. Catheters 3D model	49
3.2.1. CVC acquisition	49
3.2.2. CVC modelling with VMTK	52
3.2.3. Autodesk Meshmixer modifications and final models	55
3.3. Creation of complete CVC models	58
3.3.1. Extrusion with Solidworks	58
3.3.2. Autodesk Meshmixer modification to obtain the final models ..	60
3.4. Volume mesh creation	66
3.4.1. Surface thresholding	66
3.4.2. Mesh generation	68

4. CFD SIMULATION	73
4.1. Boundary conditions	74
4.1.1. Search of appropriate boundary conditions	74
4.1.2. Choice of the boundary condition	78
4.2. CFD simulation	83
4.2.1. Blood rheology	83
4.2.2. CFD simulations of Palindrome and Tesio cases	83
4.3. Post-processing	84
5. RESULTS	85
5.1. Velocity images of Z-axes slice	86
5.2. Velocity 3D streamlines	88
5.3. Wall Shear Stress on catheters surface	92
5.4. Pressure drop inside the catheters tube	96
5.5. Turbulent Kinetic energy	98
5.6. Particle tracking	101
6. DISCUSSION, LIMITATIONS AND FUTURE DEVELOPMENTS	105
6.1. Discussion	106
6.2. Limitations	108
6.3. Future developments	109
BIBLIOGRAPHY	110

List of figures

Figure 1.1 Hemodialysis circuit	6
Figure 1.2 The three kind of vascular access	7
Figure 1.3 Different tip design [1]	15
Figure 2.1 Palindrome lumen design	24
Figure 2.2 Palindrome tip design [2]	24
Figure 2.3 Palindrome tip design [3]	25
Figure 2.4 Palindrome position inside the body	26
Figure 2.5 Palindrome inside the right atrium	27
Figure 2.6 Tesio catheter.....	29
Figure 2.7 Tesio tip design [4]	30
Figure 2.8 Tesio section and Tesio side hole [4]	31
Figure 2.9 Tesio position inside the body	32
Figure 2.10 Simulation environment with Niagara catheter in hollow tube [5] ..	33
Figure 2.11 Different catheter tip design [6]	34
Figure 2.12 Different catheter tip design [7]	35
Figure 2.13 Different catheter tip design [8]	35
Figure 3.1 Anatomy of SVC	42
Figure 3.2 Scheme of RA, IVC and SVC	43
Figure 3.3 Extraction of VOI	43
Figure 3.4 Level set segmentation	44
Figure 3.5 Surface extracted using marching cubes	45
Figure 3.6 Surface before the smoothing	46
Figure 3.7 Surface after the smoothing	46
Figure 3.8 Final surface after Autodesk Meshmixer smoothing	48
Figure 3.9 Basis of Palindrome (117 of 4328)	49
Figure 3.10 Palindrome side holes (2021 of 4328)	49

Figure 3.11 Palindrome initial part of the tip (3385 of 4328)	50
Figure 3.12 Palindrome final part of the tip (4219 of 4328)	50
Figure 3.13 Total Palindrome scanned	50
Figure 3.14 Basis of Tesio Blu (0327 of 5420)	51
Figure 3.15 Side hole of Tesio Blu (2486 of 5420)	51
Figure 3.16 Basis of Tesio Rosso (0327 of 5420)	51
Figure 3.17 Side hole of Tesio Rosso (2486 of 5420)	51
Figure 3.18 Total Tesio Rosso and Tesio Blu scanned	51
Figure 3.19 Palindrome view in X, Y, Z planes with VMTK	53
Figure 3.20 Palindrome reconstruction with VMTK	53
Figure 3.21 Tesio Blu reconstruction with VMTK	54
Figure 3.22 Tesio Rosso reconstruction with VMTK	55
Figure 3.23 Palindrome defects viewed in Autodesk Meshmixer	56
Figure 3.24 Palindrome particular view of defects in Autodesk Meshmixer	56
Figure 3.25 Palindrome tip: final model	57
Figure 3.26 Tesio tip: final model	57
Figure 3.27 Palindrome extrusion with Solidworks	59
Figure 3.28 Tesio extrusion with Solidworks	60
Figure 3.29 Tesio extrusion with Solidworks	60
Figure 3.30 Palindrome: creation of the internal hole	61
Figure 3.31 Palindrome inner lumen hole	61
Figure 3.32 Palindrome weld boundaries	62
Figure 3.33 Palindrome: removal of the external catheter surface	62
Figure 3.34 Tesio weld boundaries	63
Figure 3.35 Tesio: removal of the external catheter surface	63
Figure 3.36 Palindrome final model	64
Figure 3.37 Palindrome final model	64
Figure 3.38 Tesio final model	65
Figure 3.39 Tesio final model	65

Figure 3.40 Palindrome threshold	67
Figure 3.41 Tesio threshold	67
Figure 3.42 Palindrome volume mesh: slice of RA	69
Figure 3.43 Palindrome volume mesh: vertical slice of RA	69
Figure 3.44 Palindrome volume mesh: view at the exit site	70
Figure 3.45 Palindrome volume mesh: slice at the level of SVC	70
Figure 3.46 Tesio volume mesh: slice of RA	71
Figure 3.47 Tesio volume mesh: vertical slice of RA	71
Figure 3.48 Tesio volume mesh: view at the exit site	72
Figure 3.49 Tesio volume mesh: slice at the level of SVC	72
Figure 4.1 Graph of blood flow velocity in the IVC [9]	74
Figure 4.2 Graph of blood flow velocity in the SVC [9]	75
Figure 4.3 Tricuspid valve outflow [10]	76
Figure 4.4 Dialysis circuit [11]	77
Figure 4.5 Matlab script for the interpolation	78
Figure 4.6 IVC curve of boundary condition	79
Figure 4.7 SVC, IJV_DX and AV_SX curve of boundary condition	80
Figure 4.8 Outflow curve from the tricuspid valve	81
Figure 4.9 Catheters waveform	82
Figure 5.1 Palindrome Z-axes slices of velocity magnitude	86
Figure 5.2 Tesio Z-axes slices of velocity magnitude	87
Figure 5.3 Palindrome streamlines Time 1.00	88
Figure 5.4 Palindrome streamlines Time 1.18	88
Figure 5.5 Palindrome streamlines Time 1.66	89
Figure 5.6 Tesio streamlines Time 1.00	90
Figure 5.7 Tesio streamlines Time 1.18	90
Figure 5.8 Tesio streamlines Time 1.66	91
Figure 5.9 Palindrome WSS: arterial side	92
Figure 5.10 Palindrome WSS: focus on arterial side hole	92

Figure 5.11 Palindrome WSS: venous side	93
Figure 5.12 Tesio WSS	93
Figure 5.13 Tesio WSS: focus on arterial side holes	94
Figure 5.14 Tesio WSS	94
Figure 5.15 Palindrome pressure drop	97
Figure 5.16 Tesio pressure drop	97
Figure 5.17 Palindrome TKE	99
Figure 5.18 Palindrome TKE	99
Figure 5.19 Tesio TKE	100
Figure 5.20 Tesio TKE	100
Figure 5.21 Palindrome particle tracking: first time step	101
Figure 5.22 Palindrome particle tracking: end step time	101
Figure 5.23 Tesio particle tracking: first time step	102
Figure 5.24 Tesio particle tracking: end step time	102

List of tables

Table 1.1 Incidence of different causes of CKD	2
Table 3.1 CFD articles studied	40

Abbreviations

CVC	Central venous catheter
AKI	Acute kidney injury
CKD	Chronic kidney disease
ESRD	End-stage renal disease
PKD	Polycystic kidney disease
GFR	Glomerular filtration rate
KDOQI	Kidney disease outcomes quality initiative
VA	Vascular access
AVF	Arteriovenous fistula
AVG	Arteriovenous graft
r-TPA	Recombinant tissue plasminogen activator
CLASBI	Central line-associated bloodstream infection
CRBSI	Catheter-related bloodstream infection
CFD	Computational fluid dynamics
SVC	Superior vena cava
IVC	Inferior vena cava
IJV	Right internal jugular vein
RA	Right atrium
VOI	Volume of interest
VMTK	Vascular modelling toolkit
WSS	Wall shear stress
TKE	Turbulent kinetic energy

1. Clinical background

The present chapter contains the physio-pathological aspects of the renal apparatus with particular reference to the vital functions and the conditions in which there are compromised, causing renal failure. Furthermore, the main kidney's replacement treatments are described, focusing on hemodialysis and the main kinds of vascular access, in particular on central venous catheters. Finally, all aspects that concern CVC are described, starting from catheterization, biomaterials, different tip design and possible complications associated to this kind of medical device.

1. CLINICAL BACKGROUND

1.1 RENAL FAILURE

Renal diseases can be divided into three principal categories:

- Acute kidney injury (AKI) results in an abrupt loss of renal function with a corresponding spike in serum creatinine concentration and decrease in urine output; however AKI is a reversible condition [12].
- Chronic kidney disease (CKD), which is characterized by a reduced glomerular filtration rate. This condition is irreversible and causes a complete loss of all renal functions.
- End-stage renal disease (ESRD) is the most devastating condition, which requires either renal transplantation or dialysis [12].

1.1.1 Etiology and classification of CKD

The etiology of renal failure can be quite various and depends upon particular event that initiates kidney damage. In the developed countries the three main causes of CKD are diabetes, high blood pressure and glomerulonephritis, a group of diseases that cause inflammation and damage to kidney's filtering units. Also inherited kidney disease, such as the polycystic kidney disease (PKD), which causes large cysts formation in the kidney damaging the surrounding tissue, is a diffuse cause of CKD. If uncorrected, any of these events can lead to renal failure [13].

Table 1.1_Incidence of different causes of CKD

CAUSES OF CKD	% OF INCIDENCE
Un-Known	24.86
Vascular	21.6
Diabetes	20.08
Glomerular nephritis	10.31
Hereditary/inborn	6.97
Partial nephrectomy	6.3
Others	4.37
Systemic	4.25
Not-specified	1.26

Table 1.1 shows the incidence of the main pathologies causing renal failure, registered in the Italian report of 2010 (<http://www.sinidt.org/web/procedure/protocollo.cfm>).

Glomerular filtration rate (GFR) has been accepted as the best index of overall kidney function in health and disease. The guidelines called Kidney Disease Outcomes Quality Initiative (KDOQI) [14] published by the National Kidney Foundation, defined several stages of CKD, which can lead to decreased GFR:

- *Stage I*: it is characterized by the presence of structural or functional abnormalities of the kidney, initially without decreased GFR ($> 90 \text{ mL/min/1.73 m}^2$), which over time can lead to decreased GFR.
- *Stage II*: it is characterized by mild reduction in GFR ($60 \text{ to } 89 \text{ mL/min/1.73 m}^2$). At this stage, patients usually have hypertension and may have laboratory abnormalities indicative of dysfunction. This condition can be determined by measurements of serum creatinine levels.
- *Stage III*: it is characterized by moderate reduction in GFR ($30 \text{ to } 59 \text{ mL/min/1.73 m}^2$). This stage is distinguished by the presence of azotemia (nitrogen metabolism) and expressed by an evaluation in serum creatinine and serum urea nitrogen.
- *Stage IV*: it is characterized by severe reduction in GFR ($15 \text{ to } 29 \text{ mL/min/1.73 m}^2$). In this extreme stage of CKD, the worsening of azotemia, anemia and other laboratory abnormalities reflect dysfunction in several organ systems.
- *Stage V*: it is characterized by kidney failure (GFR, $<15 \text{ mL/min/1.73 m}^2$). In most cases, this level of kidney dysfunction is accompanied by a constellation of symptoms and laboratory abnormalities in several organ systems. Kidney replacement therapy (dialysis or transplantation) is typically required.

1.1.2 Epidemiology of ESRD

End stage renal disease is a growing global health problem, strictly connected with progressive ageing population and increased survival rate of CKD patients. The number of patients being treated for ESRD globally was estimated to be 3.700.000 at the end of 2016 and, with a ~6% growth rate, continues to increase at a significantly higher rate than the world population. In the US, Japan and the European Union, dialysis population growth rates are significantly lower than the growth rate in regions such as Asia, Latin America, Middle East and Africa. This variation in growth rates may be

partially explained by differences in demographics and the maturity of dialysis programs in developed countries.

The survival alternatives for a patient suffering from renal failure are chronic dialysis treatments (either hemodialysis or peritoneal dialysis) and renal transplantation.

Worldwide, hundreds of thousands of patients are currently treated with dialysis due to the limited number of donors.

1.2 DIALYSIS TREATMENT

The first historical description of the dialysis procedure was published in 1913. Abel, Rowntree and Turner “dialyzed” anesthetized animals by directing their blood outside the body and through tubes with semi permeable membranes [5]. George Haas, a German doctor, was the one who performed the first attempt of dialysis involving humans. Thanks to the technical improvements in the equipment, in 1945 Willem Kolff performed the first successful dialysis treatment [6]. Doctor Kolff’s success proved the usefulness of the concepts developed by Abel and Haas: the separation of substances and the removal of water from solutions through semipermeable membranes (diffusion and osmosis processes).

There are two main types of dialysis:

- Hemodialysis: it uses an extracorporeal circuit with a special filter to clean the blood of the patient;
- Peritoneal dialysis: this treatment uses the peritoneal cavity in the abdomen as a reservoir for the dialysis solution and the thin membrane lining this cavity as a suitable barrier through which blood can be filtered.

Nowadays, hemodialysis is the most common treatment, with approximately 2.106.000 patients undergoing hemodialysis (89% of all dialysis patients) and about 252.000 patients undergoing peritoneal dialysis (11%) [15].

1.2.1 Hemodialysis treatment

Dialysis is the therapy which substitute transplants. It consists in a process of blood purification which is made using a semipermeable membrane (biological or artificial) which allows the selective passage of determinate substances between two fluid: the dirty blood and the dialysis fluid. The most common and used kind of dialysis is the hemodialysis. This therapy allows the blood depuration thanks to an artificial filter called dialyzer put inside of an extracorporeal circuit. Blood arrives to this machine thanks to a pump and it begins to circulate in the circuit; when it enters the dialyzer, thanks to different concentration of certain substances (like Na, K, Ca), the dialysis fluid purifies blood which leaves waste substances and recovers the other it needs. When the blood is purified, it returns to the patient’s body thanks to another pump of the same machine.

This therapy must be done in dedicated factories (like hospital or Dialysis Centers) from once or twice or three times for week; a single therapy lasts four or five hours depending on the volume of blood that must be purified and the patient condition.

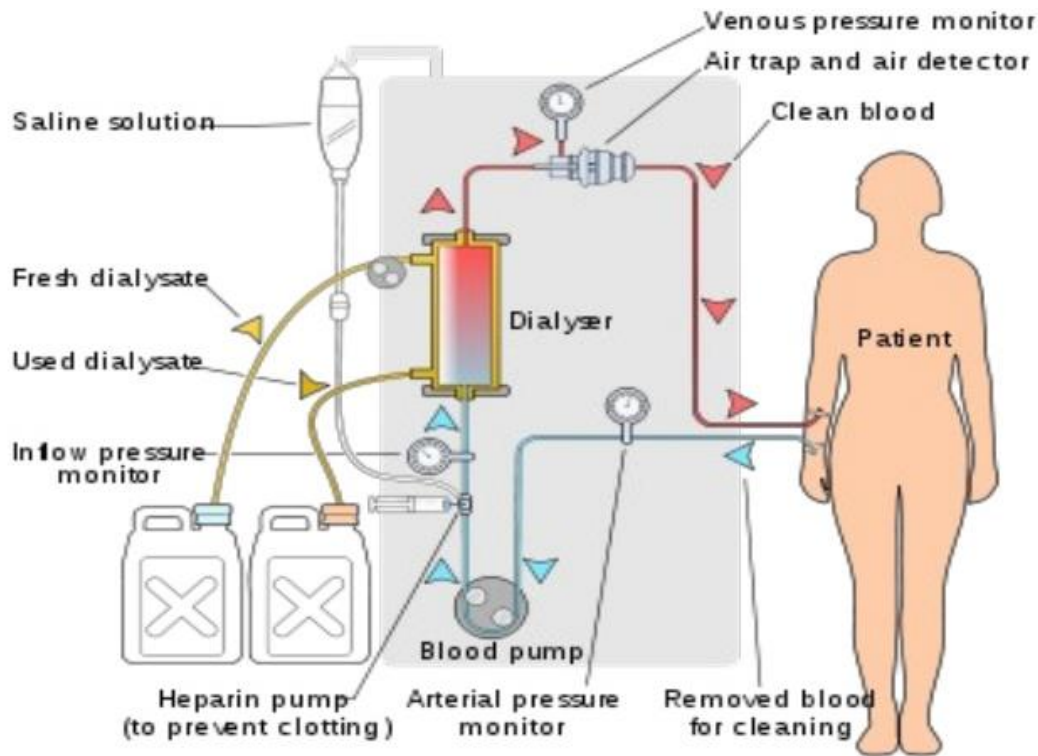


Figure 1.1_Hemodialysis circuit

1.2.2 Vascular access

Dialysis machine is attached to patient's body through a vascular access (VA); from this access, blood comes out from the patient's body, it passes throughout the dialysis machine and it returns to the patient by the same access after the deputation [15]. Clinical and instrumental evaluation is necessary to identify the type of VA, the medical and technical approach and a good follow up to check complication as early as possible. The major problems and causes of failure in hemodialysis is represented by the lack of good vascular access.

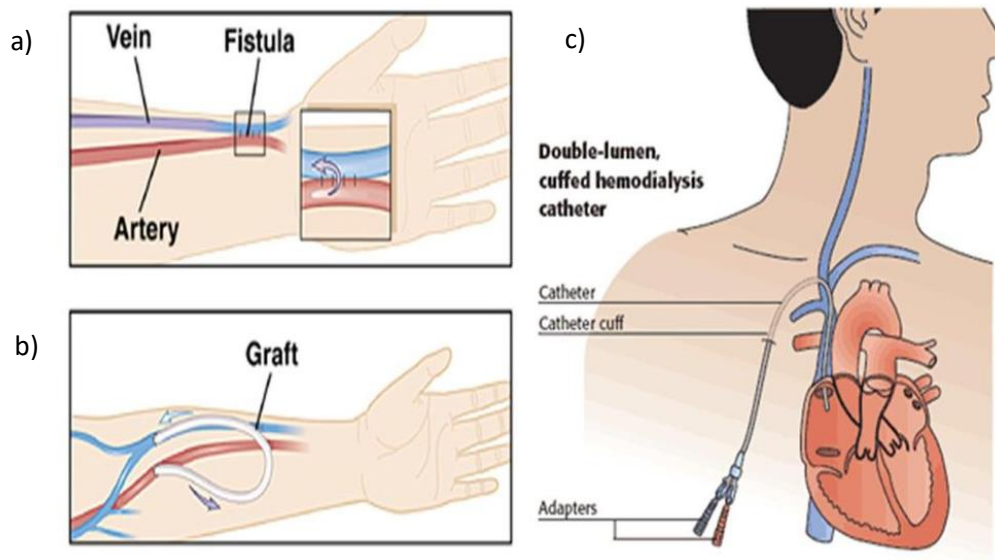


Figure 1.2_The three kind of vascular access

There are three main type of VA:

- a) The native arteriovenous fistula (AVF). It consists in a surgical connection between an artery and a vein of the patient, usually in the arm and is the first choice for vascular access. However, AVF needs a maturation time (around 40 days) before needles can be inserted in it and can be created only in presence of suitable native vessels. Therefore, despite being the preferred VA due to lower infections and biocompatibility problems, it is not possible for all patients in need of HD treatment.
- b) The prosthetic arteriovenous graft (AVG). It consists in an arteriovenous fistula made with prosthetic (graft) interposition between an artery and a vein. This is a good option for patients that had a lot of previous operations and they exhausted superficial veins or it is choose for patients with vascular fragility [16]. However, AVG presents more complications than AVF in terms of vascular stenosis and consequent thrombosis.
- c) The central venous catheters (CVCs). It is the last choice, but always selected in case of need of urgent hemodialysis. Being the focus on this thesis, CVC is widely described in the next paragraph.

1.3 CENTRAL VENOUS CATHETER

Central venous catheter represents one of the most important advances in medicine; this medical device became common in the 1960s [17]. It is very used for patients who present malfunction of the permanent access or when they need immediate dialysis therapy and they can not wait for all the AVF or AVG. Its implantation is easier than AVG and AVF: it takes at least 60 minutes and the HD can be effectuated since the day after this operation because of the immediate access to circulation of catheters. Despite of central access catheters allow an adequate blood flow rate, CVCs are evaluated as the third choice for vascular access because they are more subject to infection, vascular stenosis and thrombosis as compared to AVF or AVG [6]. CVCs are also widely used in critically ill patients or for the older ones; in this way is easily to administer medication, blood products and fluids, for example to obtain blood samples [18]. The requirements for a dialysis CVC are [19] [20]:

- High blood flow rates at moderate pressure drops.
- Minimal trauma to the vein intima to avoid thrombosis and venous stenosis.
- Prevention of bacterial migration.
- Resistance to occlusion by fibrous sheathing.
- Avoidance of contamination of the catheter lumen.
- Avoidance of clotting at the tip or within the catheter.
- Biocompatibility of the catheter surfaces.
- Avoidance of lumen collapse under negative pressure.
- Avoidance of kinking of catheters segments.
- Physical strength and integrity to avoid disconnections or breaks of any component.
- Resistance to antiseptic agents.
- Placement procedures with minimal trauma, risk and difficulty.
- Radiopaque appearance on X-ray for evaluating location during placement and after use.

There are many types of central vascular catheters and they are divided in categories depending on certain properties: the duration of their use (temporary or permanent), if they are tunneled or non-tunneled, the different biomaterial used, if there is or not a

coating and the material used for coat, the lumen and tip design, the number of pipes and the presence or not of side holes.

1.3.1 Catheterization

A careful placement of the CVC is essential to avoid catheter malposition and malfunction or complications related to the patient such as vessels' perforation or uncontrollable bleeding [21]. The correct position is evaluated using radiology instrument: the tip of the catheter must be positioned in the center of the right atrium (RA) for a correct functioning; with the radiology support, doctors can check the right position of the catheter. The catheterization may cause complications immediately after the catheter placement, such as:

- Pleural puncture: pneumothorax and hemothorax are frequent when the needle inadvertently punctures the pleural space; this complication can be recognized by a final spot radiograph of the whole chest.
- Arterial puncture: this complication can be avoid using ultrasound guidance and an identification before preparing is necessary to individuate potential issues.
- Bleeding: is very uncommon but if it happens, especially in the entry sites of CVC, it can be ameliorated with pressure.
- Arrhythmias: some accidental movement of the tip may irritate the atrioventricular node and produce supraventricular tachycardias. Despite all, this inadvertent movements are not common and can be avoid by experience.
- Air-embolism: the technological advances have decreased the rate of this complication; air-embolism is mostly related to the uncorrected position of the patient.
- Laceration of central veins: it is sufficient a close attention during the procedure on insertion to avoid the risk of laceration.

The most common technique for insertion is called "Seldinger Technique", in honor of the surgeon who developed it in the 1953 [22] [23]. The technique is composed by six steps:

- 1) A cutaneous cut with a trocar or a scalpel
- 2) Positioning the metallic guidance, which is a thine metallic wire
- 3) The trocar is withdrawn

- 4) Insertion of a dilatator to avoid a sudden admission of the catheter which may cause a serious injury of the vessel. Depending on the dimension of the catheter's lumen, it may be necessary to insert one or more dilatators before the CVC
- 5) Now the CVC can be positioned inside the patients and using the wire as a guide. When the catheter reaches the correct position, the wire is withdrawn
- 6) The area of insertion now can be checked to avoid any complications and it is well covered to decrease the risk of infections.

1.3.2 Insertion site

Preferable location for insertion is decided by instrumental analysis, usually using ultrasound, and thanks to the surgeon's ability and experience. There are four main location for the access [16]:

- Internal jugular vein: it represents the first choice for central venous catheter; the ultrasound guidance is very recommended to delete the risk of carotid puncture. This vessel is a large superficial vein; its straight course into the superior vena cava (SVC) and then inside the right atrium represents an important factor of choice. For this insertion, the patient must be optimally positioned: he lays down on the operating table with a 10° head-down tilt. An extreme rotation of the head has to be avoided because it may reduce vein diameter [24].
- External jugular vein: this vein may be chosen as an access thanks to its superficial course, so the cannulation is possible without using ultrasound guidance. The most common complication are subclavian-vein stenosis and thrombosis.
- Subclavian vein: it is considered the third choice because the risk of subclavian thrombosis is very high with complication to create a vascular access in the ipsilateral arm. So, this hemodialysis access should not be chosen if there are other central veins that can be punctured. If it is the only possibility of access, it's recommended to position the patient in the correct way to decrease the risk of air embolism and to help the distension of the vein. The main disadvantages are more risk of bleeding, pneumothorax and thrombosis.
- Common femoral vein: it is considered the second choice for inserting short-term dialysis catheter because the risk of bleeding is lower and is not required a

radiological control after the insertion. the main complication in comparison to other access is the higher frequency of catheter-associated bacteraemia.

In conclusion, the favorite location for insertion, in particular for permanent dialysis catheters, is the internal jugular vein because of the lower incidence of complication during the operation and also for the straight course to the right atrium. Moreover, the doctor may choice the right internal jugular vein (IJV) or left internal jugular vein depending on the vessels and patient conditions and the catheter length. However, the surgeon establishes the insertion point according to his experience and his preferences.

1.3.3 Temporary and permanent CVC

The principle distinction is between temporary (fewer than 3 weeks) and permanent catheters; the choice should be based on factors like duration of use, patient conditions and the therapy needed. The permanent catheters are also called “Tunneled” because, after the insertion inside the vein, the catheter’s course is moved under the skin to modify its exit position, usually just above the right nipple; this modification helps to prevent bacteremia and allows the patient a better quality of life [17]. The temporary catheters, instead, are usually called “Non-tunneled” because they are inserted directly in the vessel and they do not pass under the skin.

Temporary catheters are different because they are easier to place and remove [25]; there are also difference as regards the size because they are smaller than the permanent ones. Temporary catheters could be made up with three distinct lumen: the three-lumen design is required for patients who need urgent hemodialysis; the addition of the third lumen is helpful to allow concomitant administration of antibiotics, fluids or other medicines without the necessity of new access [21]. Temporary CVCs are used for acute renal failure, usually in bed-bound patients and for a short-term use in those patients with unexpected malfunction of permanent access [15].

Long-term tunneled catheters are inserted both after a previous temporary catheter’s installation using the same entry site or with the creation of a new access. They are larger than the temporary ones and they present a bonded cuff used to anchor the catheter to the subcutaneous tissue near the exit site of the catheter [25]. The cuff is also important because allows for fibrous sealing of the exit site; this barrier helps to prevent bacterial migration [15].

1.3.4 Biomaterials

The materials usable for CVCs must have some characteristics such as other medical devices: they must be biocompatible, hemocompatible, biostable, resistant, flexible, chemically neutral, deformable, resistant to sterilization and not affected by administered drugs [26].

Today, biomaterials used for CVC construction are silicone and polyurethane but is common to use copolymers such as polyurethane/polycarbonate copolymer. Silicone and polyurethane are both biocompatible and durable and there is no significant difference between overall duration of their function [15].

Thermoplastic polyurethanes catheters are composed of long-chain linear polymers without cross-links that are dimly bonded at room temperature, but they become free to slide past one another under the thermal energy provided by the inside of the body. The main characteristic that thermoplastic polyurethane has is that catheters may be manufactured with a higher inner lumen keeping the same outer diameter; in this way the overall catheter flow rate is improved. The main disadvantage of thinner walls is that they allow polyurethane catheters to be more prone to kinking [15] but the catheters can have a larger internal diameter without sacrificing flexibility inside the body and rigidity outside [25].

In vitro comparisons between silicone and polyurethane catheters to establish which is the best remain inconclusive. Animal models appear to attribute a decreased infection risk and thrombogenicity to polyurethane catheters over the silicone ones [27] [28]. The more difficult manufacturing process of silicone catheters may cause a greater propension to construction failures [29] [30].

Although catheter materials such as silicone and polyurethane are chosen to be biocompatible and hemocompatible, complications due to infections and thrombosis are still ineluctable [25]. However, for long-term catheters, polyurethane remains the best choice for catheters material due to the easier manufactures process that needs and the greater inner lumen provided by thinner walls.

1.3.5 Coating

To reduce the risk of complications due to thrombosis or infections or microbial colonization, it is possible to use antithrombotic and antimicrobial surface technologies

on catheters. Therefore, some catheter materials can be modified and coated with antibacterial and/or antithrombotic agents [31]. Using antithrombotic coatings there is a reduction in platelet adhesion, an inhibition of inflammatory response and a reduction in thrombus formation; antimicrobial materials, instead, reduce bacterial colonization and the incidence of bacteremia [32]. The most common catheter coatings consist in heparin, antibiotics and silver to minimize thrombosis and infections; antimicrobial coatings help to decrease microorganism adhesion and biofilm formation, so the risk of infection could be reduced.

A first type of material coating is heparin: it is a polysaccharide anticoagulant which exerts its anticoagulant effect by binding to antithrombin, then forms a complex with thrombin; this complex, formed by heparin, antithrombin and thrombin, inactivates thrombin, inhibiting its ability to convert fibrinogen to fibrin [33] [34]. Heparin coating covers both internal and external catheter surface and it is covalently bound to the polyurethane surface of the catheter material through an end-point linkage mechanism [35]. However, the flow characteristics between the uncoated and the heparin-coated are very similar and catheters with coating do not show a significant increase in catheter patency compared to uncoated catheters [35].

Another common coating hemodialysis catheter is the one with antibiotics; those catheters are impregnated with minocycline and rifampin and this coating provided antimicrobial activity on the luminal and abluminal surface. This method provides good result especially in short-term central venous catheter thanks to the half-life of antibiotic minocycline and rifampin [36]. In long-term catheters, a coating like this is not used because it will not provide good results in the long period.

The most common material coating with antimicrobial effect is silver, especially nanoparticles of silver. It is known that silver has strong biocide activity against a wide range of bacteria and it is a good biocompatible material [37]. The biocide activity of silver consists in inducing the inhibition of bacterial DNA replication and the deactivation of metabolic enzyme [38] [39]; in particular, silver nanoparticles have demonstrated strong antibacterial activity [40]. Silver is applied on the catheter using a process based on the deposition of nanoparticles using UV irradiation [41] that provides a uniform deposition and distribution of silver on the external surface. The catheter is immersed in

a 0.1% solution of silver-nanoparticles; this value represents the best compromise between the manufacturing costs and the results provided by antibacterial activity [42].

1.3.6 Tip design

The concept of “catheter functional tip” has been developed recently; tip is the part of the catheter from the most proximal side hole to the catheter tip; this part of CVC established the main differentiation between different catheters. For a correct functioning of central venous catheters, CVC tip may be positioned in the center of the right atrium and there it should stay because this position provides an adequate blood flow rate. Wrong positioning may cause venous stenosis and recirculation problems and then malfunctions in dialysis therapy, or may irritate the internal surface of the right atrium and cause arrhythmias, most commonly atrial ectopics [15]. To improve the possibility of avoiding blood recirculation, some catheters present side holes near the exit lumen; side holes can decrease the overall resistance and provide a more disturbed flow patterns near the wall and consequently a better washout near the internal wall [6]. They also provide a back-up blood path when the end hole is obstructed by a fibrin sheath or a blood clot [5]. However, their main goal is to allow the catheter in the right position at the center of the superior vena cava, avoiding the catheter surface to stick along the vessel internal wall. Number and size of side holes play an important role in blood recirculation [8]: an excessive number and size value may reduce significantly the blood flow rate from the main lumen and then causes dialysis malfunction. Their presence may promote complications due to thrombosis or creation of relative dead space at the end of the tip promoting clotting [19]. Concerned for long-term dialysis catheter, side holes provide a good method for keeping tip in the right position despite their related complications.

Over the years, many catheter tips have been designed and developed to have always a better dialysis functioning. First of all, researches for the best biomaterial allow CVC tips to be relatively rigid at room temperature to facilitate insertion, but inside the body tips become softer to minimize the potential vessel trauma [31]. Several modifications of the catheter tip design have been implemented including twin catheters, single body step-tip, split-tip and single body symmetric-tip designs. Split-tip design improve average dialysis blood flow rates compared with single body step-tip catheters but the difference is

relatively small [43]. Symmetric-tip catheters are designed to reduce recirculation and resist growth of undesired fibrin sheath [21].

In the figure 3, there are illustrated some different models of catheter tip.

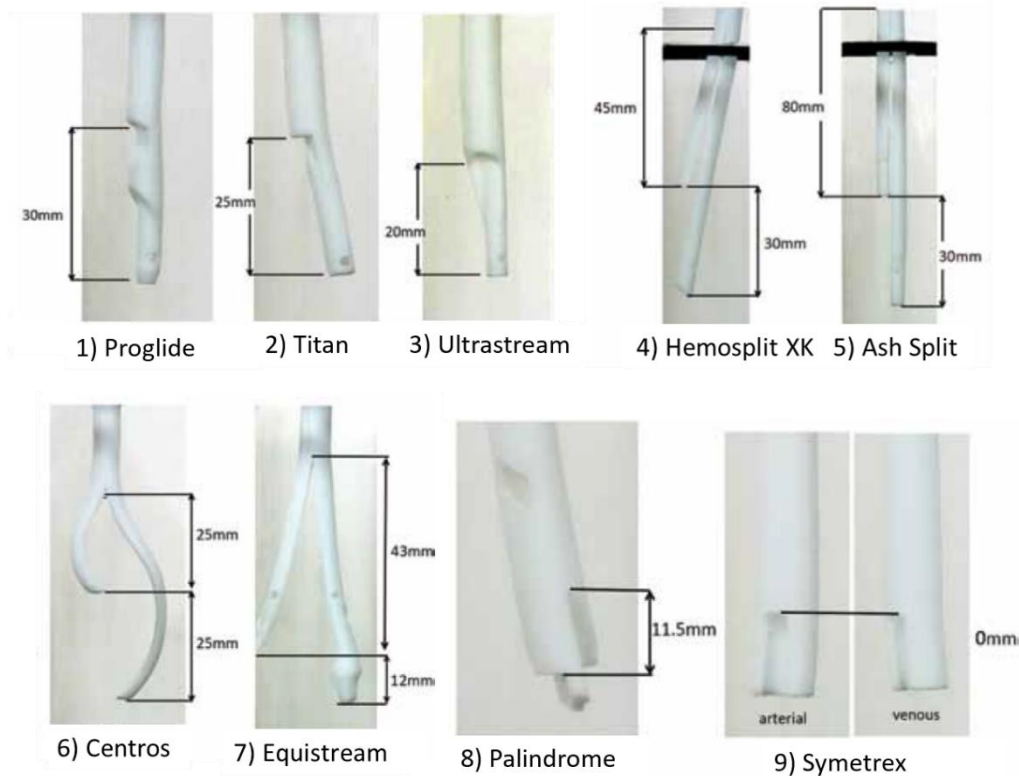


Figure 1.3_Different tip design [1]

1.3.7 Complications

CVC are medical devices which can be subject to many complication despite their relatively basic structure. Complications can be divided into two main groups:

- Short-term complications, which occurs suddenly after the catheter placement, in the first dialysis session therapy or within the following 30 days;
- Long-term complications, which occurs after at least 30 days following the placement.

If any complications do not appear, CVC's life expectative is very high: some type of tunneled and cuffed central venous catheters can survive for 8-9 years inside the patient body; the duration is influenced by patient's health state and the care with which the catheter is treated. Hemodialysis catheter are handled only during dialysis session with no irrigation between treatments. According to standard nursing procedures, the catheter exit site is cleaned with a solution and covered with permeable dressing at the end of each

dialysis session. Each time before the catheter is opened, its end-part is carefully checked for any redness, swelling, bleeding or exudate and patients should report any fever episodes [44].

There are a variety of definitions for catheter dysfunction; the National Kidney Foundation Dialysis Outcome and Quality Initiative (KDOQI) defines catheter dysfunction as failure to attain and maintain an extracorporeal blood flow of 300 mL/min or greater at a pre-pump arterial pressure more negative than -250 mmHg [45].

Short-term complications: this type of complications are usually similar to the ones that occurs during catheter insertions and described above in the part “catheterization”. Early complications that have a frequency lower than 2% are:

- Hemorrhage or hematoma;
- Catheter malposition or kinking;
- Venous perforation;
- Infection;
- Arterial puncture;
- Pneumothorax;
- Air embolism.

Catheter malposition is a typical complication in patients who have vessels in a poor condition: this happen because the course from their insertion site, that usually is internal jugular vein, to the center of right atrium is not so defined as in healthy patients. With bad conditions of vessels internal wall, CVC can proceed in a wrong direction as inside the pulmonary vein or the carotid artery. The doctor prevents this kind of complications using ultrasound guidance and with his experience; to check if the catheter is in the right position, at the end of the surgical operation a radiological control with x-ray is needed. So, early catheter dysfunction generally occurs as a result of mechanical issues such as patient malpositioning, mechanical kinking of catheter and incorrect tip location [46] [47]. To reduce the risk of dysfunction it would be better following the precaution techniques described just above. This type of problems can be resolved by repositioning the patient or adjusting the patient’s neck position, which may fix a kink or move the catheter tip away from a vessel wall [48]; to solve the problem of reaching the right atrium, the doctor should try to move carefully the CVC inside patient vessels.

Long-term complications: late dysfunctions refer to any catheter that previously functioned well but then later becomes dysfunctional, also weeks, months or even years after its insertion. These complications are:

1. Fibrin sheath: it begins to form within 24 hours of catheter insertion; the fibrin sheath is a membrane substance consisting of endothelial cells, smooth muscle cells, collagen and a combination of fibrinogen, lipoproteins, albumin and coagulation factors [49] wrapping around the central venous catheter. The sheath may partially or completely encase the catheter, extending beyond the catheter tip, leading to the disturbance of catheter blood flow [48]. The fibrin sheath begins at the point of contact between the vessel wall and the catheter and it can advance until it covers the whole length of the CVC.

The appearance of this sheath is related to the presence of biofilm; indeed, 100% of fibrin sheaths are colonized with bacteria. This biofilm is characterized by cells that attach themselves to a substratum or to each other; those cells are protected by an extracellular matrix of substances that they produce themselves. The greatest complication of the biofilm is the development of the fibrin sheath that is the most important noninfectious complication; however, the presence of biofilm does not necessarily cause the infection [32]. The presence of fibrin sheath complicates also the total replacement of central vascular catheters: total removal of failed CVC is a complicated and risky surgical operation because the doctor can not previously know how much fibrin sheath is extended; this operation can cause uncontrolled bleeding and lead in extreme cases to patient death.

The catheter can be infected in two ways, depending on the time it has remained inserted: first, within the firsts 30 days after placement, infection occurs mainly due to cutaneous microflora, the care staff's hands and thanks to internal routes; this biofilm develops a high resistance to systemic antibiotics [50] [51]. Second, dysfunction usually appears 90 days after placement [52].

Anticoagulant lock is the most commonly used preventive measure during the interdialytic period; usually heparin or citrate are used for the anticoagulant therapy.

To avoid the formation of biofilm, the ideal catheter should be biocompatible, prevent fibrin sheath formation, have a long-term effect and a wide range of

antimicrobial activity without producing resistance [53]. A strategy to reduce infections and function problems may be catheter coating with particular elements such as nanoparticles of silver, heparin, rifampicine and minocycline or chlorhexidine and silver sulfadiazine. Those anti-microbial coated catheters are expensive, so the doctor uses them only in particular cases such as young patients with a high life expectancy.

2. **Thrombosis:** it can occur in both early and late catheter dysfunction, although more commonly associated with late dysfunction [48]. Intrinsic catheter thrombosis occurs when a thrombus is formed and attached to the inner or the outer surface of the catheter. Extrinsic catheter thrombosis occurs when a thrombus is caused by the presence of catheter in the atrium of central vein [44]. This complication is recognized by the inability to aspirate or flush a catheter and all the thromboses are related to fibrin sheaths [21]. Other parameters which help to recognize thrombosis are maximal consistently achievable blood flow rate, resistance to blood flow during hemodialysis, insufficient depuration despite adequate session length.

For thrombosis prevention, the most commonly used anticoagulation locking solutions are heparin (1000 to 5000 U/mL) and trisodium citrate (4% to 47%) [54]. Comparison of citrate and heparin locks yielded similar results with citrate that has been associated to lower bleeding complications. Recombinant tissue plasminogen activator (r-TPA) is the most commonly used thrombolytic agents lock improves blood flow rates, lowers venous pressures and reduces complications [55]. The r-TPA is allowed to dwell for 1 to 4 hours and this treatment consists of filling the lumen of the catheter with this agent. If this fails, exchange of the catheter is the recommended solution.

Thrombosis of vessels around the catheter is more serious and is usually related to hypercoagulable states or poor tip position; vascular thrombosis is believed to be related to fibrin sheaths development. Intravascular thrombosis is usually asymptomatic and the only way to recognize it is by observing a catheter malfunction [21].

3. **Central Venous Stenosis:** this complication may occur after damage to the vein wall due to infection or mechanical failure. The risk of stenosis is limited if the

catheter lies in the center of a big vessel with a high flow; so, it is strictly related to right positioning of CVC. Stenosis of the central vein can cause obstruction syndrome, which in turn results in a series of symptoms and signs including swelling of the limbs, head and neck after stenosis of the vena cava systems, ulcers and infections of the limbs, and cerebral edema in severe cases [44]. For diagnosis, an angiography is required to confirm the location and extension of the obstruction.

4. Tip Malposition: tip position outside the right atrium may lead to fibrin sheath formation, thrombosis and central venous stenosis, as a result of poor flows or occlusion.
5. Catheter malposition or kinking: it occurs when the catheter is positioned in the wrong place or moves after being placed, or the CVC is curved or folded [44]. To prevent this complication, is recommended a radiological control at the end of positioning.
6. Catheter-related infections: central line-associated bloodstream infection (CLASBI), called also catheter-related bloodstream infection (CRBSI) is the most serious and common complication related to central venous catheters [56]. For this reason, CVCs are the third choice for hemodialysis vascular access: AVF and AVG are preferred for their lower infection risk. Infection is responsible for the removal of about 30-60 % of all hemodialysis CVCs, and it is the second cause of death in dialysis after cardiovascular events [32]. Infection is defined as any of the following [36]:
 - Catheter-associated bloodstream infection;
 - Catheter-related bloodstream infection;
 - Catheter-related sepsis.

CRSBI is dependent on the length of time the patient has the catheter inside his body and other factors, such as patient hygiene and precautions taken by the dialysis nurses during dialysis and the physicians during placement [57]. Catheter-related bloodstream infection is associated with high rates of morbidity and mortality with an addition of excessive costs to the care of patients [58]. The chance that a patient with central venous catheter may have developed CRSBI must be take into account in case of fever, shivers or hypotension; it is also

diagnosed if pus, redness, tenderness and/or induration greater than 2 cm along the catheter is present [44]. Most of the diagnostic methods use quantitative or semi-quantitative cultures taken both from the CVC and from a peripheral vein [59].

The risk of infection increases in relation to the insertion site: femoral catheters is associated with a higher rate of thrombosis and infection; subclavian access is preferred for infection control purpose but other factors, such as potential mechanical complication, thrombosis and operator experience should be considered and decrease the choice rate of this access [60] [61]. So, the choice of internal jugular vein is the right compromise between potential mechanical complication and risk of infection of this insertion site.

There are different type of catheter-related infections and their management varies due to severity [62]:

- Exit site infection without discharge or any symptoms involves only the exit site and not the CVC. This can be treated with catheter exchange alone from the same exit site.
- Exit site infection with discharge or local symptoms should be treated with catheter exchange with creation of a new tunnel, but the same insertion site can be used. An antibiotics therapy should follow depending on cultures and sensitivities of pus discharge.
- Tunnel infection should be treated with removal of the old catheter and insertion of a new catheter at a new venotomy and exit site.
- Catheter-related bacteremia is defined as signs of catheter infection and bacteremia with two sets of positive blood cultures. The treatment should be a removal of the catheter followed by a course of antibiotics broad spectrum at first and more specific after the culture.

In patients with tunneled hemodialysis catheter it is preferred to try keeping inside the body the CVC and start an antibiotic therapy due to the difficulty and high risk of complication of removal operation. Even though the CVC substitution is clinically advised, before the removal of a catheter it is necessary to make sure that a new site is available for insertion of a new catheter; otherwise, due to the surgeon's decision, the new catheter may be inserted in the same access site. If the

decision of the clinical team is maintaining the catheters inside the patient, a possible therapy to remove the infection is the antibiotic one. The ideal antibiotic for the treatment of hemodialysis CRBSI must [15]

- Be active towards those pathogens that are usually responsible for infection;
- Have a fast bactericide action;
- Have concentration-dependent action;
- Not be cleared via the kidneys;
- Have a long biological half-life that allows a single, daily administration after hemodialysis;
- Have a good capacity of penetration into the biofilm.

Some preventive measures for decreasing CRBSI rate are surveillance, education and quality management strategies, antiseptic dressings and catheter locks. The standard of care for infection prevention must continue to include the use of sterile gloves, a long-sleeved sterile gown, a mask, a cap and large sterile drapes during catheter insertion. Skin disinfection with 2% alcoholic chlorhexidine significantly helps to diminish the risk of presence of micro-organisms on the skin surface. During the catheterization, practical recommendations for care and surveillance include three general preventive measures: prevention and control of multi resistant bacteria spread, surveillance of nosocomial infections and hand hygiene [63].

2. Hemodynamics inside CVC

The present chapter contains the description of the two central venous catheters, Palindrome and Tesio, that characterized this thesis work. Furthermore, is described the state of art of the studies already present in literature which dealt with the computational fluid dynamics of CVC. Finally, is expressed the aim of the present study.

2. HEMODYNAMICS INSIDE CVC

2.1 PALINDROME CATHETER

Palindrome™ is a catheter used for the hemodialytic treatment; it belongs to the Palindrome precision family of chronic hemodialysis catheter, namely the group of CVC that has a particular tip design. Palindrome catheter was developed in 2005 [64]; this catheter consists in only one tube made of Carbonate (which is an aliphatic polyurethane group, based on polycarbonate) and divided in the middle to form two symmetrical “D”-shape lumen, one for the arterial needle that conducts “dirty blood” from the patient to dialysis machine, and the other for the venous needle that brings dialyzed blood from the dialysis machine to the patient.

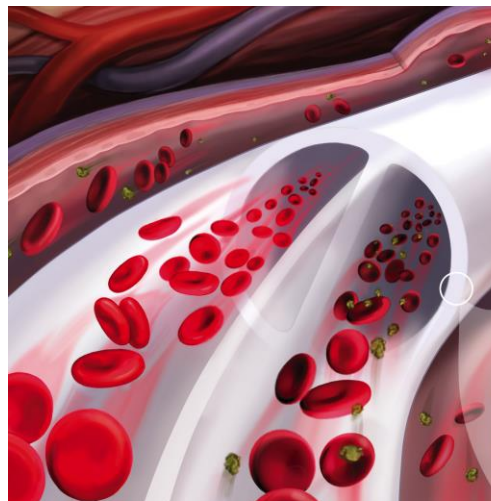


Figure 2.1_Palindrome lumen design

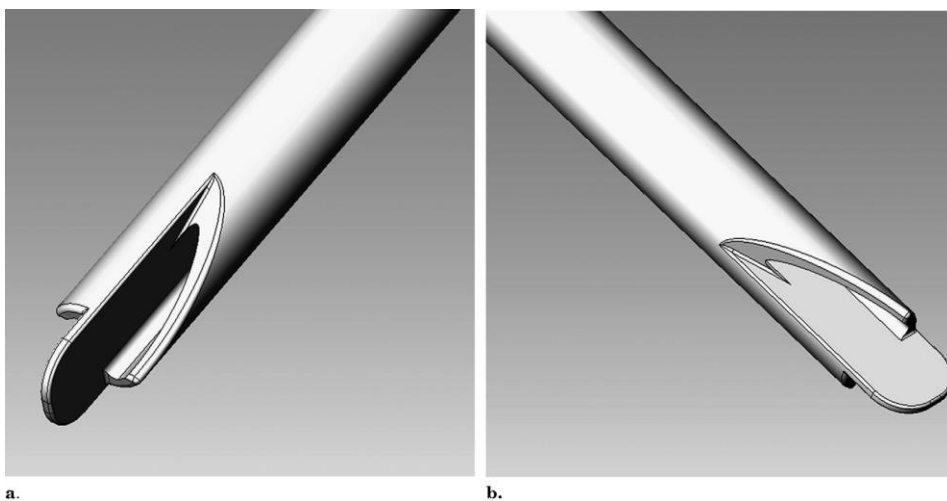


Figure 2.2_Palindrome tip design [2]

The main particular that characterized this group of catheters is the symmetrical “Z” shape tip [65]: it is designed with a symmetric, spiral tip and biased ports, with only two side holes, one on each side. The presence of side slots is due to reduce the likelihood of positional occlusion.

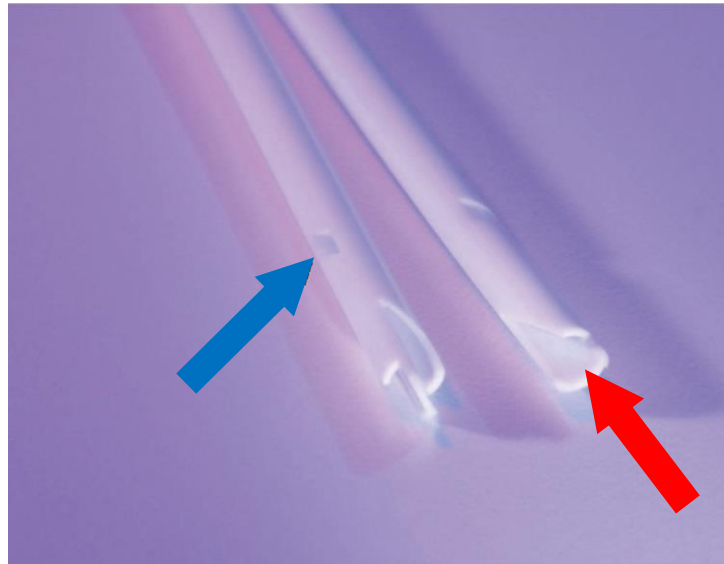


Figure 2.3_Palindrome tip design [3]

The choice of a symmetrical tip design is based on the research of recirculation risk reduction. The geometry of Palindrome tip is such that the inflow is mostly through the side hole situated about 2 cm proximal to the tip (the one indicated by the blue arrow in figure 6) and also through the most proximal part of the spiral end hole (right above the side hole) [2]. The outflow, which consists in dialyzed blood, is directed away from the catheter mainly through the spiral end hole (indicated in the figure 6 by the red arrow). This design, in addition with the septum between the catheter lumens, would prevent recirculation: Tal et al. [3] (Journal of Vascular and Interventional Radiology, 2005) conducted an animal study using a swine model: the Palindrome catheter demonstrated a reduced rate of recirculation compared with other catheters.

This study is also important because it treats a fundamental aspect that characterized Palindrome catheter: the possibility of inverting arterial lumen with the venous one due to his perfect symmetry. The authors demonstrated that, even with reversal of the dialysis lines, minimal recirculation characterizes Palindrome catheter.

In addition to the reduction of recirculation, this catheter was developed with the purpose of reducing catheter-related complications, such as fibrin sheath and infection) by

reducing thrombosis: Spector et al. [2] (Journal of Vascular and Interventional Radiology, 2008), after their single institution study, came to the conclusion that Palindrome catheter demonstrated safe and reliable use with low infection rates.

The Palindrome dialysis catheter is able to guarantee high flow rates (between 300 mL/min and 600 mL/min) due to its internal lumen design, with a diameter of 14.5 Fr (French is the measurement unit used for tube diameter; 3 Fr = 1 mm), and durable Carbothane™ material [66]. This high tensile strength material and the catheter internal lumen design optimize inner diameter integrity without compromising flexibility or kink resistance, so the internal lumens keep maintaining their “D” shape.

Several authors conduct clinical studies with the purpose of establishing which catheter was better: Hwang et al. [64] (Seminars in Dialysis, 2012) conducted a prospective randomize trial with a comparison of the Palindrome vs. Step-Tip tunneled hemodialysis catheter. They noticed that Palindrome catheter have advantages in terms of lower catheter dysfunction rate, lower recirculation with reversed blood lines, higher short-term catheter survival rate.

Li et al. [65] (Iranian Journal Kidney Diseases, 2014) arrived at the conclusion that for dialysis patients studied, Palindrome catheter was superior to Permcath catheter and comparable with the AVF in terms of the maximum blood flow, dialysis adequacy, and annual patency rate.

Ye et al. [67] (Informa Healthcare USA, 2015) conducted a retrospective study of 284 cases of chronic catheterization in 271 patients treated between 2009 and 2011 using

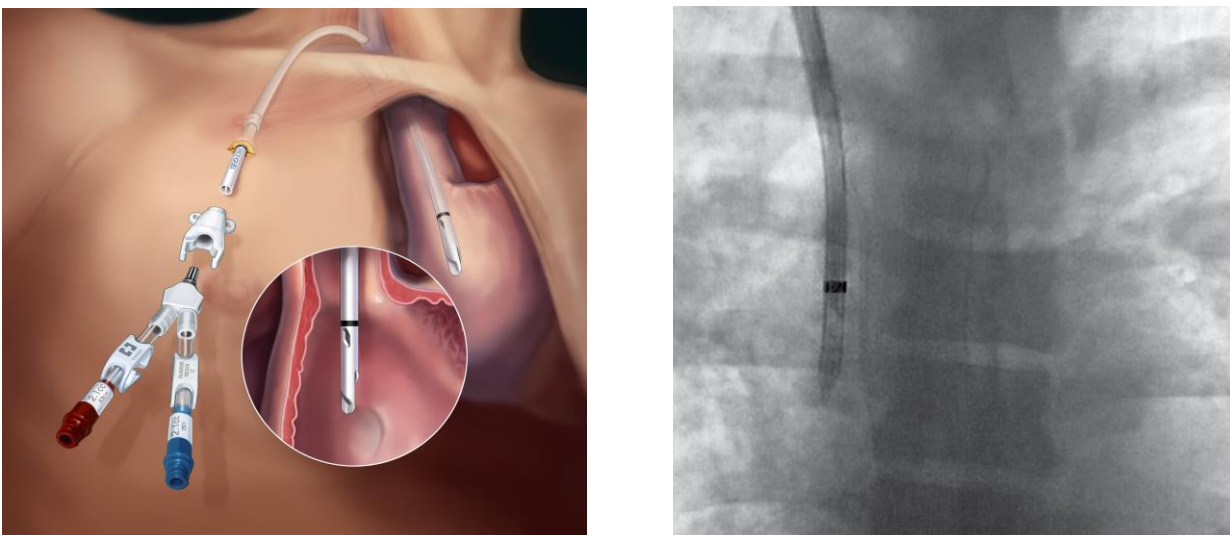


Figure 2.4_Palindrome position inside the body

Palindrome symmetrical-tip or Perm cath step-tip: Palindrome catheter was associated with a longer mean dwell time, lower incidence of low blood flow, and lower infection rate compared with the step-tip catheter.

As for other hemodialysis catheters, the optimum Palindrome tip position is the center of right atrium; this condition could be reached thanks to the metallic guide used during catheterization (specified above) and the ability of the nephrologist. The insertion procedure takes on the average 20 minutes; the duration mostly depends on the ability and the experience of the inserter. In addition, Palindrome helps nephrologist with a radiopaque tungsten marker band, positioned proximal the side holes, that allows to distinguish catheter's tip and to visualize the correct placement in the right atrium on fluoroscopy and X-ray.

Concerning catheter's tip, it is fundamental the fact that it is made with the laser cut technology: this technique allows to produce the Palindrome tip with the best possible accuracy. In particular, the laser-cut side holes have been enhanced to reduce total shear

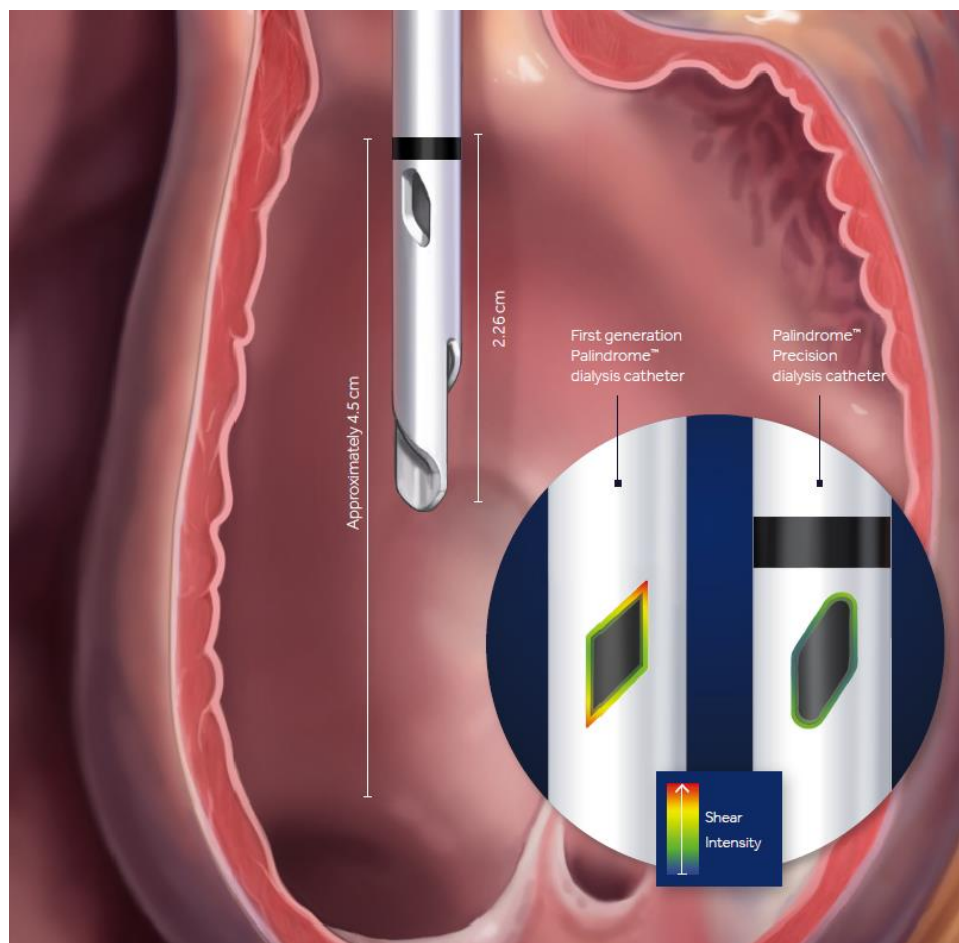


Figure 2.5_Palindrome inside the right atrium

stress on the inflow side slot and laser-cut surfaces help to discourage platelet adhesion and minimize debris attachment.

Palindrome precision family of chronic hemodialysis catheters includes several type of CVC that differ from each other for some particular [66] :

- Palindrome Precision symmetric tip dialysis catheter: is the basis one, with the marker band technology, the laser-cut side holes and without coating;
- Palindrome Precision H-heparin coated dialysis catheter: noneluting heparin coating decreases the likelihood of platelet adhesion and inhibits fibrin sheath formation;
- Palindrome Precision SI-silver ion antimicrobial dialysis catheter: a silver ion sleeve reduces colonization against a broad spectrum of bacteria on the catheter surface;
- Palindrome Precision HIS-heparin coated and silver ion antimicrobial dialysis catheter: both silver ion sleeve and heparin coating are incorporated into the catheter due to reduce the likelihood platelet adhesion and colonization against a broad spectrum of bacteria;
- Palindrome Precision RT-reverse-tunneled dialysis catheter: reverse-tunneled catheter tip is designed to allow for precise tip and cuff placement using the retrograde tunnel technique.

2.2 TESIO CATHETER

Tesio Cath is the second type of central venous catheter studied in this work: it is a kind of vascular access that allows accessing blood for dialysis. Its main particularity is the presence of two identical tube made up with the same geometry and material.

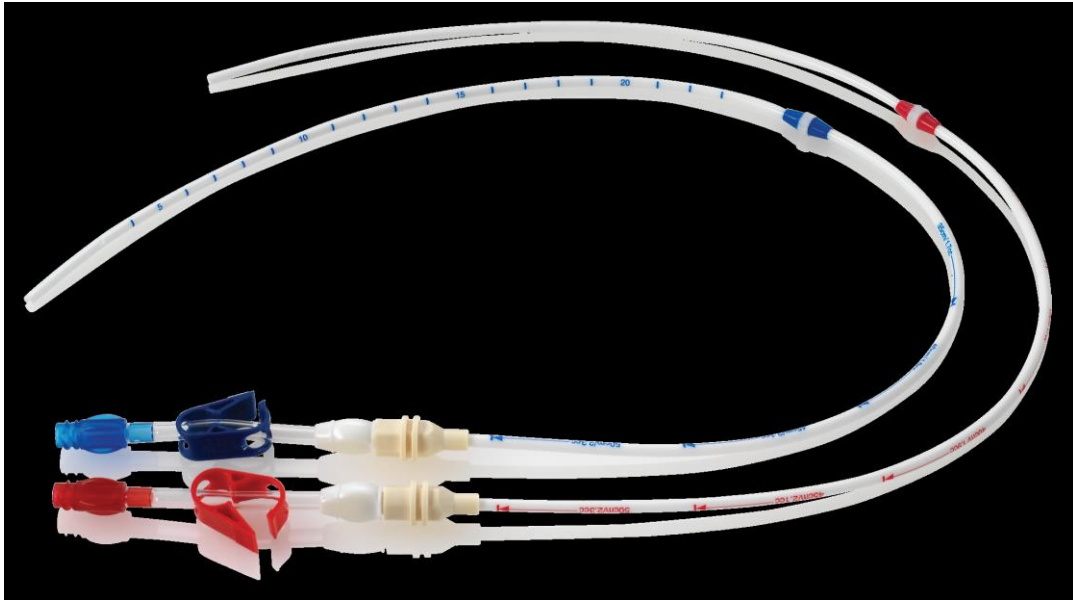


Figure 2.6_Tesio catheter

It was studied and designed by Franco Tesio: around 1980 he developed his first hemodialysis permanent catheters, which had the main problem regarding the material: he used common silicone but it was inadequate for the long-term treatment [68]. Driven by the purpose of solving this problem and other regarding mal-positioning and catheter's conformation, Tesio developed a new type of catheter, implanted for the first time in 1986. It was very similar to the one of our days: two catheters inserted both in the right internal jugular vein with the tip positioned in the center of the right atrium. The material was the spi-silicon, studied by Suzuki and Bambaour; now the material mostly used for Tesio Cath is the Bio-Flex (which gives the name Bio-Flex Tesio Cath, Medcomp) which is a carbothane with higher performance in flexibility and kinking resistance.

The presence of two distinct tube, one for the arterial line, which brings the “dirty” blood from the patient to the dialysis machine, and the other for the venous line, which brings the dialyzed blood to the patient, allows to place the two tip in the as correct as possible position, focusing on one at a time. Furthermore, if one of the two catheters went into failure, it is possible to substitute only the failed one with a new catheter, while the other tube is letting work; in this way, the dialytic therapy must not be suspended [68].

Each tube of Tesio Cath has a diameter of 10 Fr (that is equal to 3.3 mm): this allows an adequate flow rate for the dialysis therapy; the internal lumen keeps the circular shape for all the catheter's length.

Concerning the tip, both catheters have the same identical geometry: a huge hole at the end of the tube but also six side holes spirally placed starting from the exit site [4]. Each side hole has a diameter of 15 mm and they make the catheter tip approximately 50 mm long.

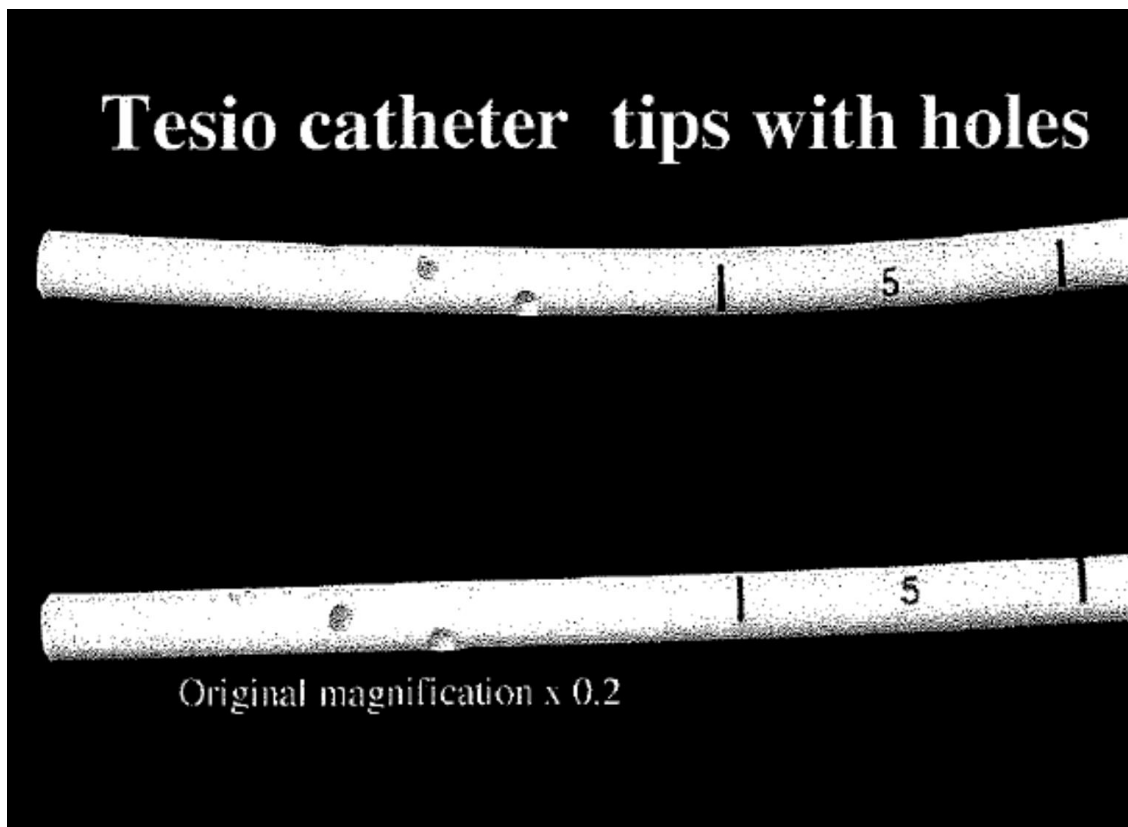


Figure 2.7_Tesio tip design [4]

The side holes have the task of avoiding that the final part of the tube will attach to the internal wall of the vein and letting an adequate blood flow rate even in case of fibrin sheet formation and the eventual occlusion of the end site or someone of the side hole.

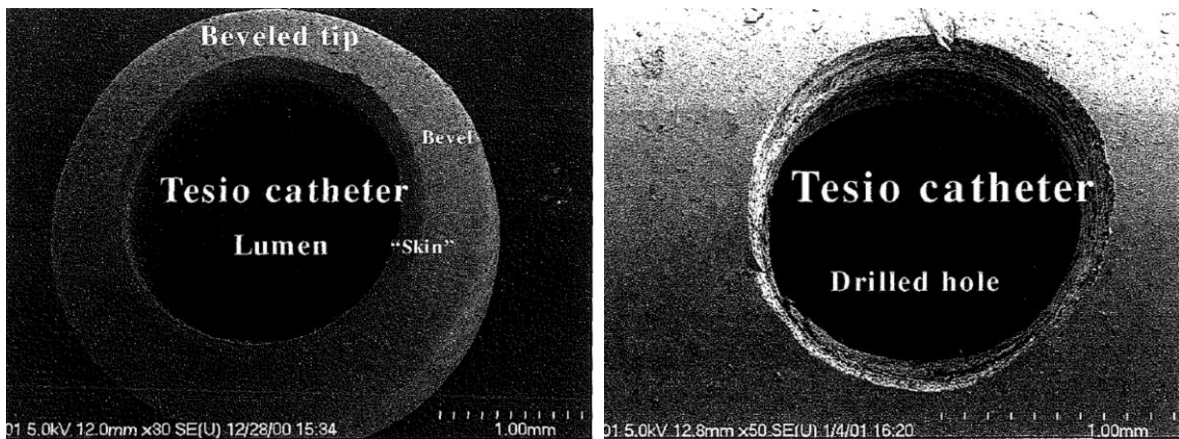


Figure 2.8_ Tesio section and Tesio side hole [4]

For Tesio Cath is fundamental that the tip of both catheters must be positioned in the correct way: the optimal position is the same of other catheter (the center of the right atrium); in addition, the venous catheter must be positioned above the arterial one, about 2-3 cm of distance, closer to the tricuspid valve. This reciprocal position of the inflow and the outflow tubes allows to avoid a high rate of recirculation; an eventual malposition could make the dialytic therapy useless. To prevent the risk of uncorrected positioning, the nephrologist must be careful during the procedure: after the insertion of the tubes, he checks by X-ray their position; once observed the result images, he eventually assesses some arrangements to obtain the correct tip position. This condition is maintained due to the cuff previously described that anchors the catheters in the right position.

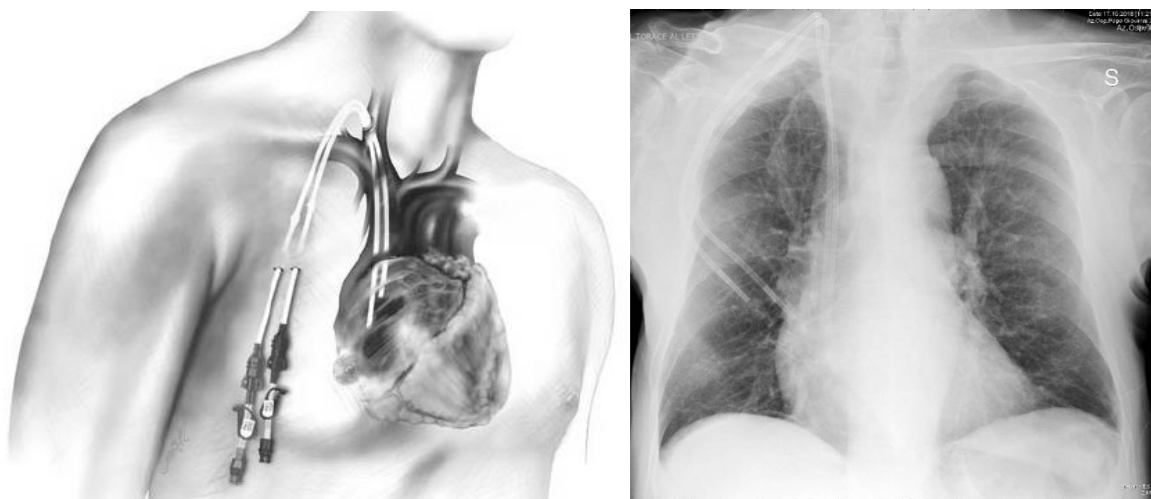


Figure 2.9_ Tesio position inside the body

The procedure of insertion for the Tesio Cath takes more time compared to the one for the Palindrome: due to the fact that Tesio Cath are two different tube, this procedure can last at least 45 minutes.

The inflow, that is the blood flow in the venous line, is mainly through the main hole at the end site and it exploits less the side holes. Instead, the outflow is mainly through the two or three most distal side holes.

There are different type of Bio-Flex Tesio Cath available: they difference each other for the length between the end part of the tip and the cuff position; the correct length is chosen by the nephrologist on the basis of the patient's size.

2.3 STATE OF THE ART OF CFD INSIDE CVC

Computational Fluid Dynamics (CFD) is the numerical analysis of physical phenomenon such as flow of fluids, gases or heat. This analysis technique is increasingly used in developing medical devices and studying their behavior for clinical applications. Indeed, thanks to CFD software, fluid flow problems are analyzed with a huge saving of time because the fabrication and characterization of experimental set-up is unnecessary.

A literature research provides a first vision of the studies present which concern the application of CFD techniques to hemodialysis CVC.

Mareels et al [5] (Artificial Organs, 2004) studied the Niagara catheter using CFD simulation technique. In particular, they studied the influence of side holes in different situations: totally open side holes, totally closed side holes and side holes with reduced size. They evaluated the insertion of the catheter first in a simple hollow cylinder placed concentrically around the CVC (simulating the superior vena cava) and after using a 3D model of right atrium reconstructed from axial cryosection images of a male cadaver. They used CAD package SolidWorks 2000 (SolidWorks Corporation, Concord, MA, U.S.A) to construct the model of Niagara catheter; concerning on CFD simulation, the CFD software they choose to simulate blood flow was Fluent 6.1 (Fluent Inc., Lebanon, NH, U.S.A.).

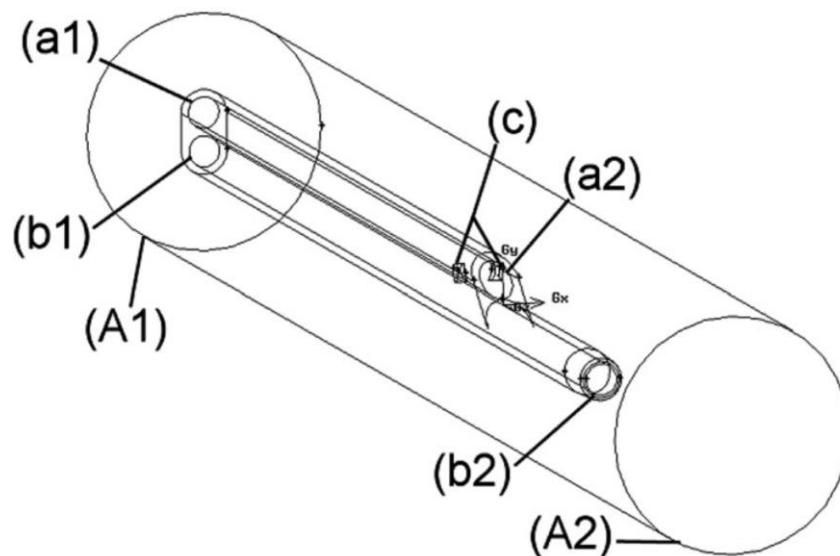


Figure 2.10_Simulation environment with Niagara catheter in hollow tube [5]

The same authors compared seven CVC designs using CFD simulation [6] (American Society of Artificial Internal Organs, 2007). The different catheter designs studied were Cut straight, Cut straight sleeve, Cut angle, Cut straight hole, Concentric, Cut angle hole and Ash split. All catheter models were constructed in *in vivo* scale in the CAD package SolidWorks 2003; concerning CFD simulation, catheter models were inserted concentrically in an *in vivo*-scaled rigid cylinder representing the superior vena cava and the software used was Fluent 6.2.

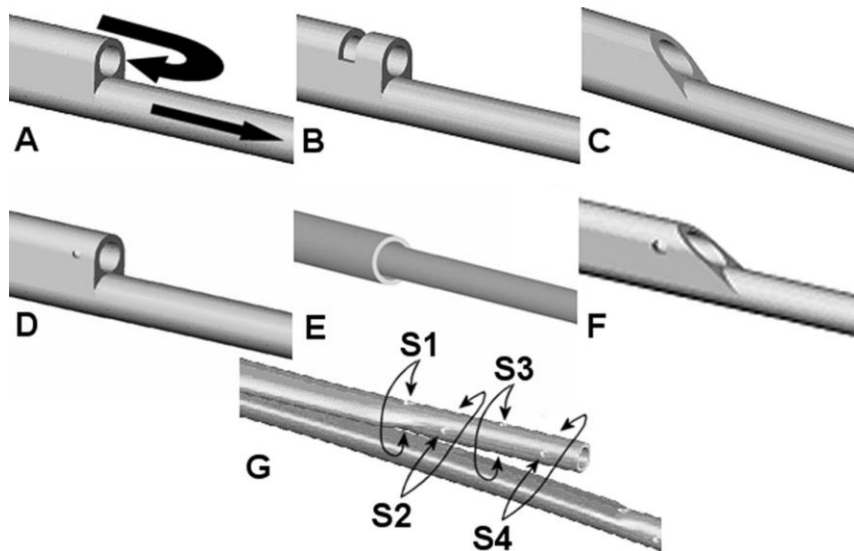


Figure 2.11_Different catheter tip design [6]

Elkhoury et al [69] (International Mechanical Engineering Congress & Exposition, 2010) compare the performance of three hemodialysis catheters: Niagara double lumen, Flexxicon II double lumen and Hemosplit long-term catheters in terms of blood flow rate and shorter exposure time, focusing on the comparison of shear rates. For the study, authors used catheter's geometries constructed with SolidWorks 2007; with this software they also modelled the superior vena cava, in which catheters are placed, with a simple hollow cylinder. The hemodynamics were evaluated using Fluent 6.3 software.

Clark et al [7] (Seminars in Dialysis, 2012) examined flow characteristics of two CVC: VectorFlow catheter and Palindrome catheter. They examined the behavior of these catheters in three settings: a simulated model using computational flow dynamics, a bench model of hemodialysis and an animal model (to measure recirculation at varying rates of flow). Furthermore, they compare the results of this catheter with other dialysis catheter designs, in particular the ones studied by Mareels et al. (2007). In this study, Clark created catheters' design using SolidWorks software; these virtual catheters were placed within

a hollow cylinder representing the superior vena cava. The software used for CFD simulation was Fluent 6.2.

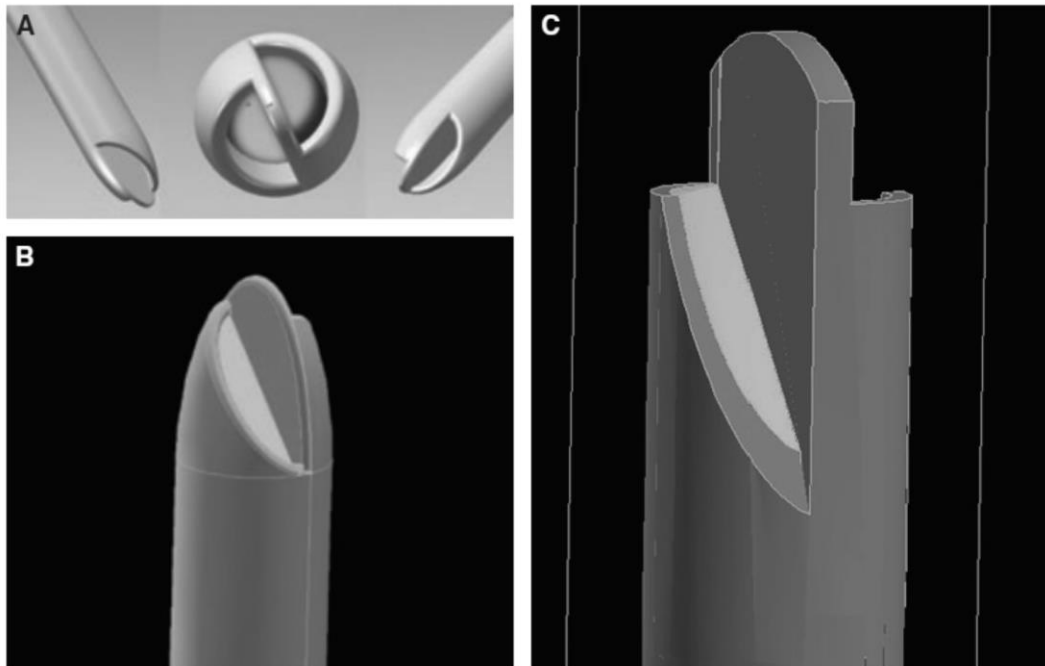


Figure 2.12_Different catheter tip design [7]

Again Clark et al. [8] (Journal of Vascular and Interventional Radiology, 2015) compared three different catheters' design: Palindrome, VectorFlow and GlidePath. They obtained catheters' geometry in three different way: Palindrome catheter was measured with a touch probe coordinate machine; to generate a 3D model they used SolidWorks starting from the resultant measurements previously obtained. Concerning to GlidePath catheter, thanks to a high-resolution industrial computed tomography system (GKS Services, Minneapolis, Minnesota) they obtained a scan of internal and external surfaces and the resulting 3D model was rendered into SolidWorks. Finally, the VectorFlow catheter was rendered by using design-control SolidWorks files. To compute CFD simulation, these

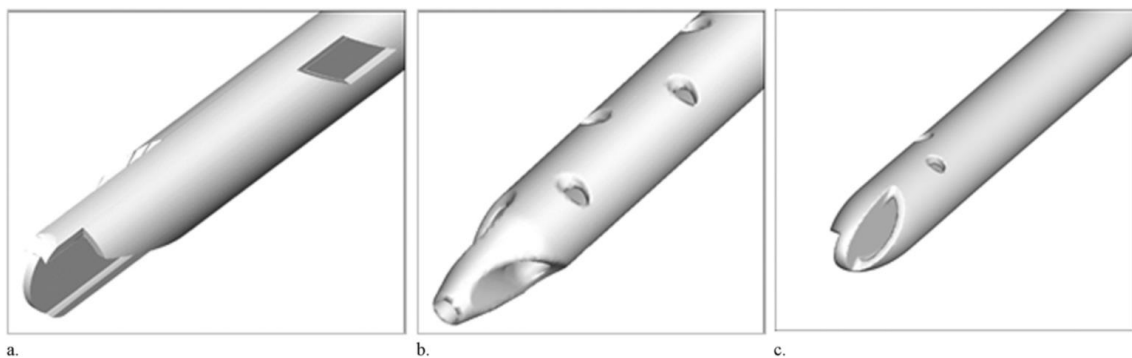


Figure 2.13_Different catheter tip design [8]

3D models were coaxially placed inside a cylindrical conduit which ideally represents superior vena cava. In this study, the CFD software used was Fluent (ANSYS).

Despite limitations and approximations present in these studies, computational fluid dynamics represents a valid technique in studying and comparing different catheters' designs. This approach could be a strong support for valuation of CVC clinical efficiency and for eventual future development of new catheter's

2.4 AIM OF THE STUDY

Differences in catheter design can produce significant differences in hemodynamic conditions during hemodialysis, and in turn can have important implications for catheter thrombogenicity, recirculation, and other critical parameters of catheter performance. However, a number of studies provided only very limited and simplified evaluations of CVC hemodynamic conditions.

The present thesis was aimed at setting up a reliable method for the characterization of hemodynamic condition in patient-specific conditions, coupling imaging techniques and high-resolution CFD. In particular for this work, the main goal was to identify a methodology for the comparison between the fluid dynamic conditions of two particular catheters, Palindrome and Tesio, once inserted in the patient's body.

3. Computational mesh creation

The present chapter contains guidelines to perform 3D reconstruction of patient specific and catheter model starting from DICOM files. The first part is about the reconstruction of the precise part of the patient's body starting from a CT acquired at the Hospital Papa Giovanni XXIII (Bergamo). The second part described the procedure of acquisition of the two catheters Palindrome and Tesio, starting from the samples to the 3D model. The second part is about the generation of final models and then the creation of the volume mesh.

3. COMPUTATIONAL MESH CREATION

3.1 3D MODEL OF THE VEINS

3.1.1 Overview of geometry used in studied articles

The literature search performed during the first weeks of this work, has given way to evaluate the previous CFD studies about different central venous catheters.

ARTICLES (First name, Journal of publication, Year)	CVC POSITION	EXTERNAL GEOMETRY	LENGTH (mm)	DIAMETER (mm)
Mareels, Artificial organs, 2004	SVC or IVC	Simple hollow cylinder	150	16
Mareels, AmSocArtificial InternalOrgans, 2007	SVC	Cylinder	NA	18
Elkhouhry, IMECE, 2010	SVC	Simple hollow cylinder	NA	16
Clark, SeminarsInDialysis, 2012	SVC	Cylinder	120	18
Clark, JVascIntervRadiol, 2015	SVC	Cylinder	480	18

Table 3.1_CFD articles studied

Table 3.1 shows the external geometry where catheters were inserted for the fluid dynamics simulations. In these articles, it was specified that the simulations would recreate the situation in which the catheter is positioned in the centre of the SVC; all the authors used a simple geometry (a hollow cylinder) to model the SVC. These cylinders are similar as regard the internal diameter: their values are 16 mm or 18 mm; their length was not specified in two articles and the others assumed different values: 120, 150 and 480 mm. We compared these values to the physiological ones found in literature [70]. The diameter of superior vena cava is about 22 mm (healthy adult man), so it is comparable to the values used in the articles. Instead, the physiological length is about 70 mm, very different from the ones used in articles; this difference is not relevant because vessel length in CFD simulation plays a fundamental rule allowing the correct blood flow development, so it may not be the same of physiological one.

On the basis of this bibliography review, we decided to improve the geometry in which the catheter is inserted during CFD simulation and make it as realistic as possible. One

aspect that we have decided to improve is the position of catheter's tip: the centre of the SVC is described as critical situation or malposition. Both the literature search [21] and the interview with the nephrologist has showed that the optimal position of catheter's tip is the centre of right atrium, just below the junction between SVC and right atrium. This is the optimal position because the blood flow could meet the requirements of dialytic therapy, without risks to the patient. In fact, a catheter positioned "shorter", namely with the tip located in the SVC, above the junction between SVC and right atrium, may pose several health risks, including increasing incidence of thrombotic events and damage to the internal wall of the vein. On the other hand, a catheter positioned "longer", spanning the whole right atrium is located in proximity of the junction between IVC and right atrium or near the tricuspid valve and right ventricle. This mal positioning may generate arrhythmia, valve damage or atrial thrombosis, in addition to all complication described above (paragraph 1.3.7).

3.1.2 Description of the geometry chosen

In order to have a geometry as realistic as possible, we decided to take the model starting from a CT of a patient (75 years old man) acquired at the Hospital Papa Giovanni XXIII (Bergamo). After a briefing with the nephrologist, we decided to include in our model the right atrium, the tricuspid valve, the IVC, the SVC, the right internal jugular vein and the left anonymous vein.

The right atrium, one of the four chambers of heart, is located in the upper right corner of the heart, superior to the right ventricle and divided from this by the tricuspid valve. The right atrium receives deoxygenated blood from the superior and the inferior vena cava; when the tricuspid valve is open, the right atrium pumps the blood into the right ventricle to be send to the lung circulation, where it becomes oxygenated. The normal dimensions for the right atrium are: superior-inferior, 3.4 to 4.9 cm; medial-lateral, 3.1 to 4.5 cm [9]. The tricuspid valve divides the right atrium and right ventricle; it is an atrioventricular valve consisting of three membranes (cusps) that deny to the blood to flow backwards from the right ventricle to the right atrium. In our simplified geometry, we decided to idealize this valve with a cylinder starting perpendicularly from the right atrium and, located in the same position of the tricuspid valve. Thanks to this, the blood flowing away from the right atrium to the right ventricle can be taken into account.

The IVC opens into the most caudal part of the right atrium [9]; it returns deoxygenated blood from the lower half of the body. Its orifice is larger than that of the SVC. The diameter of the IVC proximal to the right atrium ranges from 1.2 to 2.3 cm [9].

The SVC opens into the cranial and posterior part of the right atrium; its position allows the blood entering the atrium to be directed toward the atrioventricular opening [9]. Usually, SVC has a diameter of about 22 mm and a length of 70 mm. SVC returns the deoxygenated blood from the cranial half of the body; this blood flows in SVC from the left and right brachiocephalic veins (or innominate veins). We decided to include in our model the left innominate vein and the IJV; for the right brachiocephalic veins, we decided to include only IJV because the CVC is inserted into the blood circulation from this vein.

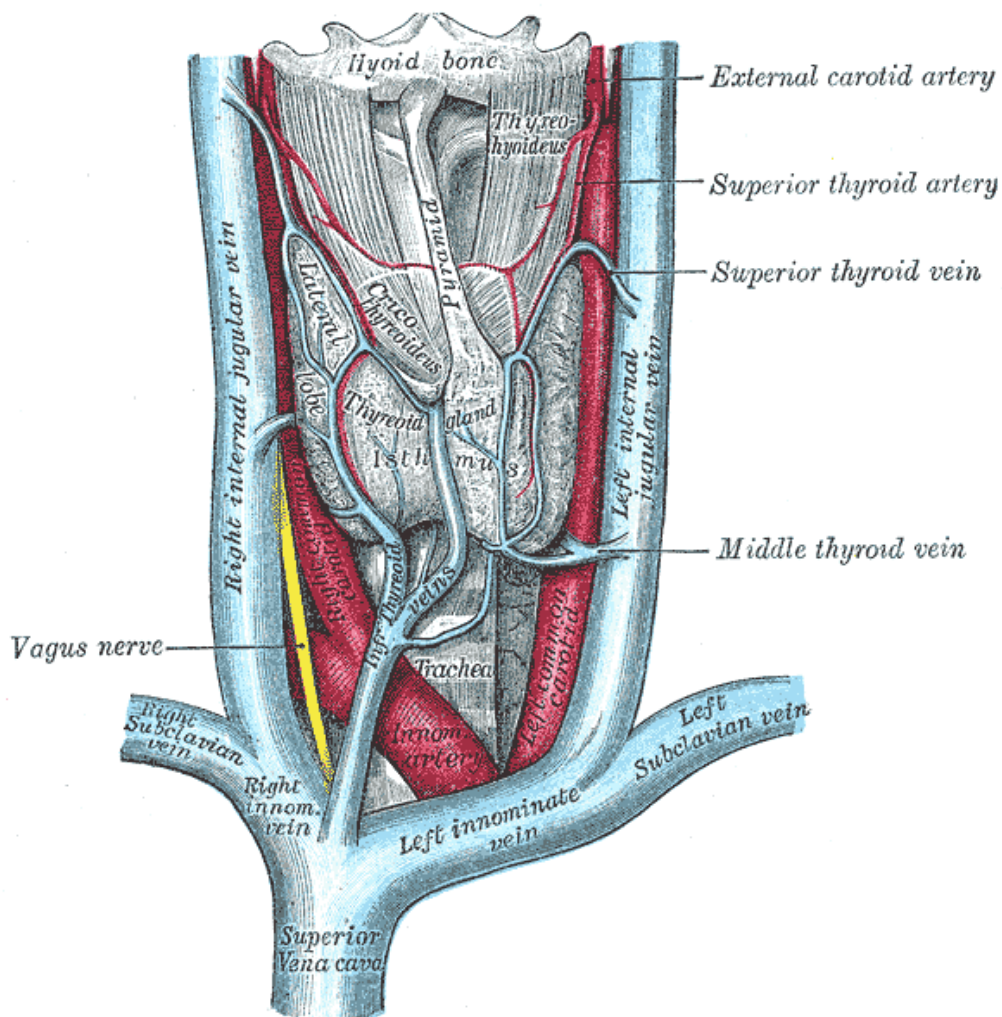


Figure 3.1_Anatomy of SVC

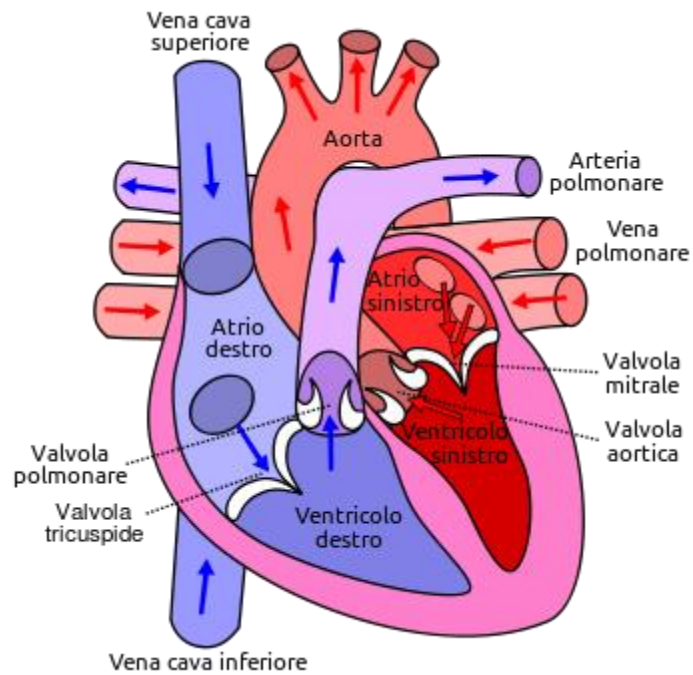


Figure 3.2 _Scheme of RA, IVC and SVC

3.1.3 Reading DICOM files and selecting a Volume of Interest (VOI)

The 3D model reconstruction has been realized with the Vascular Modelling toolkit (VMTK) [71].

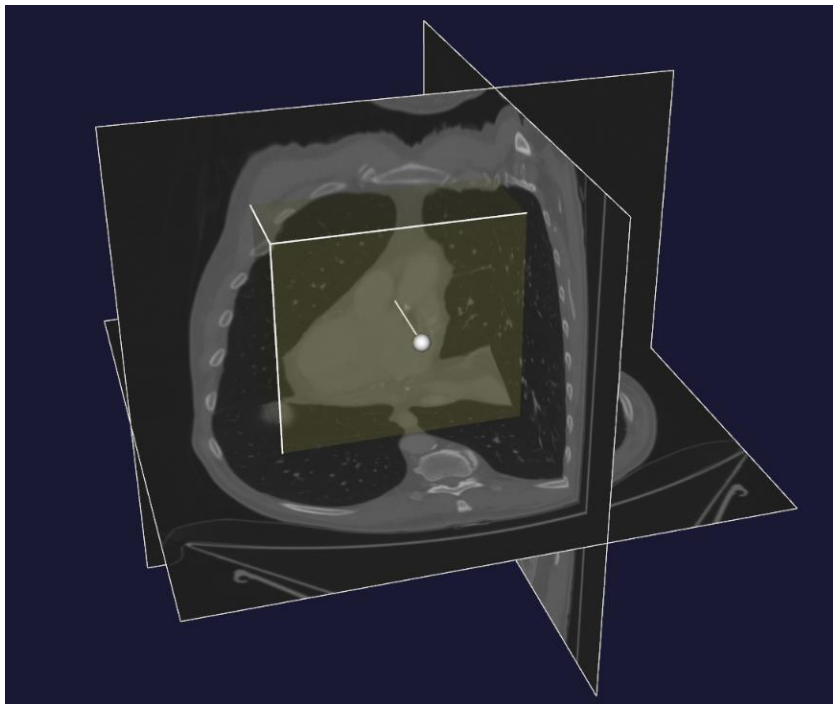


Figure 3.3_Extraction of VOI

Once the position of veins of interest has been identified, a volume of interest (VOI) containing the part of the body that we want to include in the 3D model (Figure 3.3) is extracted.

3.1.4 Level set segmentation

Level sets [72] are a kind of deformable model in which the deformable surface is not represented by a set of points and triangles, but rather described by a 3D function (basically another image) whose contour at level zero is the surface in question. The advantage of using a deformable model is that the location of the surface does not depend on the chosen level, but on the regions corresponding to the steepest change of image intensity across the vessel wall, which is a robust and objective criterion.

For this work it has been decided to use the Colliding Fronts method, because of its effectiveness in initializing the tract of a vessel. With a manual choice of the two seeds, the model results more accurate and it includes only determined parts of vessels.

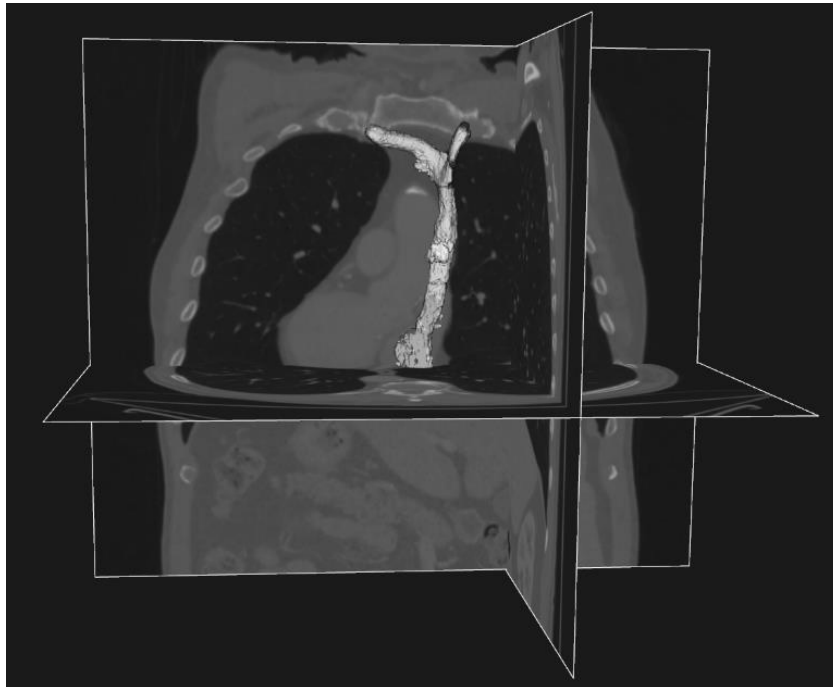


Figure 3.4 _Level set segmentation

In order to control the level sets some parameters has to be set:

- *Number of iterations*: the number of deformation steps that the model performs;
- *Propagation scaling*: the weight assigned to model inflation;
- *Curvature scaling*: the weight assigned to model surface regularization;

- *Advection scaling*: the weight that regulates the attraction of the surface of image gradient modulus ridges.

In this model the parameters set are respectively 300 0 0 1. Setting advection to 1 and propagation and curvature to 0 can robustly lead to reproducible results and setting the number of iterations at 300 should make the level set not to move anymore. The Figure 3.4 shows an example of segmentations with level set.

3.1.5 Generating the vessel wall surface with marching cubes

The algorithm marching cubes [73] uses a “divide-and-conquer” approach to generate inter-slice connectivity and then creates a topology surface based on triangles. Figure 3.5 shows an example surface extracted with marching cubes:



Figure 3.5_Surface extracted using marching cubes

3.1.6 Surface smoothing and conversion to .stl format

Image segmentation can result in bumpy surfaces, especially if the image quality is rather poor. Since a bumpy surface can result in spurious flow features and affect wall shear stress distributions, it is important to smooth the surface prior to generating the mesh.

The parameters that have to be set are the method (Taubin is better than Laplacian method because it avoids the loss of geometrical features), the number of iterations (after making some attempts, the number of iterations considered the most precise was 30), and the passband (set to 0.01).

A comparison between the surface before and after the smoothing is shown in Figure 3.6 and 3.7.



Figure 3.6_Surface before the smoothing



Figure 3.7_Surface after the smoothing

The resulting smoothed surface still presents some imperfections; in order to reduce them, we decided to perform a manual smoothing using Autodesk MeshMixer (Autodesk, Inc., San Rafael, Calif.). We used this program also to add flow extensions to the IVC, the right internal jugular vein, the left anonymous vein and the tricuspid valve; these changes ensure fully development of blood flow. Autodesk Meshmixer works with files which are in the *.stl* (stereolithography) format.

3.1.7 Modified with Autodesk Meshmixer

Autodesk Meshmixer allows to correct the imperfections and protrusions that the initial reconstruction with VMTK has included due to the low resolution of CT images. With the “sculpt” tool we made a manual smoothing of the veins and the right atrium removing one by one every protrusion making all the structure as smoothly as possible. These changes modified only the external surface: the dimension of right atrium and diameters of veins have remained the same.

Autodesk Meshmixer allows also to add the flow extensions that ensure the fully development of blood flow. We added four cylindrical additions to the inlet accesses, namely the IVC, the right internal jugular vein and the left anonymous vein, and to the outlet, the tricuspid valve. For each access, we selected the area involved and then used the “extrusion” tool choosing the correct direction to ensure the fully development of flow.

The next step consisted in a surface remeshing in which the triangle edges were resized in order to obtain a uniform distribution, without altering the structure of the geometry. The Autodesk Meshmixer allows, with its “Remesh” tool, to re-tile a mesh with a new set of triangles; we performed the remeshing to the whole structure in order to have a uniform distribution of all triangles.

For our structure we have chosen to remesh the model surface using the “Relative density”, maintaining thus the same density of edges but increasing the regularity in order to obtain triangles more “regular” or roughly equilateral.

The final step regards the capping of each inflow / outflow access of the model. The “Plane Cut” tool allows slicing a mesh with a plane to create a regular surface at the end of each vein and the tricuspid valve’s extrusion. With this tool we positioned the cutting plane in the correct way and, by choosing the Cut type, the portion of the model that is rendered as semi-transparent will be deleted.

The final geometry of the structure in which insert the catheter is so completed: it consists in 35.526 number of triangles, and it is length 92.4 mm on X-axes, 79.7 mm on Y-axes and 314.9 in Z-axes (Figure 3.8).

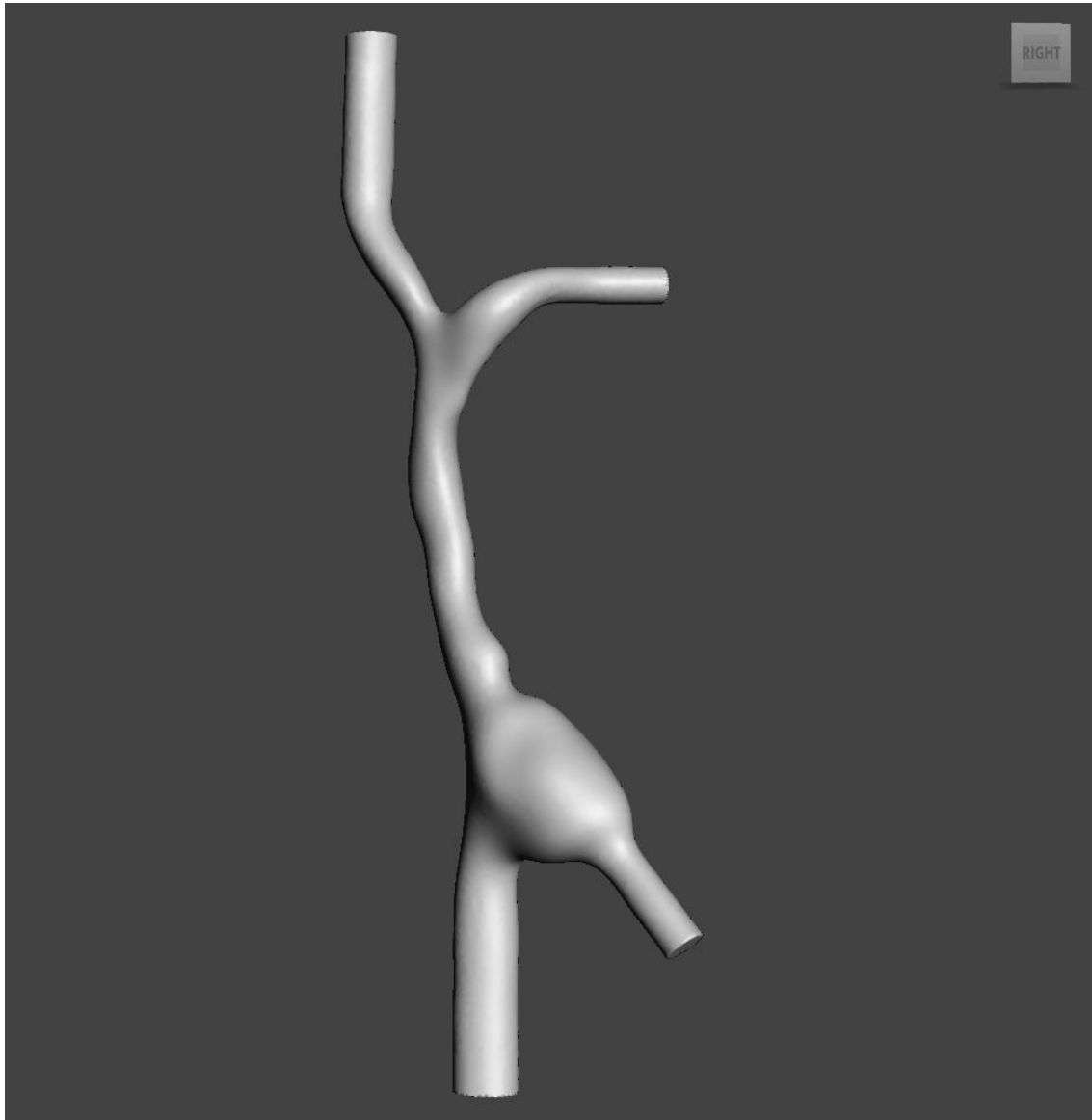


Figure 3.8_Final surface after Autodesk Meshmixer smoothing

3.2 CATHETERS 3D MODEL

3.2.1 CVC acquisition

The tips of a Palindrome and a Tesio CVC were extracted from two different patients by the Hospital's nephrologist. In both cases the failure consisted in the formation of fibrin sheath inside the CVC. After these delicate removal operations, both catheters were carefully washed, cleaned and made as sterile as possible with hot water and bleach solution to eliminate all blood and organic residuals.

Once samples were completely cleaned, we scanned them using micro-CT; this instrument is located in the "Laboratory of Renal Biophysics" of the "Mario Negri Institute".

The first catheter studied was Palindrome, the acquisition scan took up two hours (2h:11') and resulting in 4328 image files, each one containing the picture of every section; each section was taken at 8.95 μm of distance from the previous one. The total length of scanned catheter underwent was 38.74 mm.

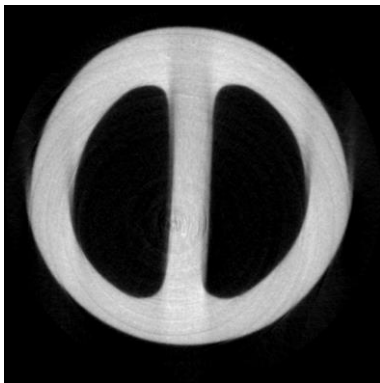


Figure 3.9_Basis of Palindrome (117 of 4328)

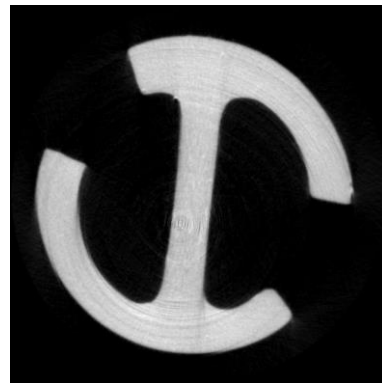


Figure 3.10_Palindrome side holes (2021 of 4328)

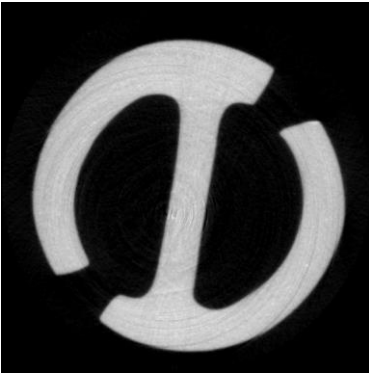


Figure 3.11_Palindrome initial part of the tip
(3385 of 4328)

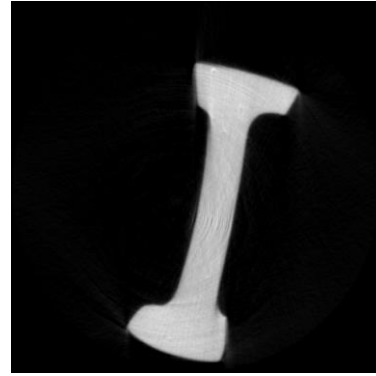


Figure 3.12_Palindrome final part of the tip
(4219 of 4328)

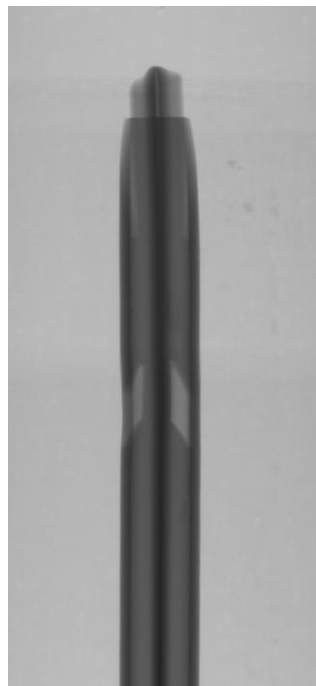


Figure 3.13_Total Palindrome scanned

The same method was performed for the Tesio catheter. This catheter is composed of two distinct single-lumen ducts, but we scanned them together keeping the distinction between the venous one and the arterial one. This scan took up two hours (2h:08') and provided us 5420 files for each duct. Every single file included the picture of every single section and each section was taken every 8.95 μm of distance from the previous one, for a total length of scanned catheter of 48.53 mm, a little bit more than the Palindrome. This is due to the presence of 6 side holes which make the Tesio tip longer.

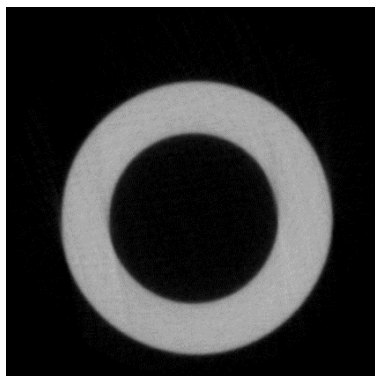


Figure 3.14_Basis of Tesio Blu
(0327 of 5420)

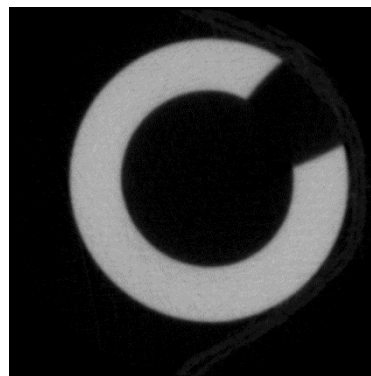


Figure 3.15_Side hole of Tesio Blu
(2486 of 5420)

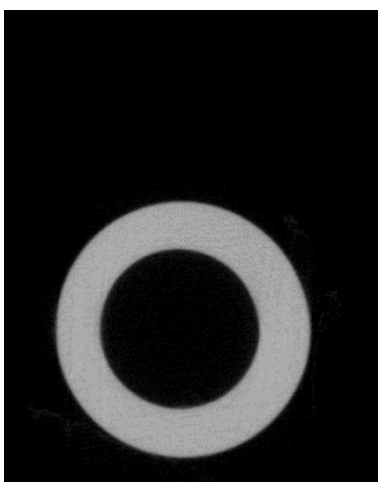


Figure 3.16_Basis of Tesio Rosso
(0327 of 5420)

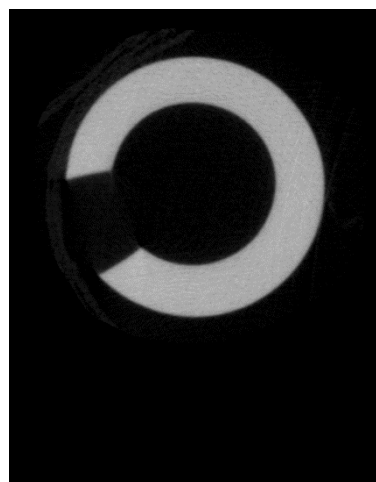


Figure 3.17_Side hole of Tesio Rosso
(2486 of 5420)

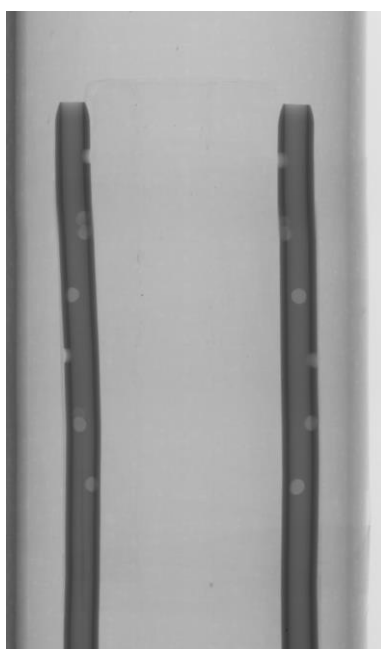


Figure 3.18_Total Tesio rosso and Tesio Blu scanned

3.2.2 CVC modelling with VMTK

Thanks to the images acquired by Micro-CT, we were able to create 3D of the real CVC tips. The proceeding for the creation of 3D models was the same both for Palindrome and for Tesio, from the slice images to the final models using the VMTK software. In this case, images were saved as DICOM files (".dcm"). The procedure we performed was the following:

- 1) A VOI was selected to reduce the image data to only the region containing the tip catheter and a little segment of the catheter's duct. This VOI isolation helped us to reduce computational and time costs (command used: "*vmtkimagevoiselector*");
- 2) The CVC surface was segmented using an algorithm in which we inserted specified values that identified catheter's surface. In this case we used the Threshold method because the catheter was characterized by the same value of grey (command used: "*vmtklevelsetsegmentation*");
- 3) A marching cubes algorithm was applied to construct a surface model (command used: "*vmtkmarchingcubes*");
- 4) Finally, this file was converted from the VTP extension to the stereolithographic (STL) file format which is fundamental for the next step of our work (command used: "*vmtksurfacewriter*").

The firsts scan images we treated were those of Palindrome catheter. Once selected the first image of the raw, VMTK showed all the pictures stacked in the correct order, showing only one figure for each plane (X, Y, Z).

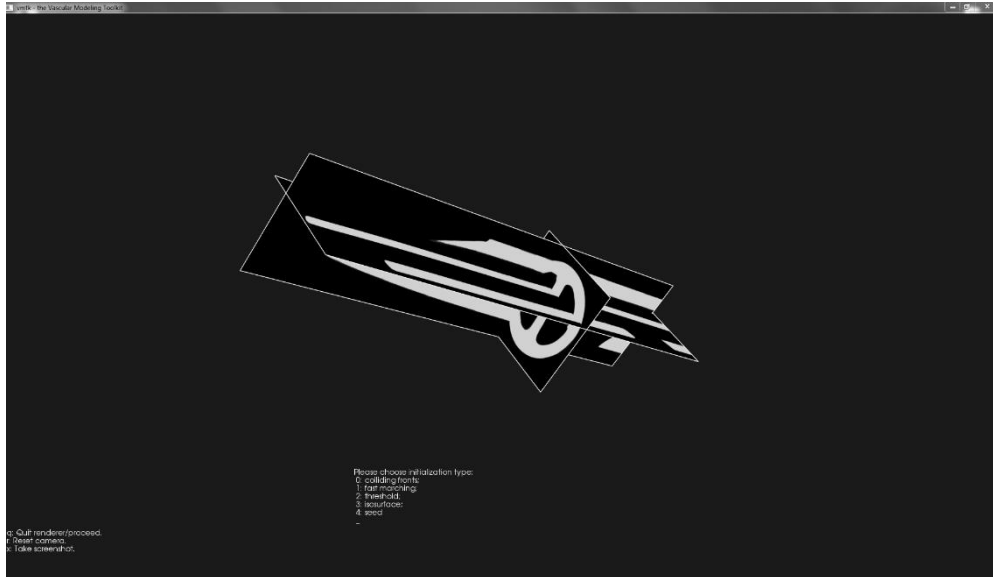


Figure 3.19_Palindrome view in X, Y, Z planes with VMTK

The selection of a VOI that excluded unnecessary part was fundamental in this case because taking all the catheters acquired made VMTK crash due to the elevated dimension of files studied. Once the correct VOI was selected, the identification of values associated to catheters' surface was immediate because the background, which was black, was in contrast with the CVC, totally white. Due to the high number of images, this procedure had an elevated time cost, but resolution and accuracy of all details made the obtained 3D model the perfect copy of the real catheter. Moreover, the conversion to

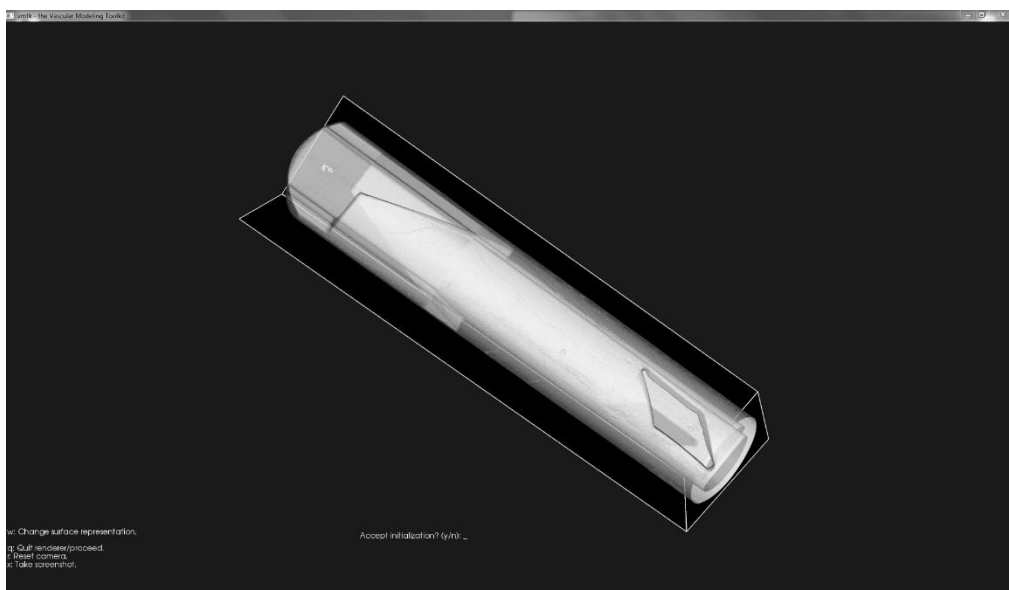


Figure 3.20_Palindrome reconstruction with VMTK

stereolithographic file format allowed us to observe the 3D model with other programs without changing or reducing the quality of the acquired model (Figure 3.20).

The procedure of 3D reconstruction was the same performed for Palindrome CVC, with the same steps carried out in the same order. We treated first the slice images of the first duct called “Tesio Blu” and we obtained the 3D model showed in Figure 3.21.



Figure 3.21_ Tesio Blu reconstruction with VMTK

The acquisition and reconstruction of the second duct (“Tesio Rosso”) was performed in the same way of the previous ones. Once selected the appropriate VOI and the correct values for the level set segmentation, the model presented a curve which entailed a warp of the catheter’s tip, as shown in the Figure 3.22.

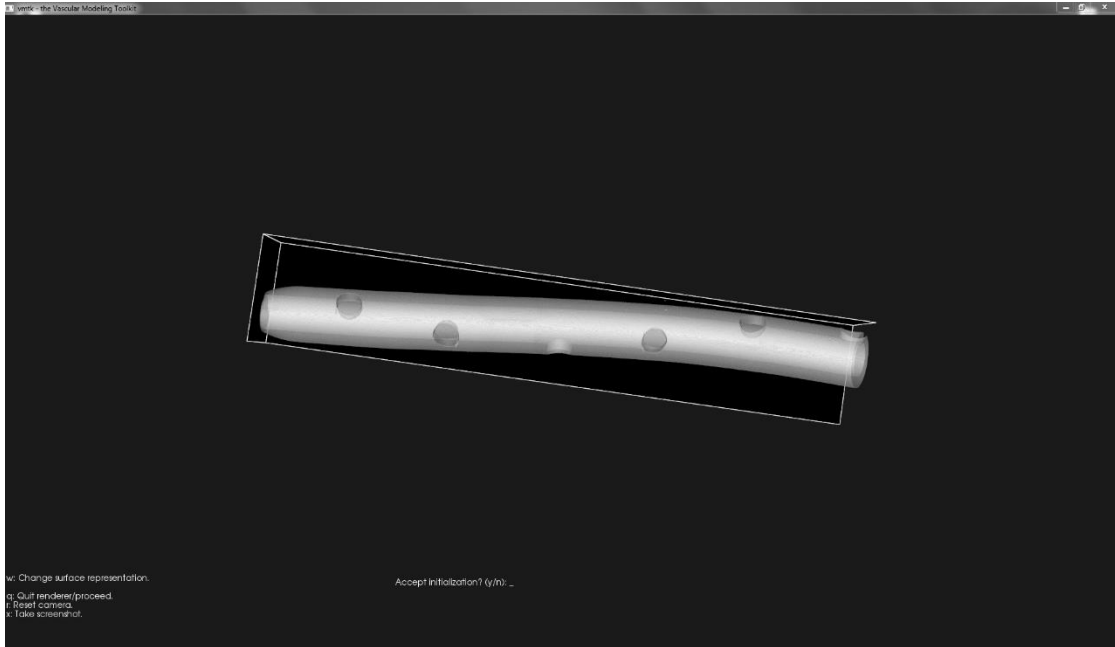


Figure 3.22_Tesio Rosso reconstruction with VMTK

This defect, probably caused by a malposition of the sample during the scansion with Micro-CT, made the 3D model unusable for the creation of a good geometry so we decided to discard it. However, since Tesio Rosso and Tesio Blu has identical tips, we decided to use the 3D reconstruction of Tesio Blu for both catheters.

Once obtained these structures, we need to change the extensions from `.vtp` to `.stl` with the command `vmtnsurfacewriter`. With this file we can work on Autodesk Meshmixer to make the last changes to our models.

3.2.3 Autodesk Meshmixer modifications and final models

The `.stl` file format of each catheter was processed in Autodesk Meshmixer; the last modifications applied on these models were basically the same that we had done for the veins model (Chapter 3.1.7), excluding the last part with the “Plane cut” tool.

First, we used the “Sculpt” tool to perform a manual smoothing, in particular to remove the artifacts included by the high-precision Micro-CT scan: these defects probably were due to a non-perfect cleaning before the scan. This step was important in order to have a perfect surface that replicate real catheter’s tip. These defects were present in particular on the Palindrome catheter surface.

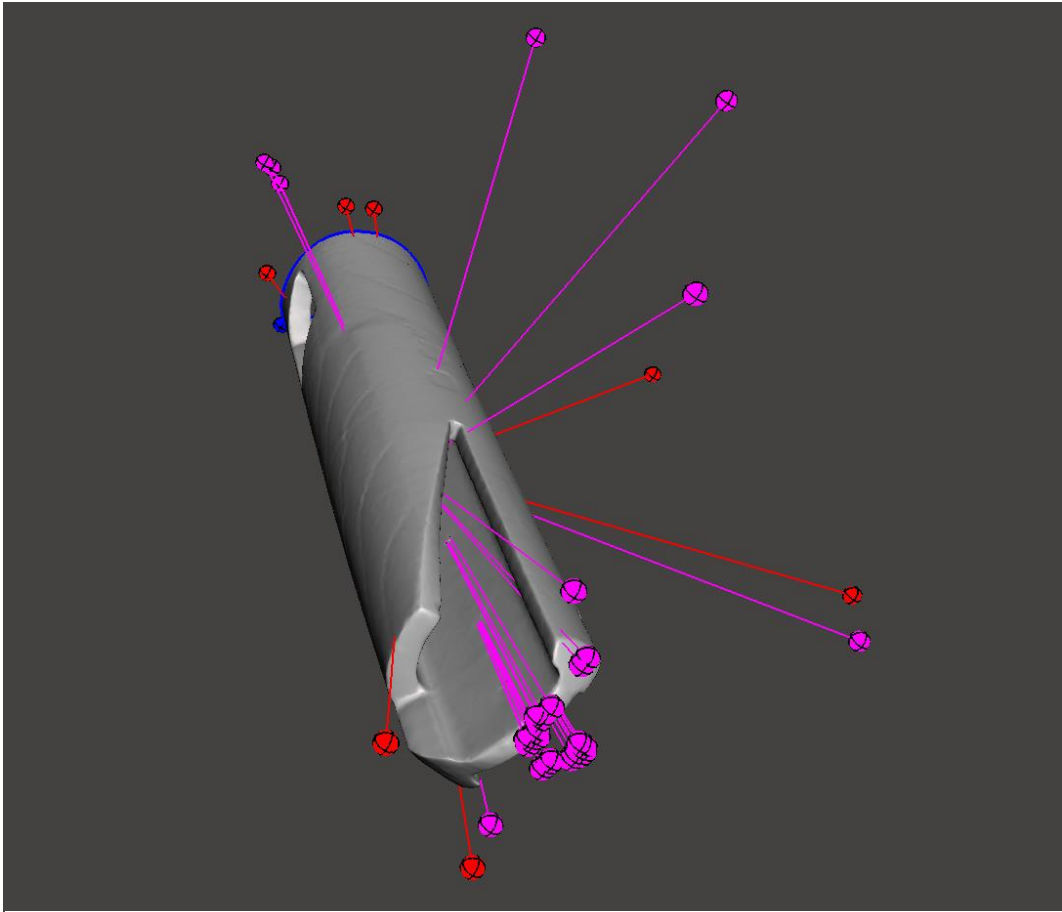


Figure 3.23_Palindrome defects viewed in Autodesk Meshmixer

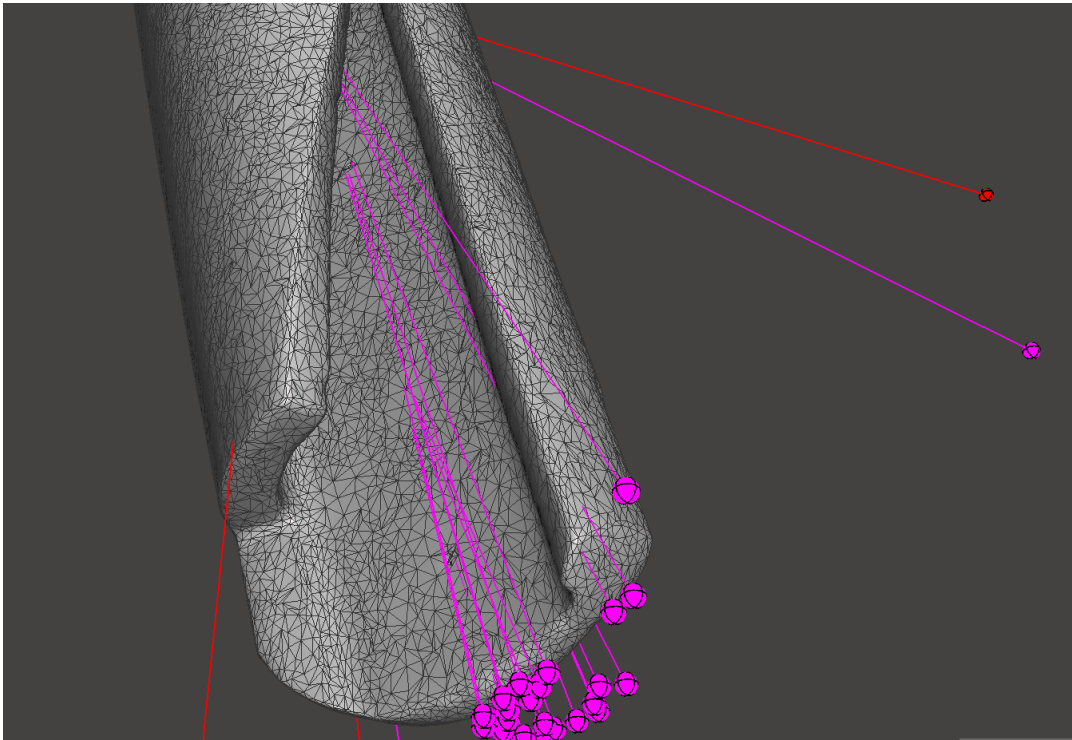


Figure 3.24_Palindrome particular view of defects in Autodesk Meshmixer

Subsequently, we selected the whole area to perform a total remeshing. We selected again the “Relative density” mode, maintaining the same number of edges but with a uniform distribution and a more regularity in the disposition of triangles. We noticed that varying the density percentage or the mode used for remeshing, there were deformations that changed the shape of catheter’s tip.

Concerning the Palindrome catheter tip, the final model that we obtained is made of 11.946 uniformly distributed polygons (Figure 3.25).

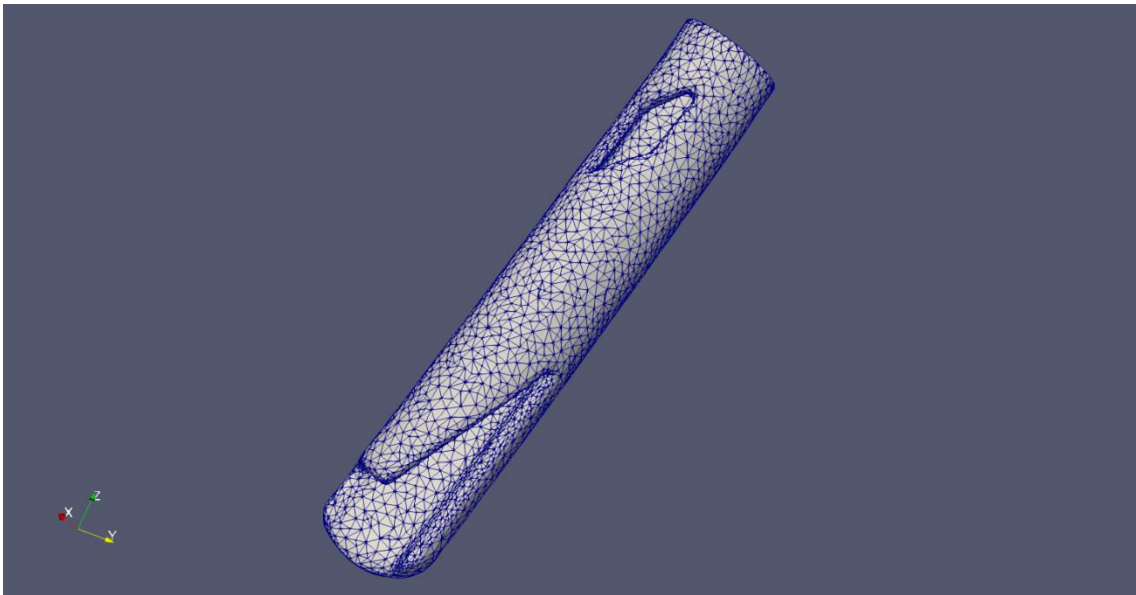


Figure 3.25_Palindrome tip: final model

Concerning the Tesio catheter, the final model that we obtained is made of 28.987 uniformly distributed polygons (Figure 1.25).

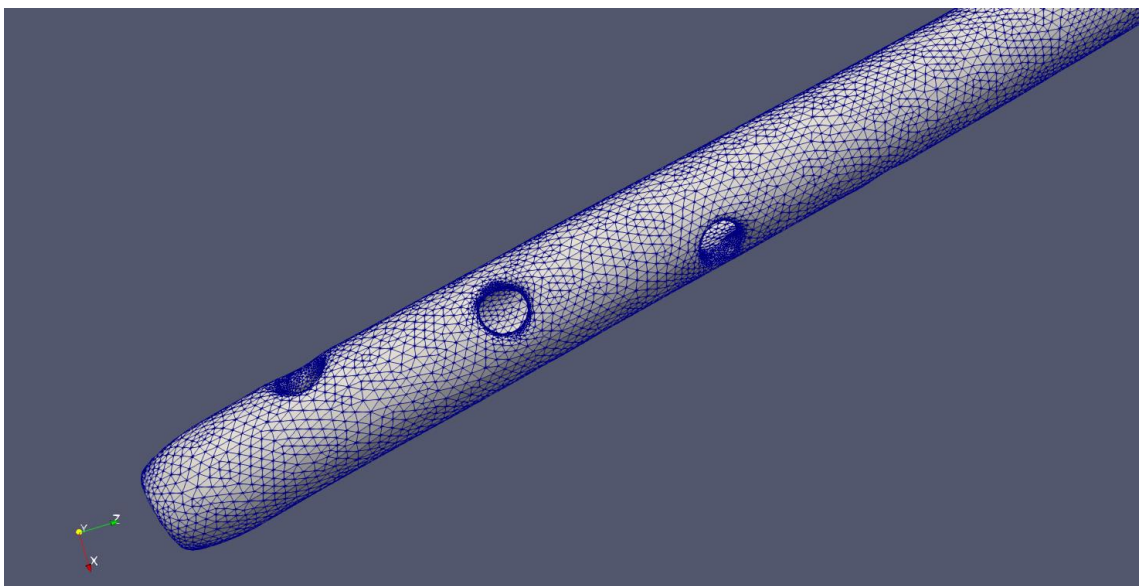


Figure 3.26_Tesio tip: final model

3.3 CREATION OF COMPLETE CVC MODELS

3.3.1. Extrusion with Solidworks

Once obtained the final model of the Palindrome and Tesio tip and the one of the external structure, the next step was to insert the catheter's tip in the right position inside the right atrium. In order to perform this task, we decided to use the Solidworks2018 software (SOLIDWORKS Corp, Waltham, Massachusetts, USA): it is a computer-aided design (CAD) software based on parametric computation which allows to create 3D forms from basic geometric shapes but also to modify 3D models previously generated.

The sequence of steps to follow is the same for both Palindrome and Tesio.

First, we imported in Solidworks the 3D model of right atrium and the veins, setting it as the fixed geometry. Second, we imported the model of catheter's tip; this was the mobile model at the beginning because we had to place it in the correct position; once obtained this task, we fixed this part in order to proceed with the next steps.

The next step was important to design the final models: the extrusion of the end part of catheter's tip along the SVC and the IJV and the consequent exit out of this vein. The extrusion was made with the catheter positioned in the centre of the vessels to avoid the adhesion between the catheter and the internal surface of vessels. For the Tesio catheter, this condition was harder to respect because of two separate tube; furthermore, this main characteristic of Tesio implied another condition: avoiding the contact between the two different ducts.

The extrusion was performed by the following steps:

- Extraction of the shape involved in the extrusion identified by the insertion of a plane in the end part of catheter's tip;
- Construction of a spline starting perpendicular from the plane before created; this spline is a curve used to avoid the creation of sharp pointed making the model as realistic as possible. This spline requires the direction of the catheters along the SVC and the right internal jugular vein in order to respect the conditions described above;

- Using the Solidworks tool “Sweep” we imposed that the extrusion of the shape identified in the previous step must follow the course of the spline.

For the Palindrome catheter, the extrusion made by Solidworks took about 4 hours of computer-work. The Figure 3.27 shows a step of the extrusion process.

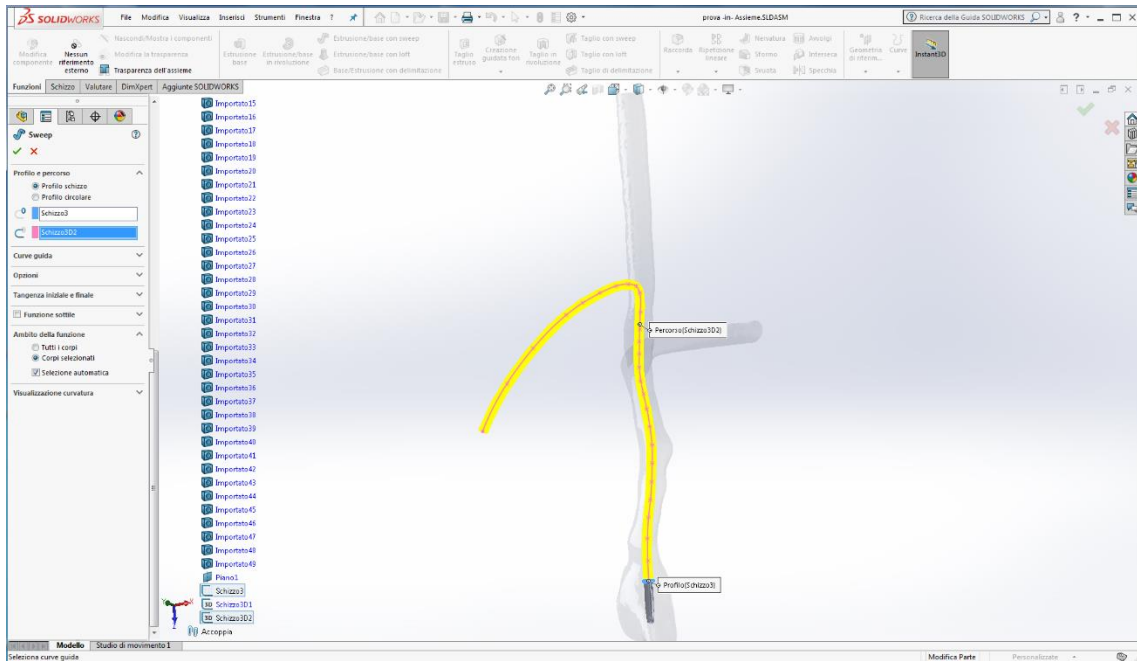


Figure 3.27_Palindrome extrusion with Solidworks

Concerning to the Tesio catheter, the extrusion took about 8 hours, about twice as much as for the Palindrome; this was due to the fact that the Tesio catheter is composed by two distinct tube and the extrusion was performed for one tube at time. The Figure 3.28 and 3.29 show that the catheter outside the vessels follows a path that depart itself from the veins: this shape tries to emulate the one assumed in the reality, where the catheter’s tube, once out of the right internal jugular vein, passes over the clavicle and goes just under the skin up to the exit point.

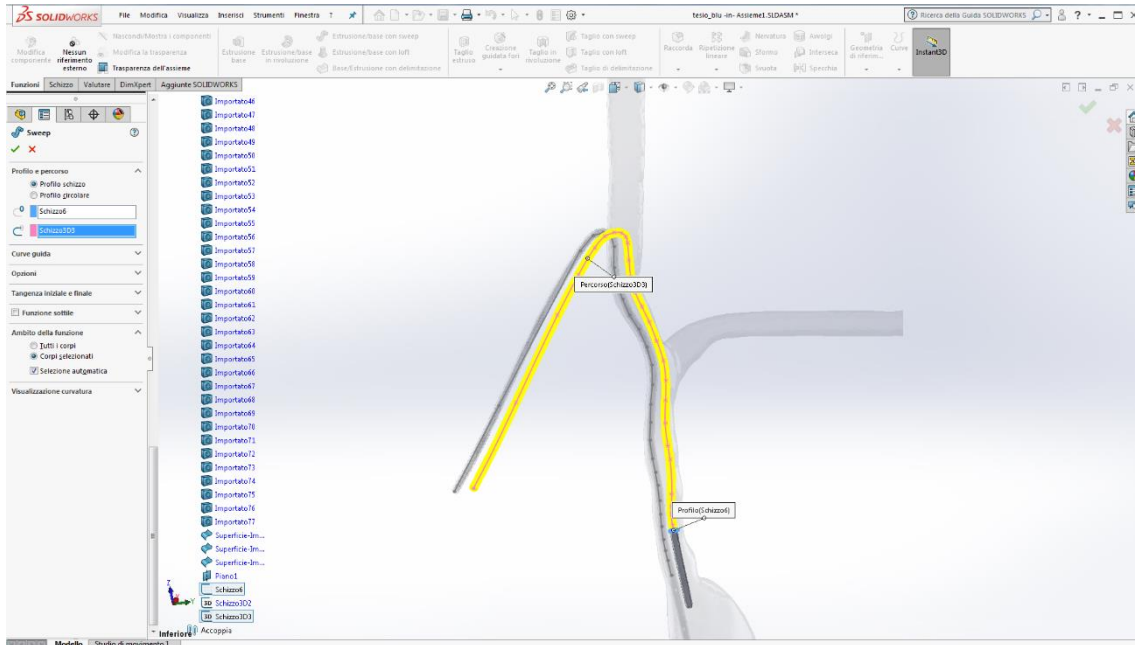


Figure 3.28_ Tesio extrusion with Solidworks

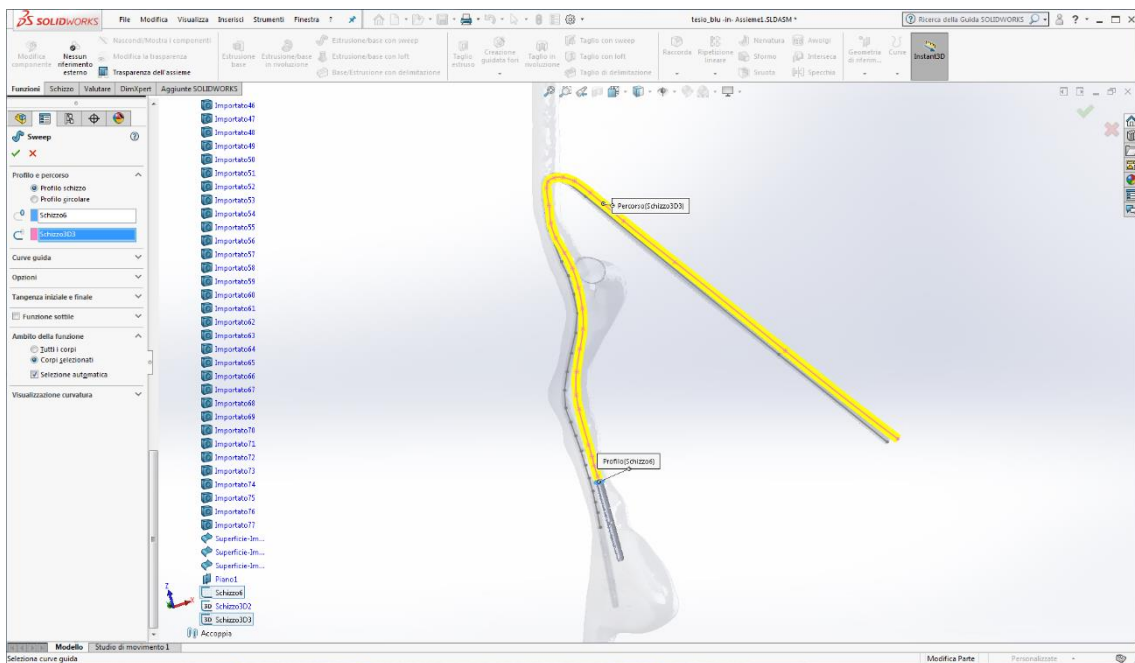


Figure 3.29_ Tesio extrusion with Solidworks

3.3.2 Autodesk Meshmixer refinement to obtain the final models

The file obtained with Solidworks was then modified with the Autodesk Meshmixer software in order to obtain the definitive 3D model. First, we used the same procedure described in paragraph 3.2.3. to readapt the surface triangle edges distribution on the extruded part of the catheter just created. In this way we obtained a uniform distribution

in all catheter's surfaces: the edges of the triangles assumed roughly the same dimension. The second step involved the leaving site placed in the IJV. With Autodesk Meshmixer we eliminated the part of the vein wall placed at the level of the catheter's inner lumen; in this way we created a hole and we cleared the path inside the catheter. For this activity, we selected the surface triangles that we wanted to delete and the "Discard" tool allows to delete the selected part.

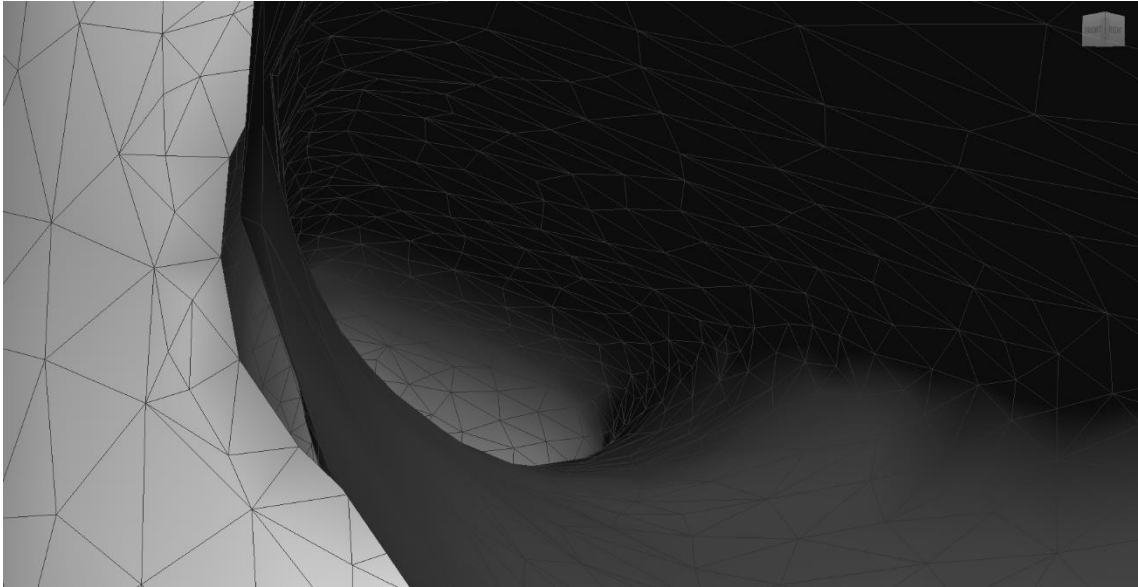


Figure 3.30_Palindrome: creation of the internal hole

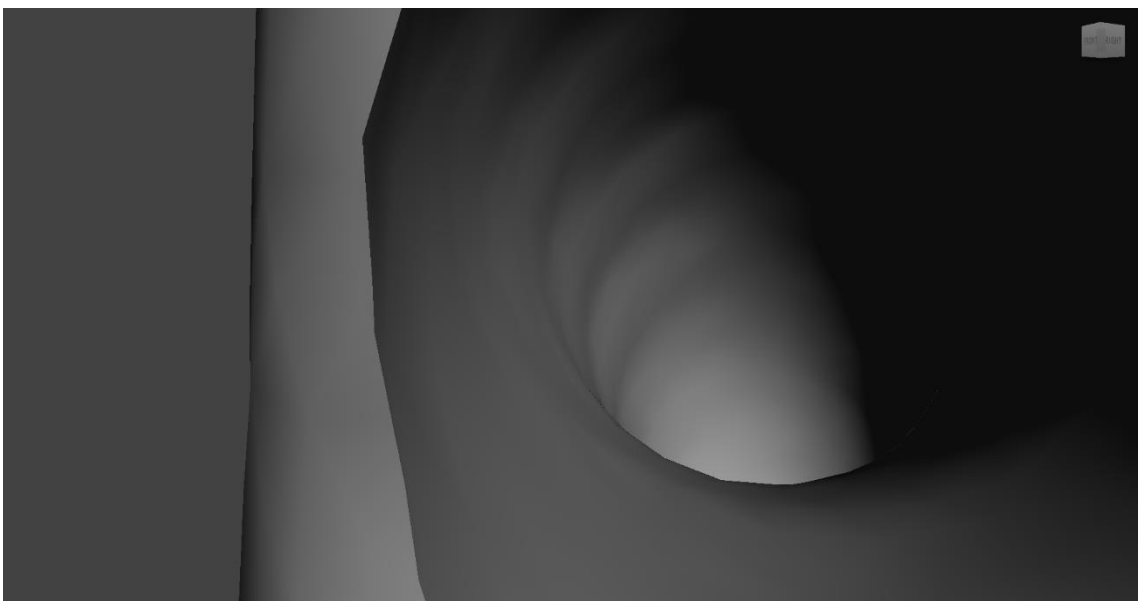


Figure 3.31_Palindrome inner lumen hole

Furthermore, we removed the external surface of the CVC from the exit side to the end of the tube, in order to decrease the final mesh file size. Finally, we joined the right internal jugular vein wall with the external surface of the catheter in order to avoid surface holes in the whole structure. To perform this step, we selected the parts involved and we used the Autodesk Meshmixer tool “Weld Boundaries” so that the two surfaces joined each other.

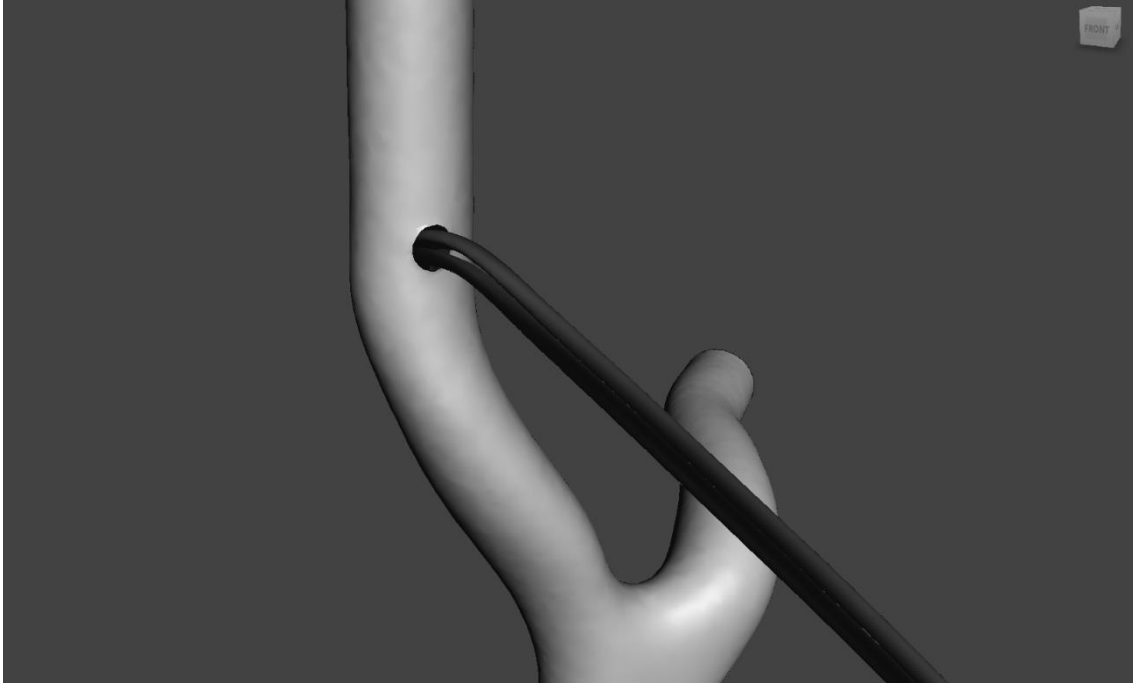


Figure 3.32_Palindrome weld boundaries

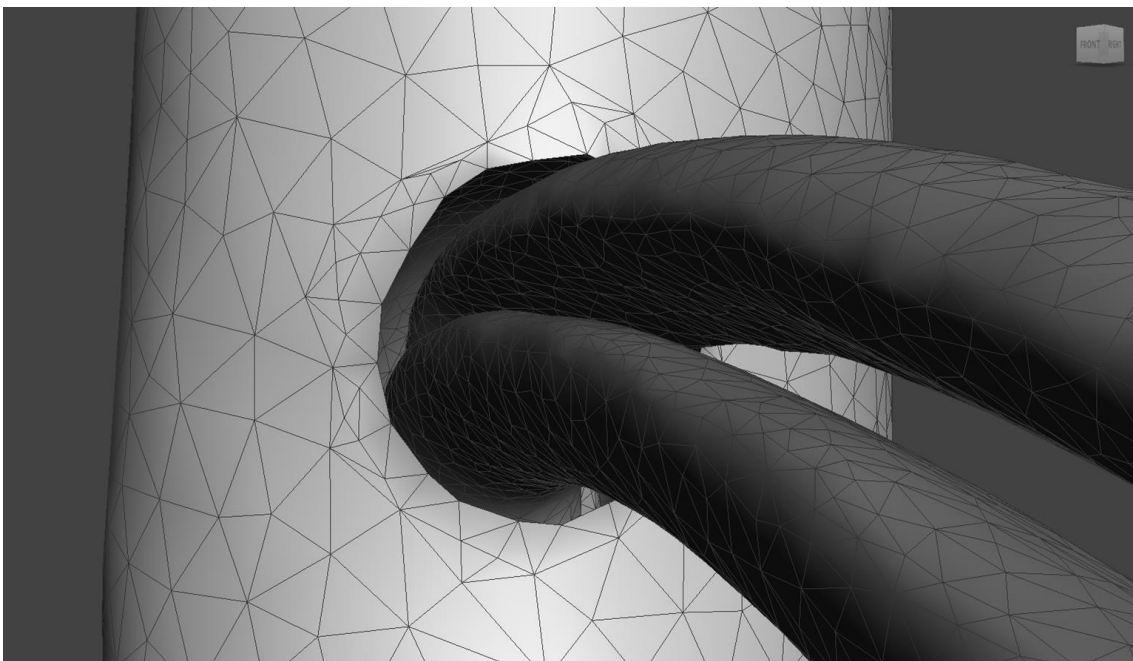


Figure 3.33_Palindrome: removal of the external catheter surface

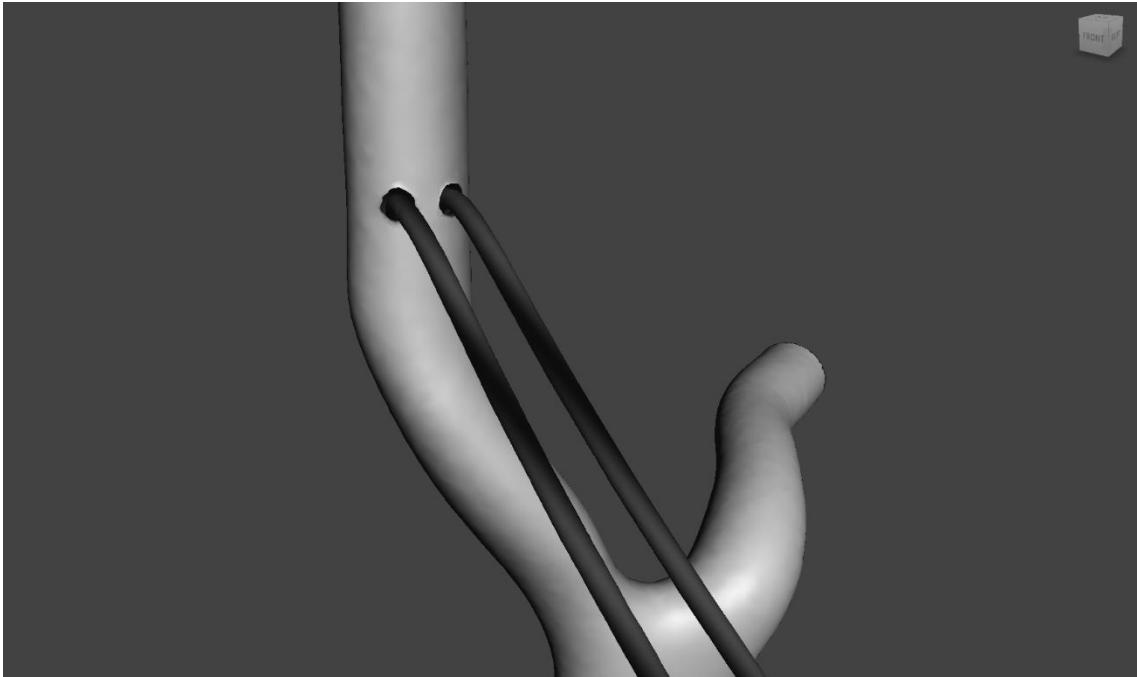


Figure 3.34_Tesio weld boudaries

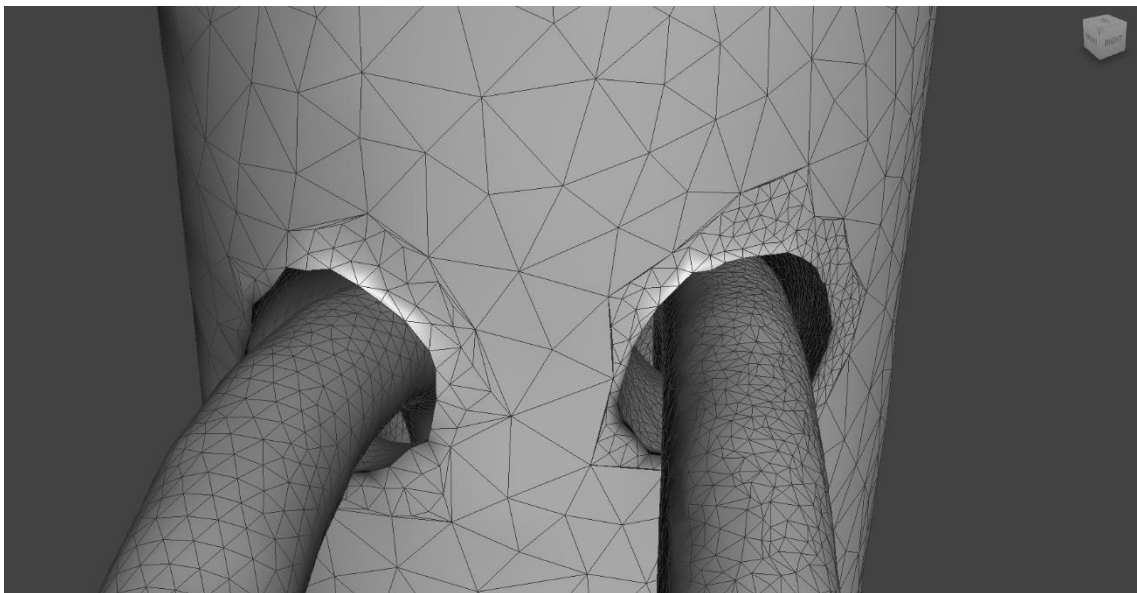


Figure 3.35_Tesio: removal of the external catheter surface

At the end of these steps, we obtained the final 3D model for both the catheters; the Palindrome one is composed of 133.538 triangles while the Tesio one of 333.886 triangles. Figure 3.36 and 3.37 show two views of the final model of the Palindrome catheter (the catheter in yellow). Figure 3.38 and 3.39 show two views of the final model of Tesio; the venous tube is blue, instead the arterial tube is red.

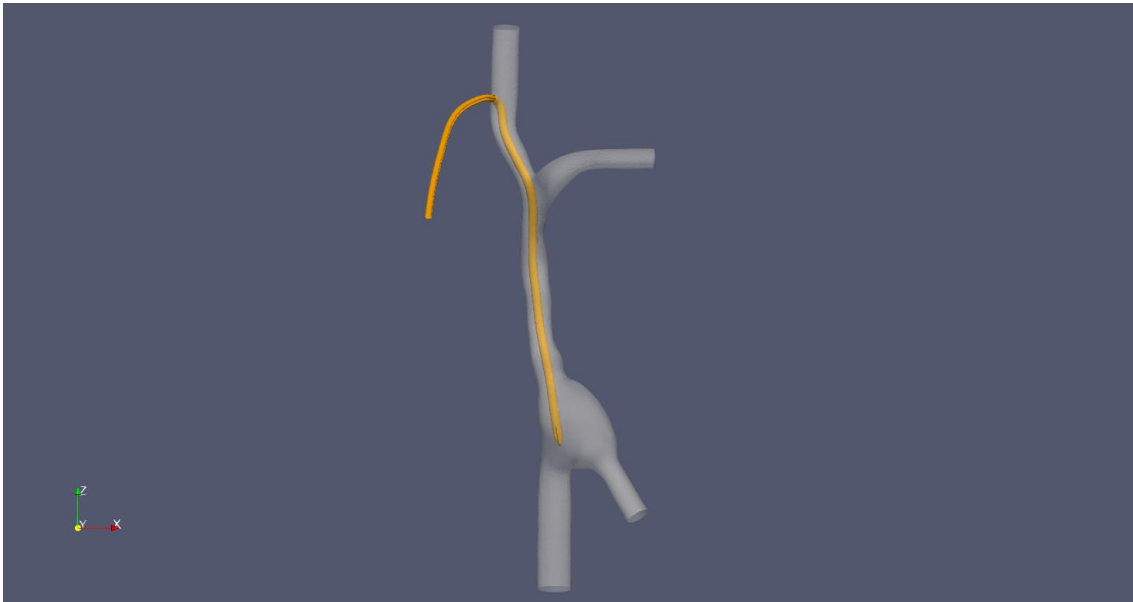


Figure 3.36_Palindrome final model

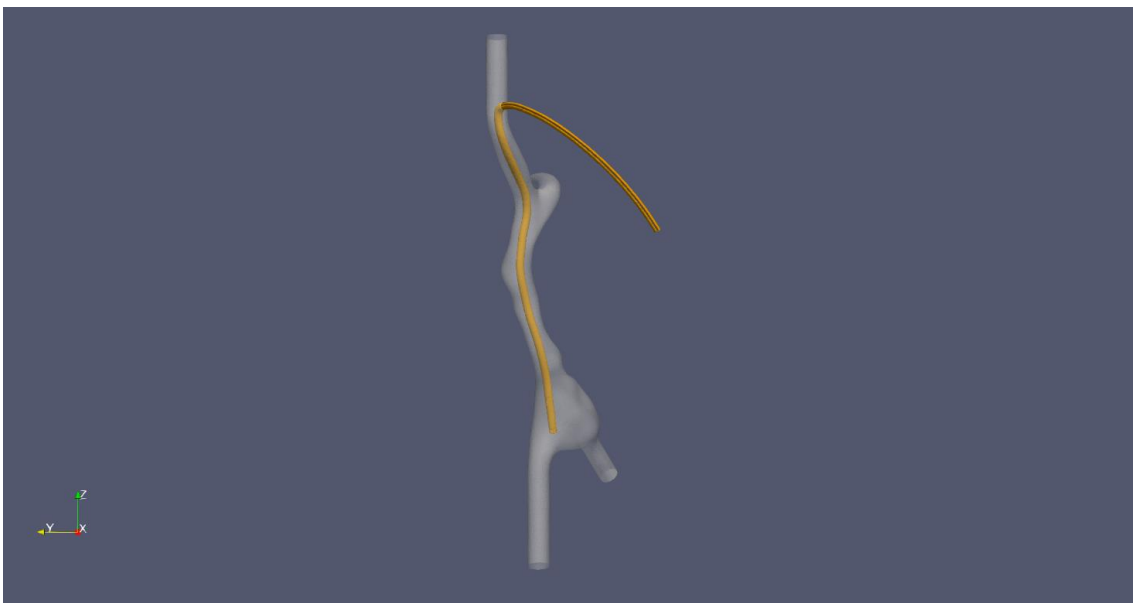


Figure 3.37_Palindrome final model

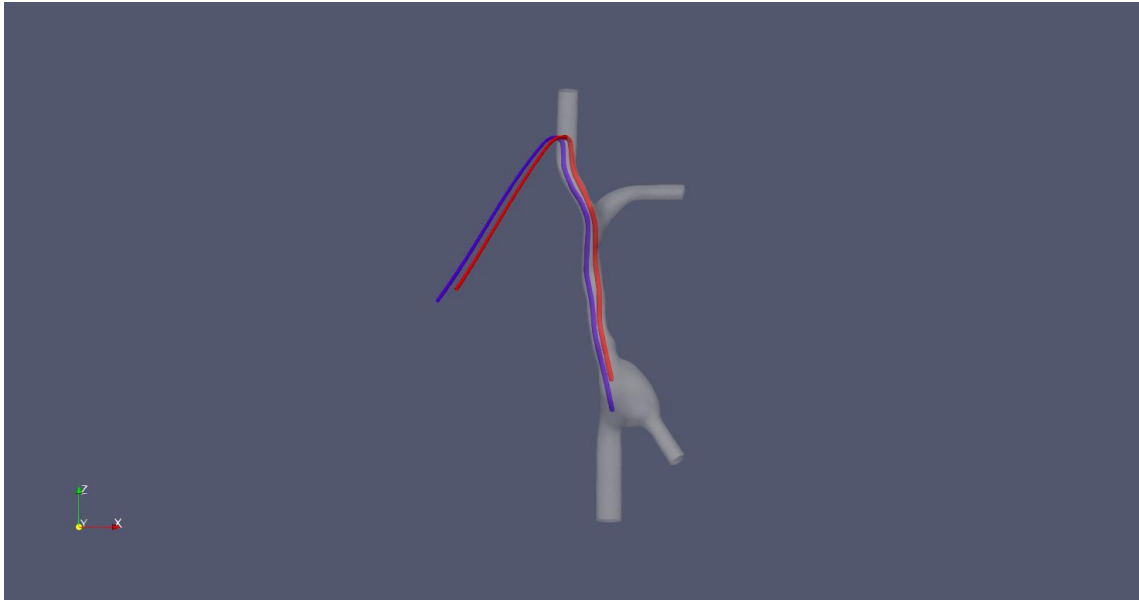


Figure 3.38_Tesio final model

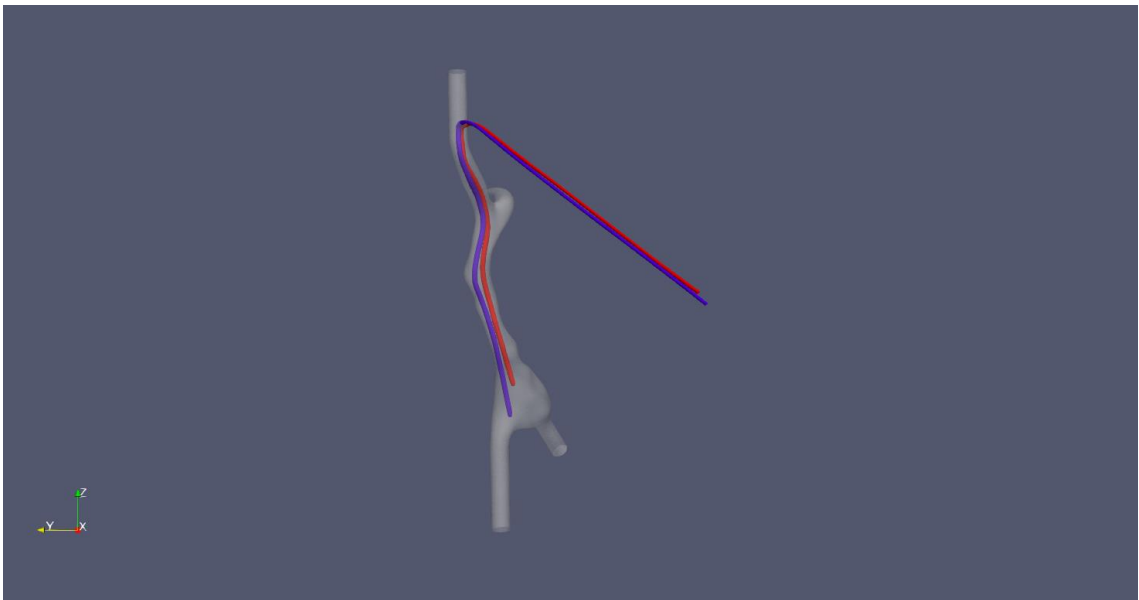


Figure 3.39_Tesio final model

3.4 VOLUME MESH CREATION

The creation of an accurate mesh is fundamental to perform a correct CFD simulation. The mesh is an integral part of the numerical strategy and must satisfy certain criteria to ensure a valid and accurate solution

3.4.1 Surface thresholding

The first step for generating the mesh consisted in separating the surfaces composing the whole geometry. We performed this task using the software Paraview (<http://www.paraview.org/>), an open source application for data analysis and visualisation. Once opened the .stl file of the 3D model, we applied four filters in the sequence below to individuate each single surface of our models:

1. Applied the filter “Extract surface”: it extracts a 2D boundary surface using neighbour relations to eliminate internal faces.
2. Applied the filter “Generate Surface Normals”: it produces surface. The parameter “Feature Angle” was imposed to 40 (the default value was 30/100): this value allows individuating the single surface involved.
3. Applied the filter “Connectivity”: this filter marks connected components with integer point attribute array. This filter assigns a region ID to connected components of the input data set. After the application of this filter, the number of surfaces individuated was displayed: if it was uncorrected, we had to return to the previous steps and applied the correct changes. In our models, the correct Palindrome number of surfaces are 8 and for Tesio there are 9.
4. Applied the filter “Threshold”: this filter extracts the portions of the input dataset whose scalars lie within the specified range. To extrapolate each surface, a values equal to RegionID must assigned to the minimum and the maximum.

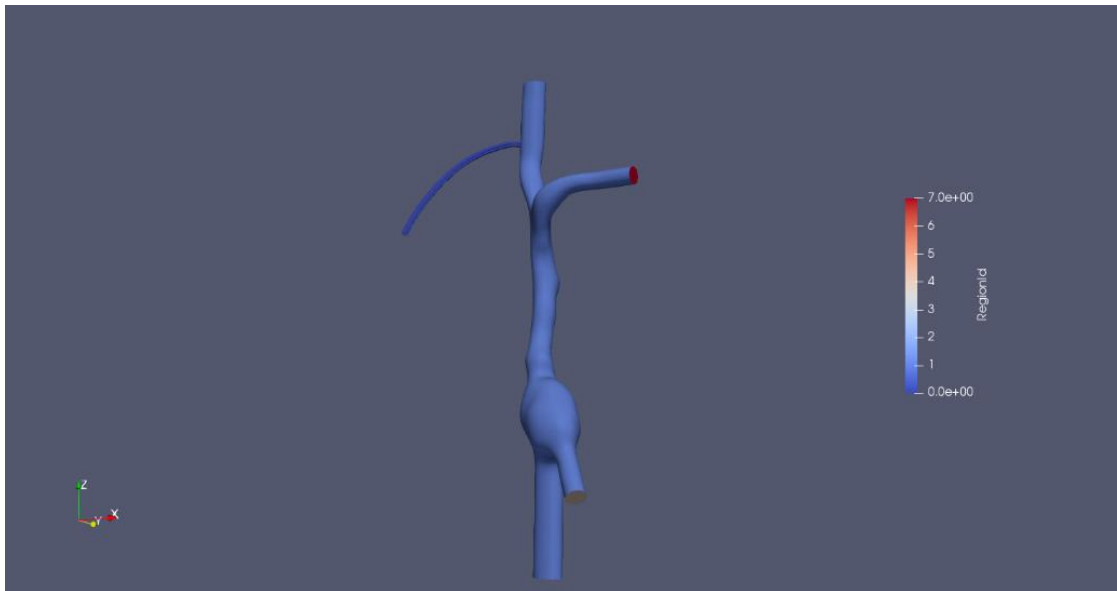


Figure 3.40_Palindrome threshold

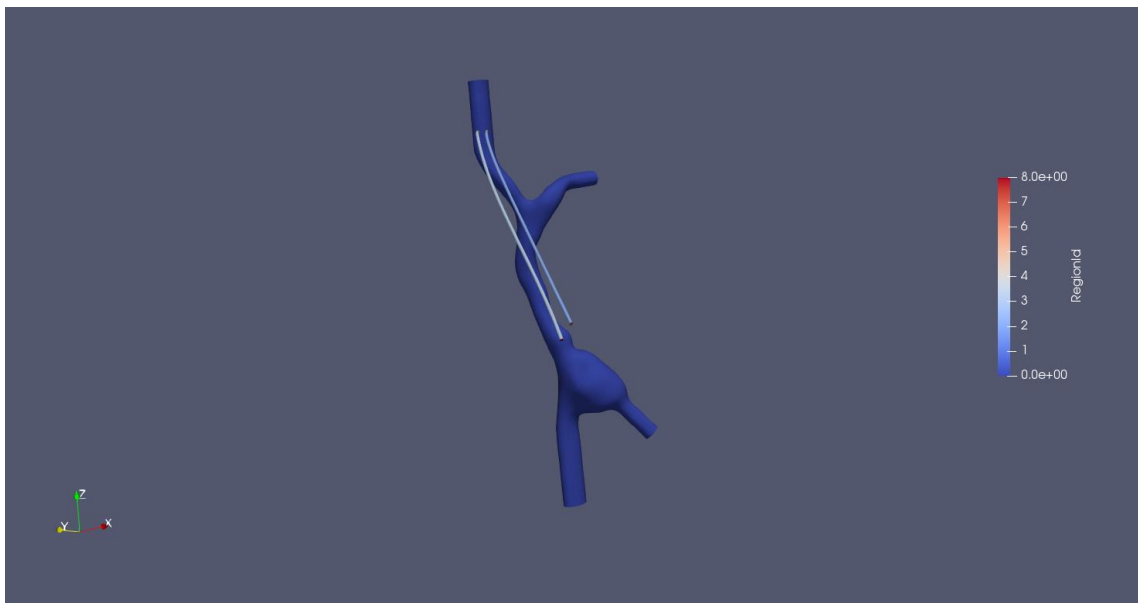


Figure 3.41_Tesio threshold

We then called with the same name the surfaces that identify the external structure, which were present in both 3D models:

- `ivc_in`: the surface for the inlet IVC;
- `ijv_dx_in`: the surface for the inlet right internal jugular vein;
- `av_sx_in`: the surface for the inlet left anonymous vein;
- `valve_out`: the surface for the outlet tricuspid valve;
- `wall_blood`: the surface which include wall vessels and the right atrium.

For each model, there was a different number of surfaces identified. Concerning to Palindrome 3D model, there were three regions to identify:

- `cvc_pal_in`: the surface of the inner light that contains the blood which flows from the dialysis machine to the patient (venous needle);
- `cvc_pal_out`: the surface of the inner light that contains the blood which flows from the patient to the dialysis machine (arterial needle);
- `cvc_pal_wall`: the surface of the catheter.

Concerning to the Tesio 3D model, there were four regions to identify:

- `tesio_blu_in`: the surface of the inner light of the tube in which the blood flows from the dialysis machine to the patient (venous needle);
- `tesio_blu_wall`: the surface of the tube with the function of venous needle;
- `tesio_rosso_out`: the surface of the inner light of the tube in which the blood flows from the patient to the dialysis machine (arterial needle);
- `tesio_rosso_wall`: the surface of the tube with the function of arterial needle.

To save each region, the filter “Extract Surface” must be applied after each threshold. In this way, we saved one by one every surface with its exact name, in the file format `.stl`, choosing the file format ASCII. Once obtained single surface files, these were assembled in a unique file (`.STL ASCII` format) by using the command `cat`.

3.4.2 Mesh generation

We used the *foamyHexMesh* mesh generator that is part of the OpenFOAM package (www.openfoam.org) to create the 3D mesh of our catheters. For both models the procedure was the same, also with the same value of certain parameters; the main difference between the generation of the two meshes was the name of the surfaces that composed the different catheters. This mesher generates polygonal, mainly hexahedra, cells inside a closed 3D triangular surface (`stl`), namely the surface models of our catheters.

Once obtained the mesh of both models, we opened the result files in Paraview in order to see more in detail the quality of the mesh.

Concerning the Palindrome, the mesh was composed of 1.644.212 cells, of which 587.860 were hexahedra.

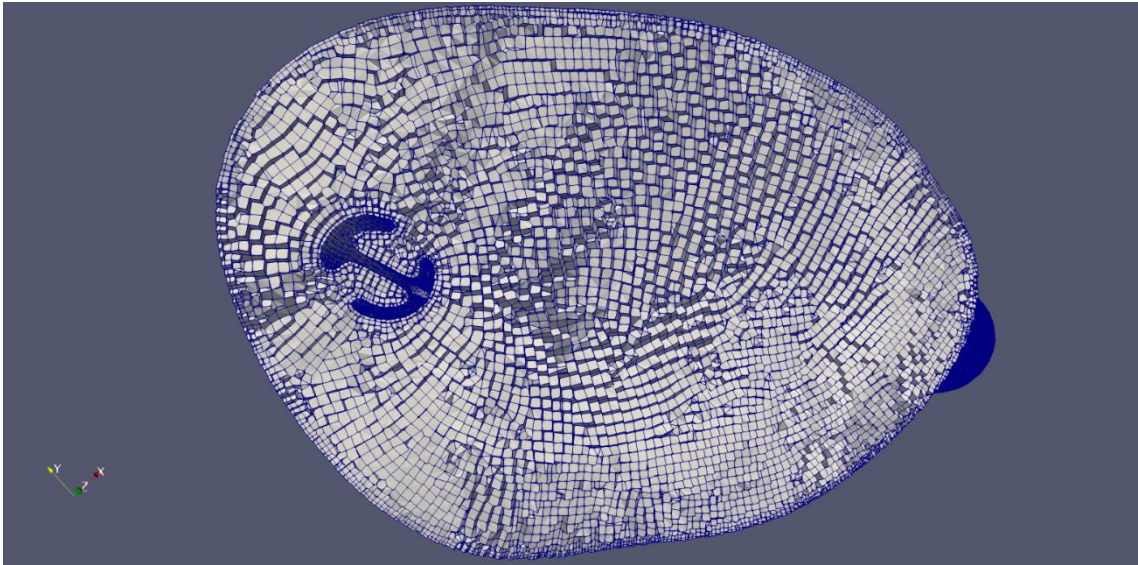


Figure 3.42_Palindrome volume mesh: slice of RA

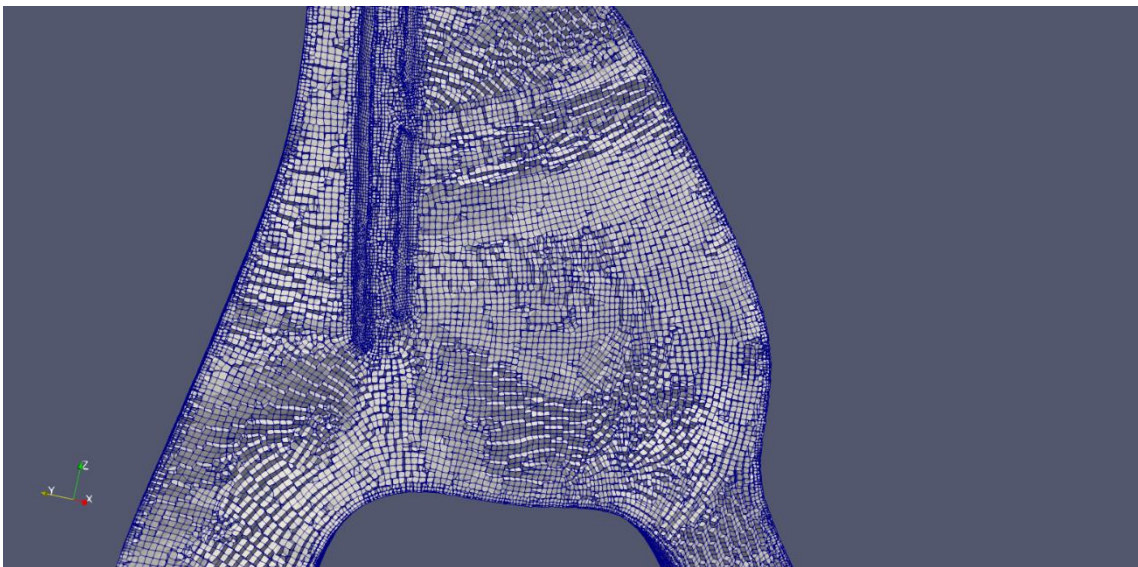


Figure 3.43_Palindrome volume mesh: vertical slice of RA

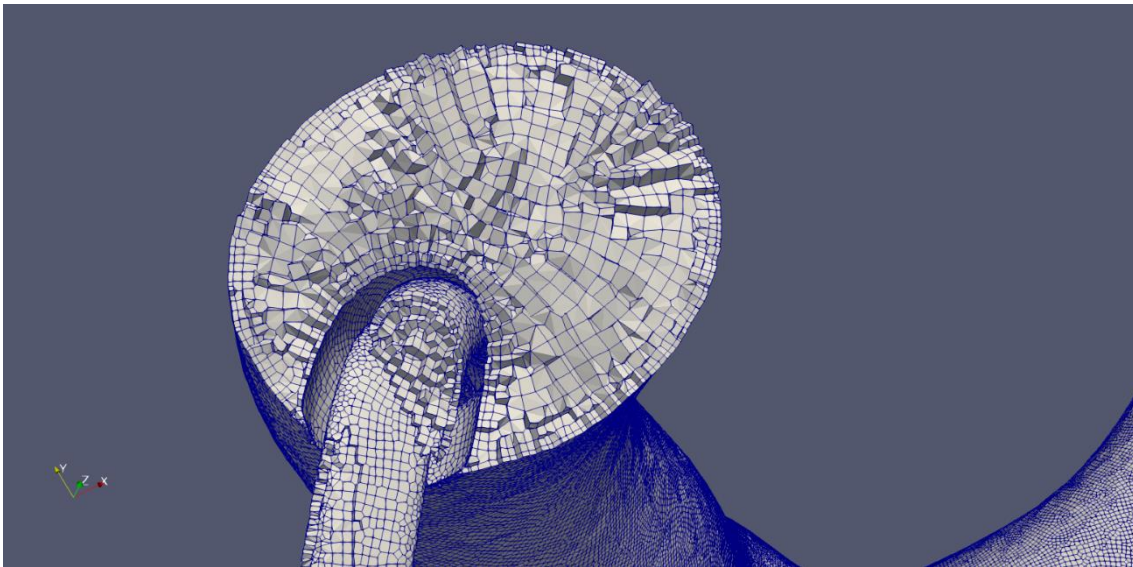


Figure 3.44_ Palindrome volume mesh: view at the exit site

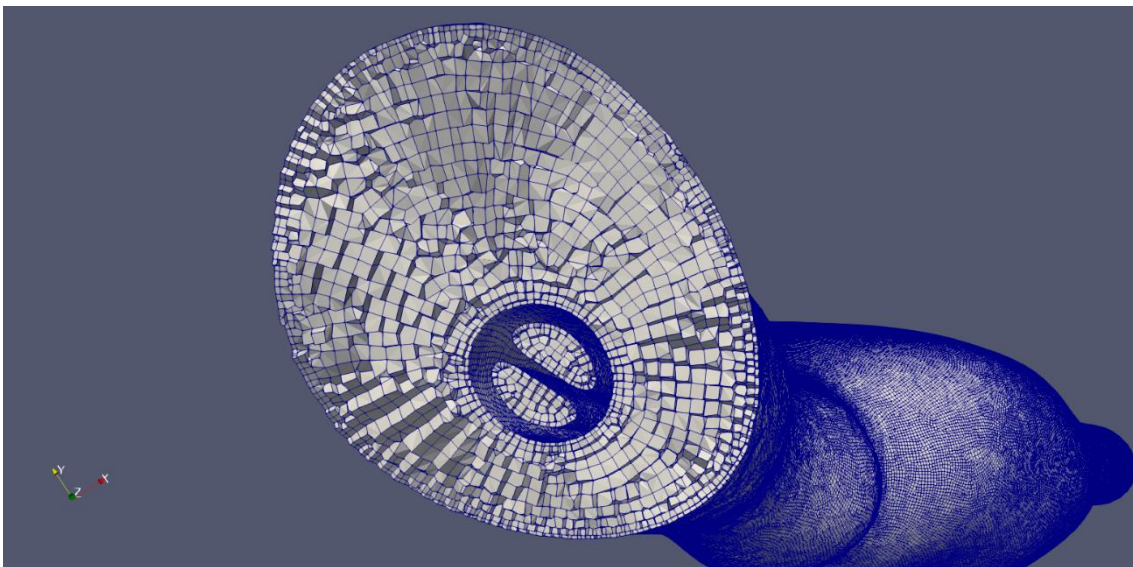


Figure 3.45_ Palindrome volume mesh: slice at the level of SVC

The figure 3.42, 3.43, 3.44 and 3.45 show more in detail the composition of the internal mesh: we can notice that, near the internal wall of vessels or near the surface of the catheter, cells assumed a smaller edge. The presence of smaller cells in these particular areas ensures a greater precision in the realization of the mesh.

The Tesio mesh is composed of 1.740.522 cells, of which 590.148 were hexahedra. We can notice that the two tubes of Tesio catheter did not touch themselves or the internal wall of the veins. Figure 3.46, 3.47, 3.48 and 3.49 show more in detail the composition of internal mesh.

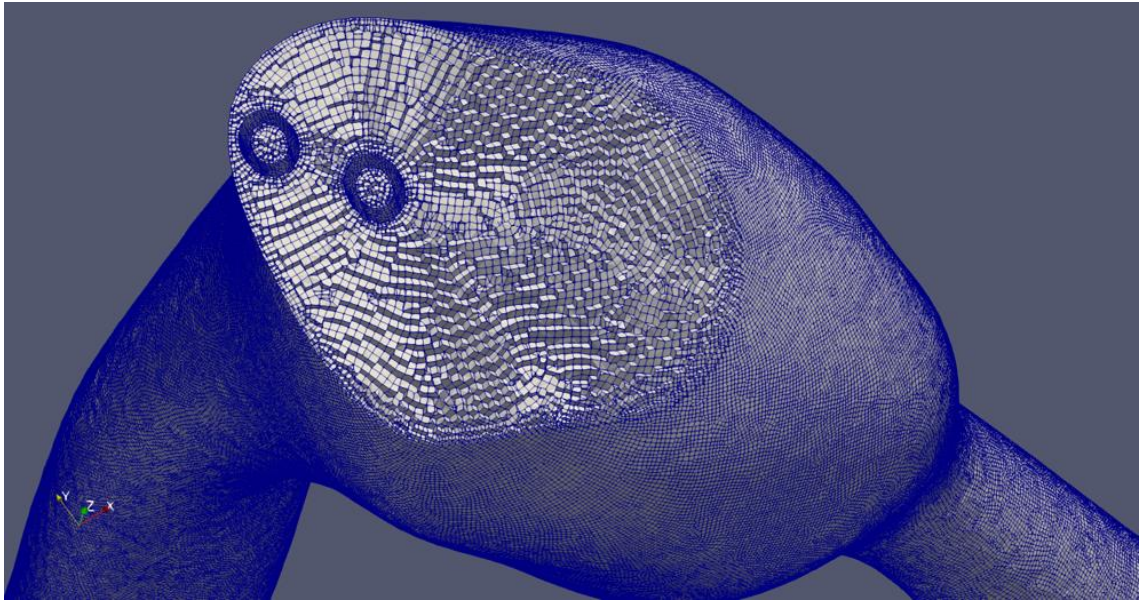


Figure 3.46_Tesio volume mesh: slice of RA

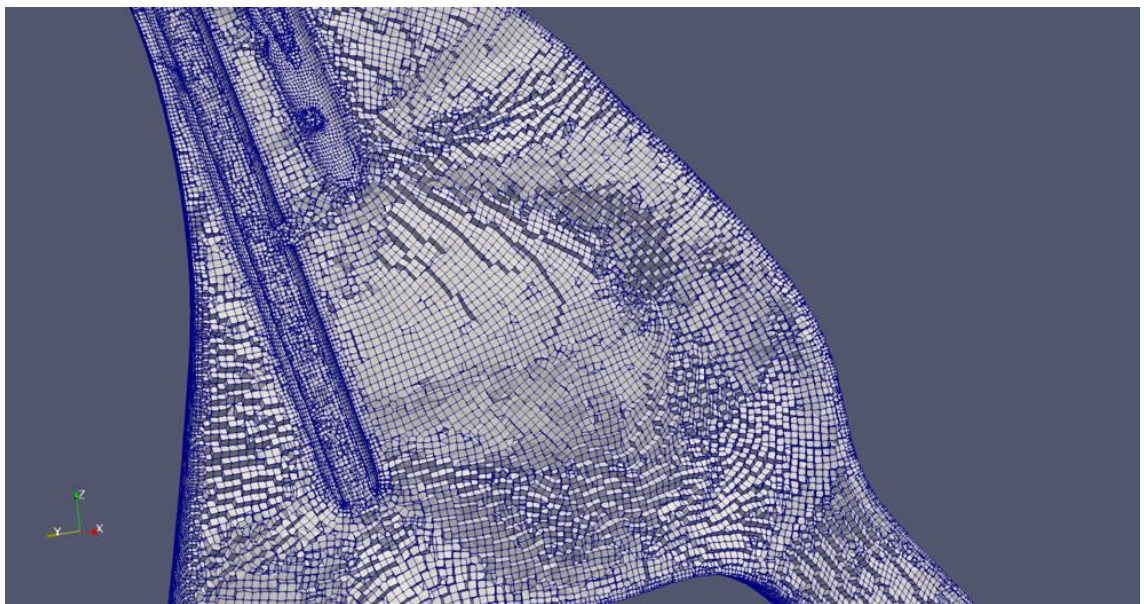


Figure 3.47_Tesio volume mesh: vertical slice of RA

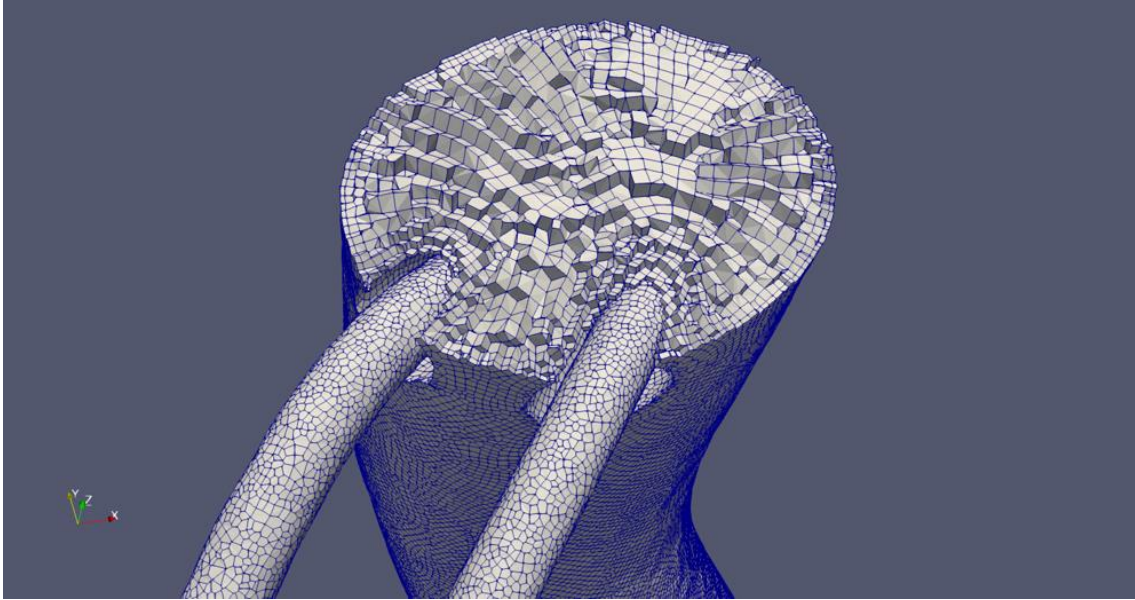


Figure 3.48_Tesio volume mesh: view at the exit site

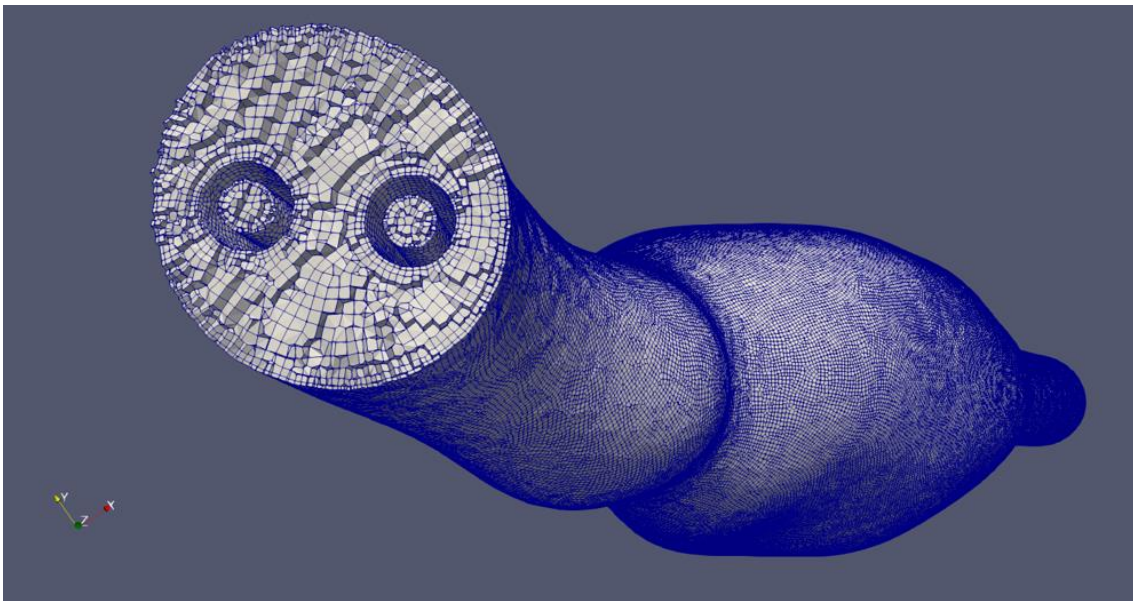


Figure 3.49_Tesio volume mesh: slice at the level of SVC

4. CFD simulations

The present chapter contains the CFD simulations. In the first part there is the description and the explanation of the boundary conditions chosen for every specific vein (IJV, left anonymous vein, IVC and tricuspid valve) and the ones chosen for the two lumens (venous and arterial) of both CVC. The second part of the chapter contains the description of the variables and parameters used for the CFD simulation.

4. CFD SIMULATION

4.1 BOUNDARY CONDITIONS

4.1.1 Search of appropriate boundary conditions

We searched in literature reference waveforms to be imposed as boundary conditions.

Regarding the IVC, we found an article that described in detail the anatomy of this vein and report the graph of blood flow velocity (Figure 4.1) [9].

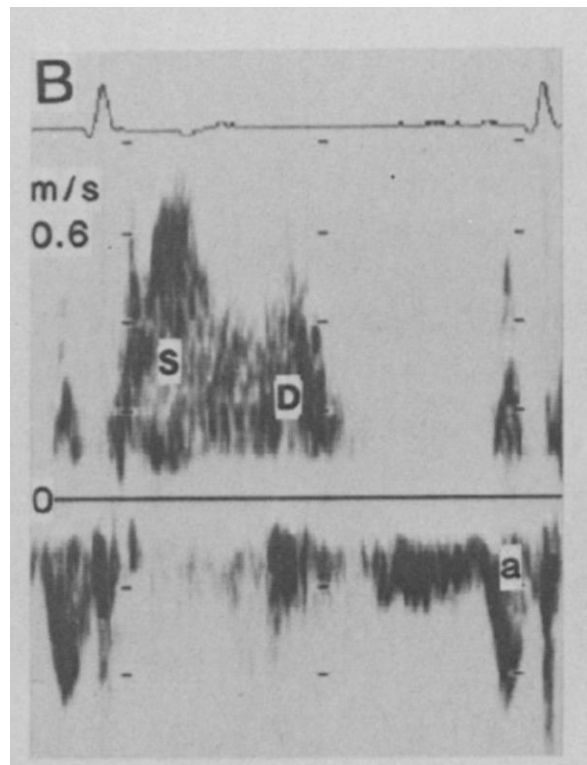


Figure 4.1_Graph of blood flow velocity in the IVC [9]

This graph represents the right ventricular inflow tract viewed with the pulsed-wave Doppler sample volume in the IVC above the diaphragm. We can notice that this measurement is taken synchronized with the electrocardiogram: these conditions allowed us to correlate each blood flow value with the cardiac activity. The flow graph is characterized by three distinct waveforms. The largest is the S wave, which occurs in ventricular systole: is caused by relaxation of the right atrium and descent of the tricuspid ring associated with right ventricular systole. A second distinct peak (the D wave) occurs during rapid ventricular filling when the tricuspid valve is open. In normal adult, the peak of S wave occurs around midsystole while the peak of the D wave occurs in early diastole

with tricuspid flow [9]. The third wave form is the A wave, which occurs with right atrial contraction and represents reverse flow. The A wave is small in normal adult man and, especially, may not be recorded during inspiration because it decreases in size.

Concerning the IJV and the left anonymous vein, both converge to form SVC.

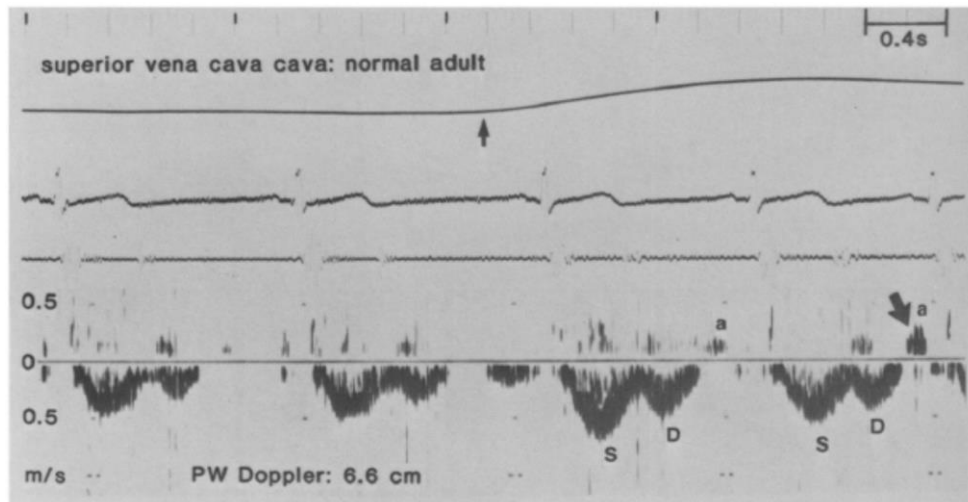


Figure 4.2_Graph of blood flow velocity in the SVC [9]

The Figure 4.2 shows a pulsed-wave Doppler ultrasound flow velocity curve from the SVC of a normal adult [9]. The upper line shows respiration with the vertical arrow that indicates onset of inspiration. Electrocardiogram and phonocardiogram are in the middle, the flow is in the lower part of the Figure; we can notice that the values are mainly negative due to the fact that the flow below the zero reference line is directed toward the right atrium. We also notice the presence of the same waves (S, D, A) described for the IVC graph.

Regarding the flow in the tricuspid valve, we found a graph showing the normal right ventricular inflow curve for measurements obtained across the tricuspid valve orifice [10]. As shown in the Figure 4.3, the curve is biphasic, with two distinct peaks that represent early and late diastolic inflow. In contrast with the two graphs described before, this curve represents the blood flow and not the blood flow velocity, but it is not synchronized with the electrocardiogram. The arrow at B indicates the peak flow during early diastolic filling, while the arrow at E indicates the peak flow during late diastolic filling.

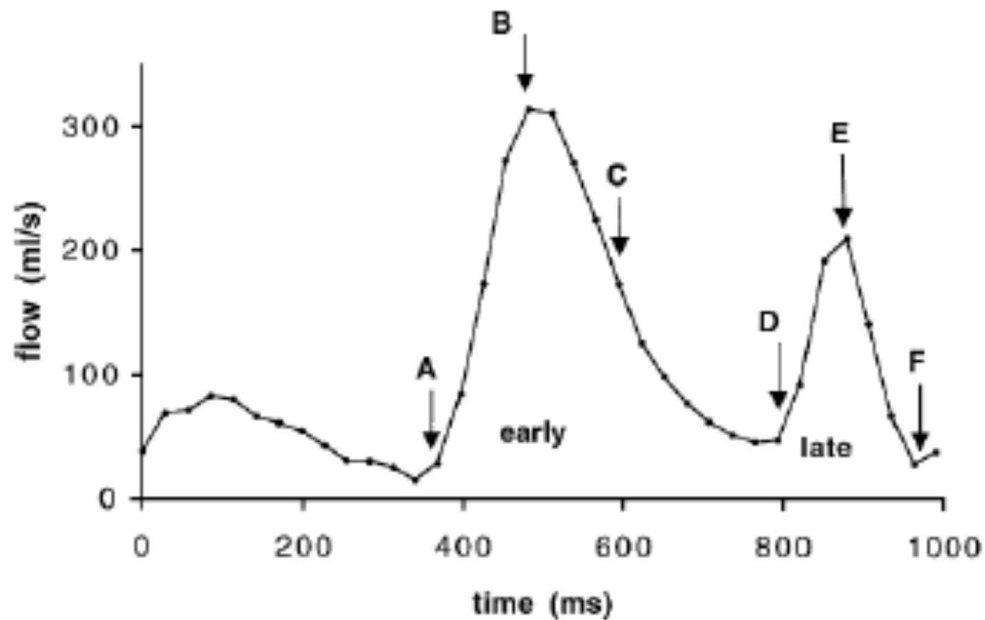


Figure 4.3_ Tricuspid valve outflow [10]

Regarding to the flow inside the catheters, the nephrologist told us that, thanks to the dialysis machine, it is possible to set the blood flow inside the catheters; usually, he set a constant value, equal to 300 mL/min. After a literature search, we found that the graph of blood flow at the arterial and venous needle is not constant but it oscillates about a fixed value [11]. We can notice from the Figure 4.4 that the curve that represents the blood flow velocity in the arterial needle assumes a regular sinusoidal shape, while the curve of the venous needle it is more constant. This difference is probably due to the resistance that the dialysis machine causes to the venous blood flow; the arterial blood flow, which doesn't suffer from this resistance, continues to have a more evident sinusoidal evolution. The graphs show the velocity waveform as measured by Doppler ultrasound in different points of the hemodialysis extracorporeal circuit.

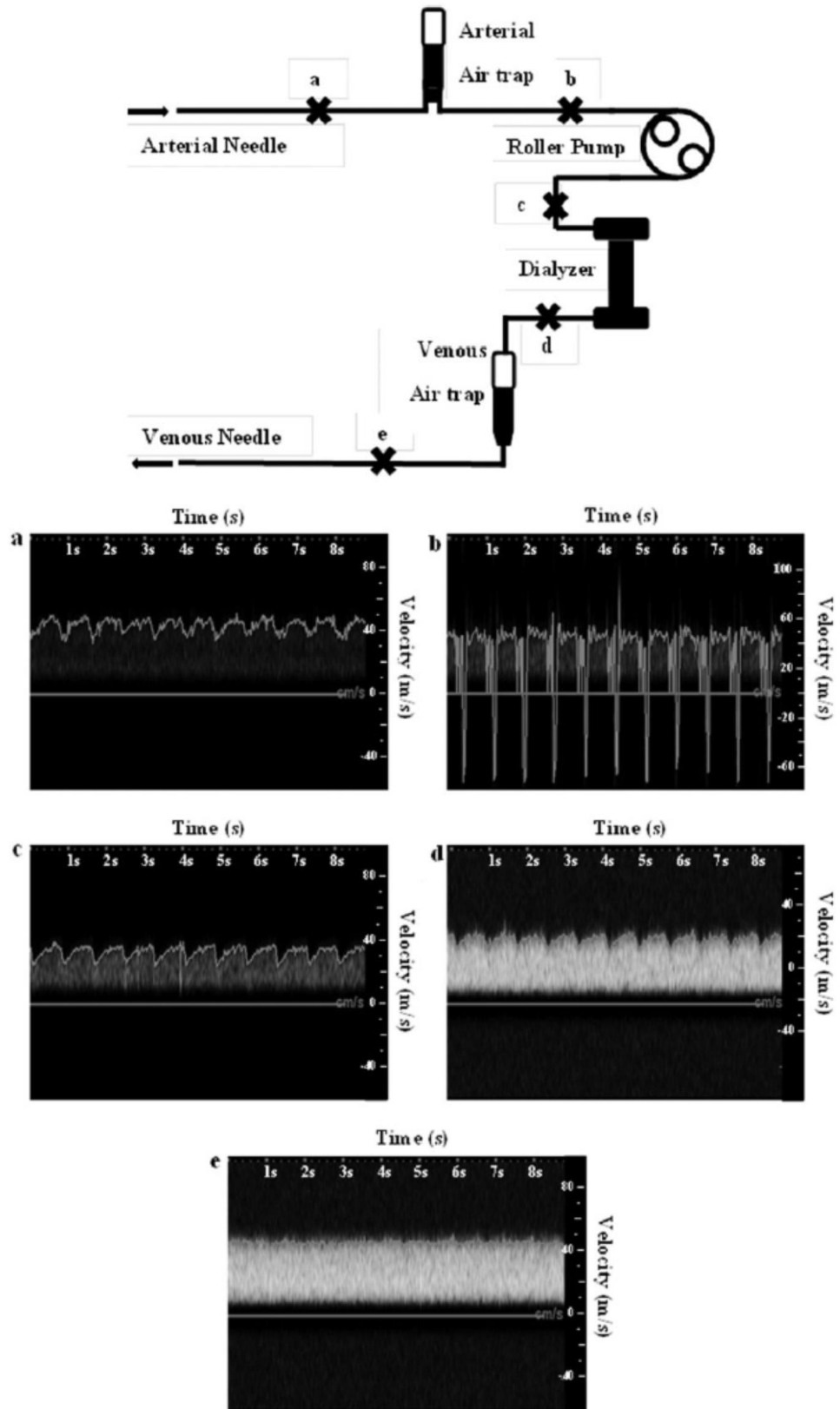
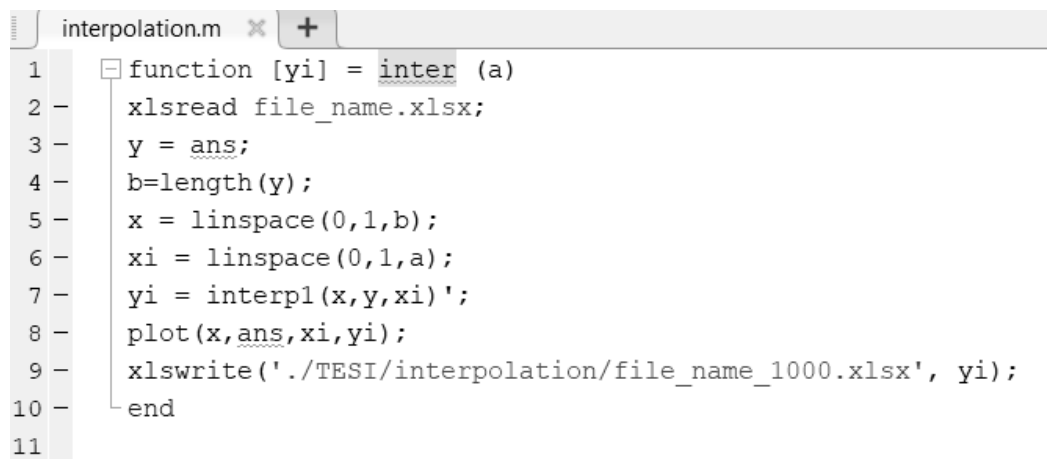


Figure 4.4_Dialysis circuit [11]

4.1.2 Choice of the boundary condition

The first step was to open the image of the graph with the software ImageJ (v. 1.43, National Institute of Health, Bethesda, Maryland, USA). Using the “Pen” tool, we delineated the contour of the curve, made it binary in order to have only black and white colours. Thanks to a “macro” written in house, the graph is transformed: the total black graphs is substituted by vertical stripes, alternating one black stripe to one white stripe, each one with a width of one pixel. To obtain the numerical value of each stripe, we used the ImageJ function “Analyze Particles” which returns the number pixel of each stripe. Therefore, to obtain the real values we had to multiply the pixel values with the relative scaling factor.

The number of values was not the same for each graph because it depended on the number of vertical black stripes contained in the binary image. In order to obtain 1000 values for each graph, we implemented a script (Figure 4.5) in Matlab2019 (The MathWorks, Natick, MA, USA). This function uses linear interpolation to elaborate a new file containing 1000 values whose starting from the initial values.

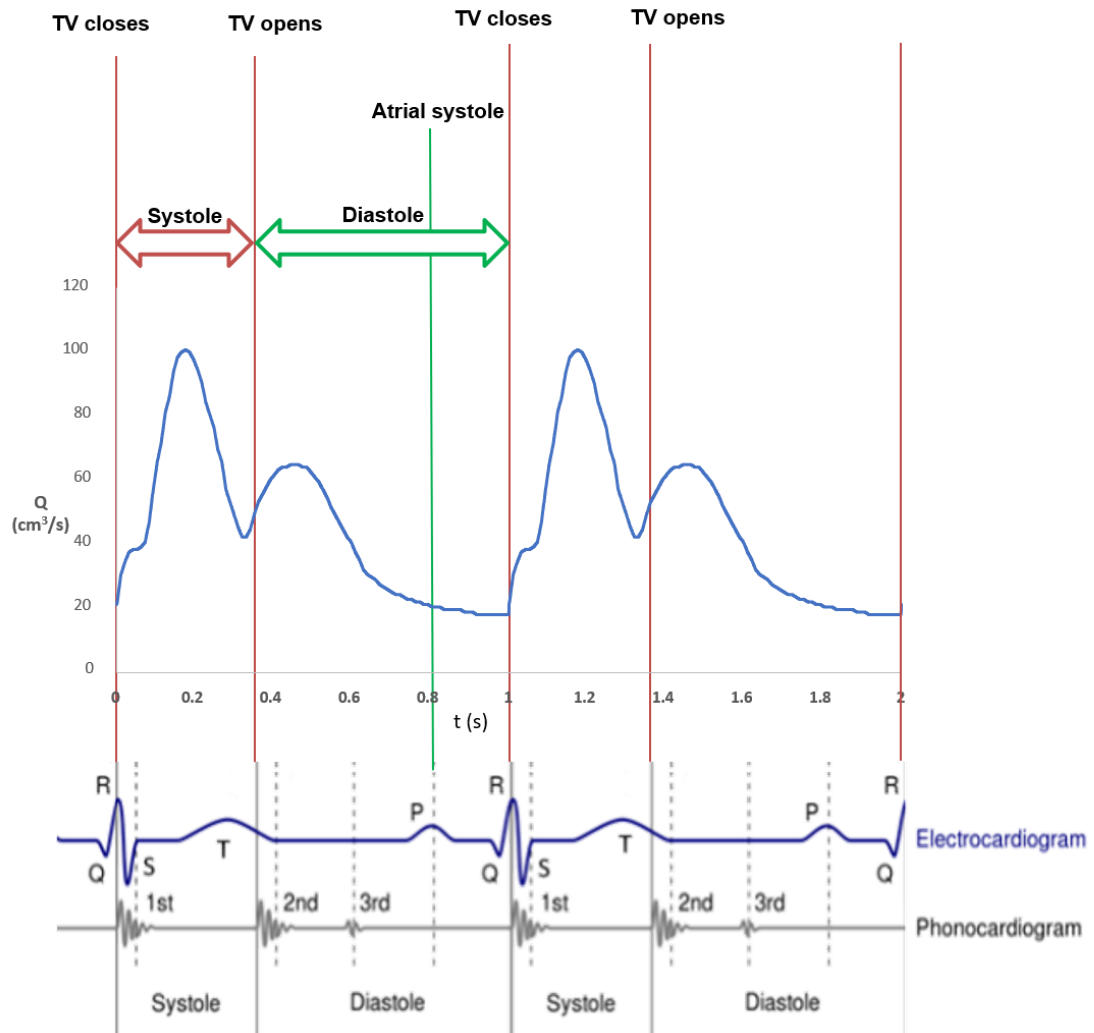


```
interpolation.m x +
1 function [yi] = inter (a)
2     xlsread file_name.xlsx;
3     y = ans;
4     b=length(y);
5     x = linspace(0,1,b);
6     xi = linspace(0,1,a);
7     yi = interp1(x,y,xi)';
8     plot(x,ans,xi,yi);
9     xlswrite('./TESI/interpolation/file_name_1000.xlsx', yi);
10 end
11
```

Figure 4.5_Matlab script for the interpolation

Concerning the IVC, we impose a plug-flow, volumetric flow rate boundary condition following the curve shown in Figure 4.6 during the cardiac cycle.

Q IVC



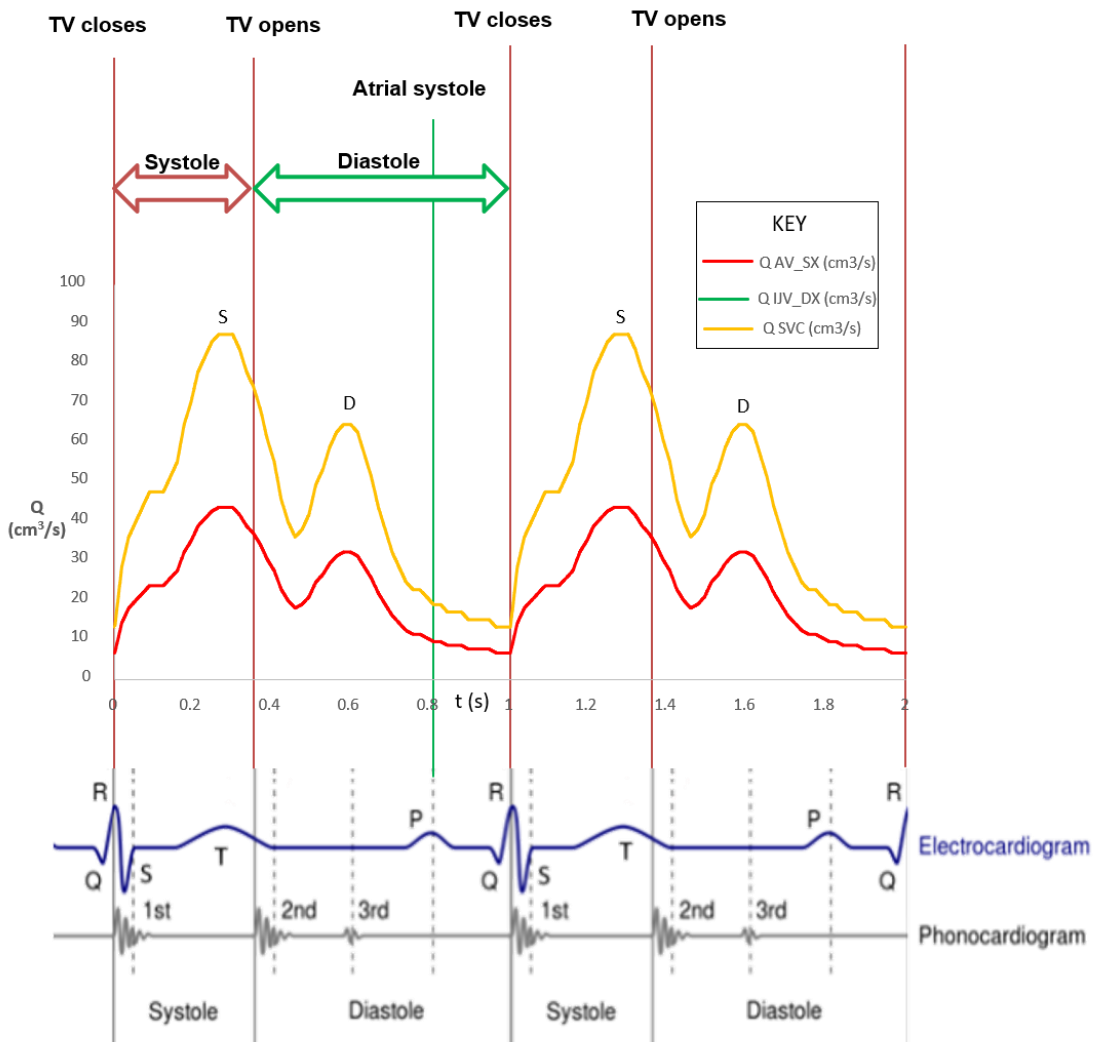
The right ventricular inflow tract (R VIT) view with the pulsed-wave Doppler sample volume in the **inferior vena cava (IVC) above the diaphragm**

Reynolds, JAmSocEchoCardio, 1991

Figure 4.6_IVC curve of boundary condition

We assumed a 50:50% contribution of the IJV and of the left anonymous vein to the total flow of SVC. Accordingly, the value of the SVC curve was two equal parts to obtain the flow rate of IJV and of the left anonymous vein. These graphs are shown in the Figure 4.7.

Q SVC, IJV_DX, AV_SX

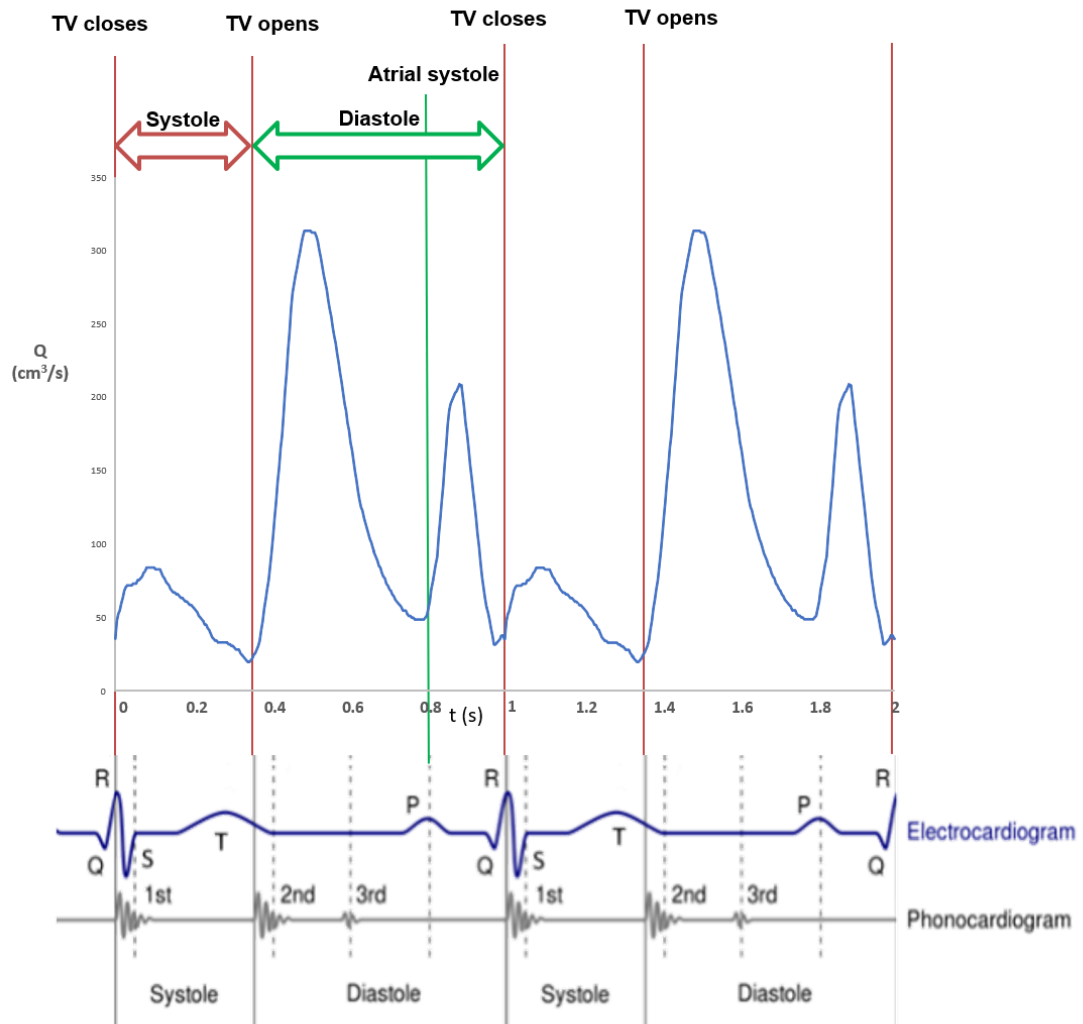


SVC Flow is composed by IJV_DX flow and **AV_SX** flow, each one contributes for half of the total

Figure 4.7_SVC, IJV_DX and AV_SX curve of boundary condition

As regards the tricuspid valve, the waveform of the flow rate imposed is shown in Figure 4.8.

Q VALVE OUT



The curve is **biphasic**, with two distinct peaks that represent **early and late diastolic inflow**.

Kroft et al., Radiology, 2000

Figure 4.8_Outflow curve from the tricuspid valve

It is important to remember that flows in IVC, IJV and left anonymous vein are inflows, all entering the domain and heading towards the right atrium. Instead, the flow through the tricuspid valve is an outflow and directs away from the right atrium. The sum of all inflow values provides a mean blood flow rate of 5.5 L/min representing the average cardiac output of a normal healthy man.

As regards catheters' values, we were able to obtain from the graph only the trace of the venous needle. We then decided to use a sine function to represent the flow curve of the arterial needle:

$$\text{Fun} = A \frac{\text{ml}}{\text{s}} * \sin(2\pi * (B)) + C \frac{\text{ml}}{\text{s}}$$

where $A = 1.25 \text{ mL/s}$ is the amplitude, $B = 1$ is the period of the function (namely 1 s is the period of a cardiac cycle), $C = 5 \text{ mL/s}$ is the vertical shift.

we assumed that the flow inside the two different lumens has a cycle-averaged value equal to 300 mL/min, with the waveform as shown in the Figure 4.9 below.

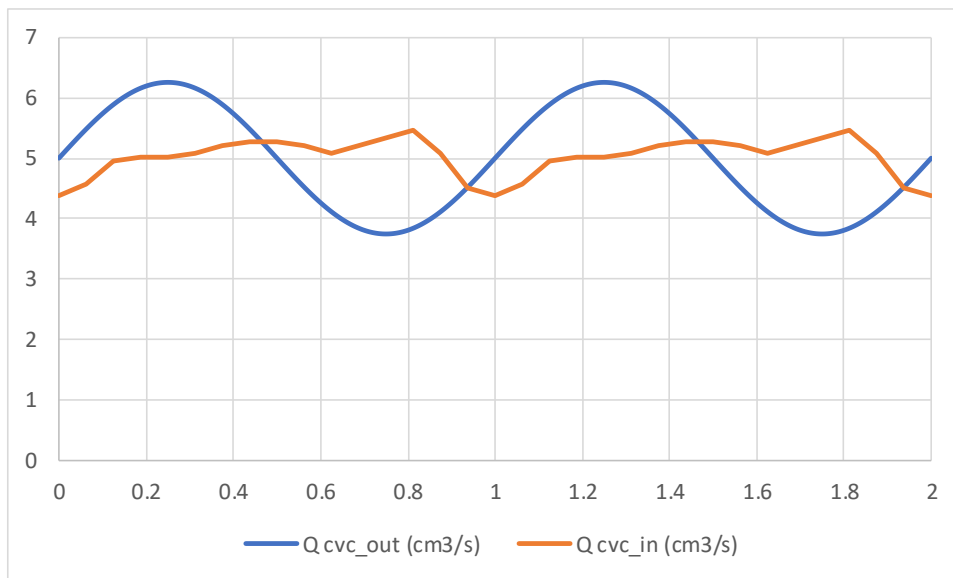


Figure 4.9_Catheters waveform

4.2 CFD SIMULATION

4.2.1 Blood rheology

A Bird-Carreau model was adopted to describe the non-Newtonian viscosity of blood [74]:

$$\mu = \mu_{\infty} + (\mu_0 - \mu_{\infty}) * (1 + \lambda^2 \dot{\gamma}^2)^{\frac{n-1}{2}}$$

where μ is the dynamic viscosity, μ_0 and μ_{∞} are the viscosity values as the shear rate goes to zero and infinity, λ is the shear rate, $\dot{\gamma}$ is the time constant and n is the power-law index.

We assumed $\mu_0 = 0.161905 \text{ m}^2/\text{s}$, $\mu_{\infty} = 0.0300822302 \text{ m}^2/\text{s}$, $\dot{\gamma} = 1 \text{ s}$, $n = 0.5$.

Blood density was assumed as $\rho = 1.045 \text{ g/cm}^3$.

4.2.2 CFD simulations of Palindrome and Tesio cases

We performed transient simulations of blood using the pimpleFoam solver of the OpenFOAM toolbox. The pimpleFoam solver was set to operate with second order backward time integration scheme, with automatic adjustment of the time step base on a maximum CFL number, which we set to 1.

As boundary conditions, we imposed the flow rate waveforms shown above while traction-free condition was set at the tricuspid valve. We considered vessel walls as being rigid and applied here the no-slip condition.

For post-processing purposes, we decided to save the numerical results every 0.01 s obtaining 100 steps time per cycle. Palindrome and Tesio simulations took about the same computational time work: about 24 hours achieve 2 cycles running in parallel on 12 CPU.

4.3 POST-PROCESSING

The hemodynamic parameters of interest have been post-processed using Paraview (<http://www.paraview.org>), an open-source multiple-platform application for scientific visualization.

In particular, we evaluated the velocity contours of certain slices along the whole geometry, the 3D streamlines and the wall shears stress (WSS) for both the vessel and catheters walls. We also performed the analysis of the pressure drop between the two inner lumens of the catheters, the evaluation of the turbulent kinetic energy and the particle tracing.

5. Results

The present chapter contains the results obtained by CFD. Numerical results of the CFD simulations were analyzed in order to characterize the hemodynamic conditions in the presence of both catheters. A special attention has been focused on particular parameters, such as WSS on catheters surface, TKE and the pressure drop; furthermore, there is a focus on velocity images of Z-axes slices, velocity 3D streamlines and particle tracking.

5. RESULTS

5.1 Velocity images of Z-axes slice

We evaluated the magnitude of blood flow velocity (U) inside the vessels and the catheters; to visualize the evolution of the velocity in different points inside the vessels we made multiple slices along the Z-axis. These results are important for the evaluation of a correct CFD simulation.

Figure 5.1 shows the velocity contours for the Palindrome came in the moment of the first peak of blood flow in the veins; this peak had the maximum value in the whole cardiac cycle.

The results show, as expected, high values in the tract that represents the tricuspid valve. We can observe high values also inside the catheter due to the small area of the catheter's lumen.

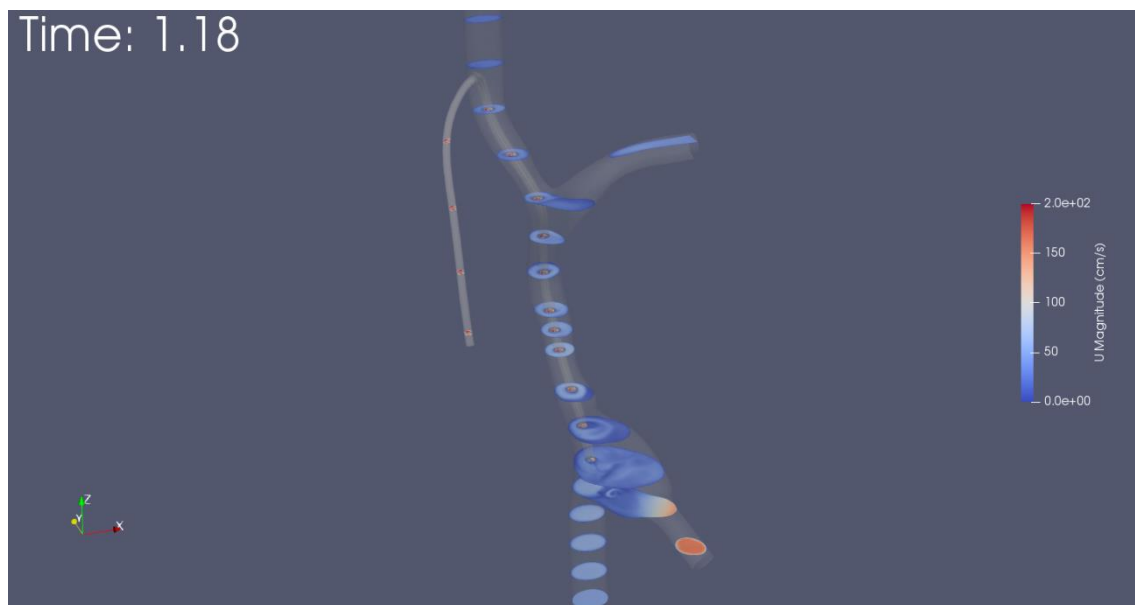


Figure 5.1 _Palindrome Z-axes slices of velocity magnitude

Figure 5.2 shows the velocity contours for the Tesio case in the same moment of the Palindrome one, the moment of the first peak of blood flow in the veins.

The results show, as expected, high values in the tract that represent the tricuspid valve and also inside both catheter's tube, due to their small lumen.

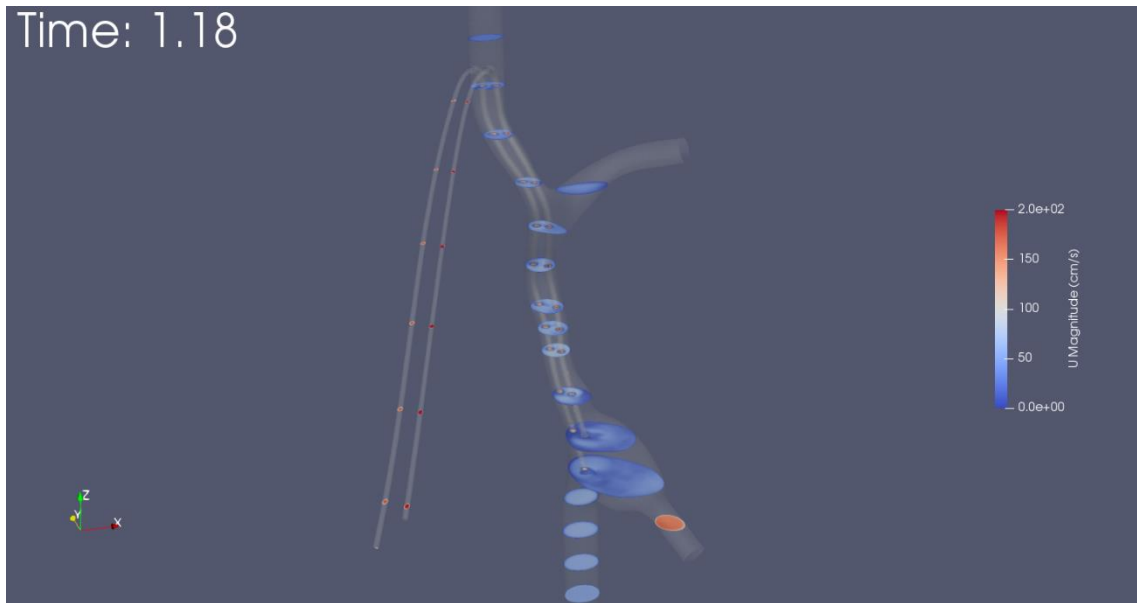


Figure 5.2_Tesio Z-axes slices of velocity magnitude

5.2 Velocity 3D streamlines

Streamlines are curves that are instantaneously tangent to the velocity vectors of the flow.

In our cases, we analysed the 3D streamlines which were generated in catheters' inner lumen and the behaviour of flow at the catheters' tip during the whole cardiac cycle.

In our cases, we distinguished the venous streamlines by the arterial streamlines assigning them different colours: blue represents the venous blood flow instead red stands for the arterial blood. Depending on the magnitude of velocity, the streamlines assume a darker colour if the velocity is lower while it becomes whiter with greater velocity.

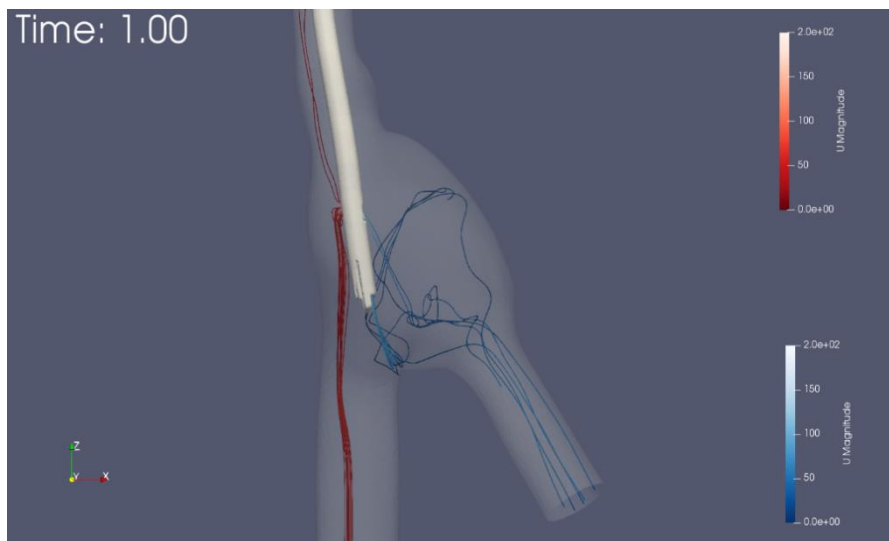


Figure 5.3_Palindrome streamlines Time 1.00



Figure 5.4_Palindrome streamlines Time 1.18

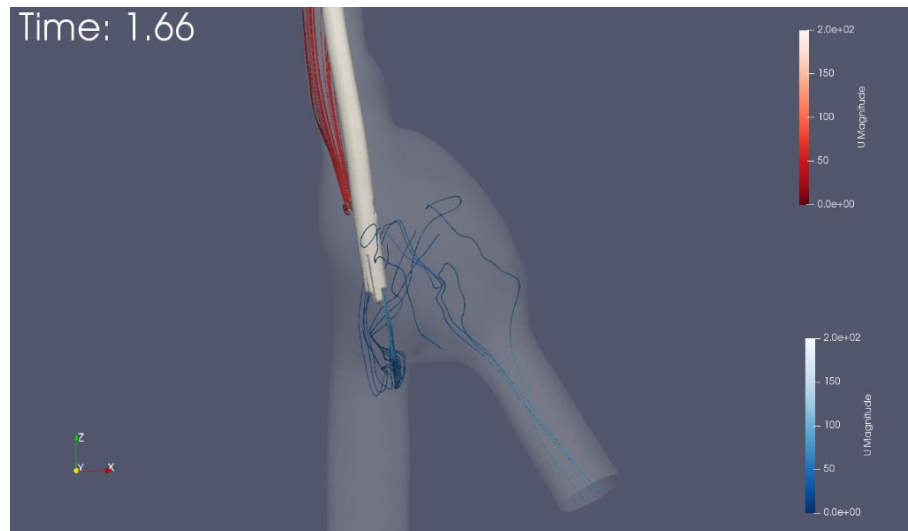


Figure 5.5_Palindrome Streamlines Time 1.66

Figure 5.3, 5.4 and 5.5 show the 3D streamlines in the case of Palindrome catheter in different time steps. This analysis shows that the venous flow comes out mostly from the principal hole instead from the side hole. As regards the arterial flow, the analysis of the whole cardiac cycle has showed the opposite: the side hole is the mostly used by the blood flow to come into the inner light. This particular is very important because reduces the likelihood of recirculation. From Figure 5.4 we can notice that blood flows directly from the CVC to the exit site; instead, blue streamlines in the Figure 5.5 show the presence of eddies in the right atrium and blood does not flows directly as in Figure 5.4. This behaviour is due to the different values of blood flow in veins during the cardiac cycle: when the blood flow is higher (in the first half of cardiac cycle there are the two peaks of maximum value) the blood flows directly from the CVC to the tricuspid valve while, during the second half of the cycle, lower values of blood flow cause eddies in the right atrium.

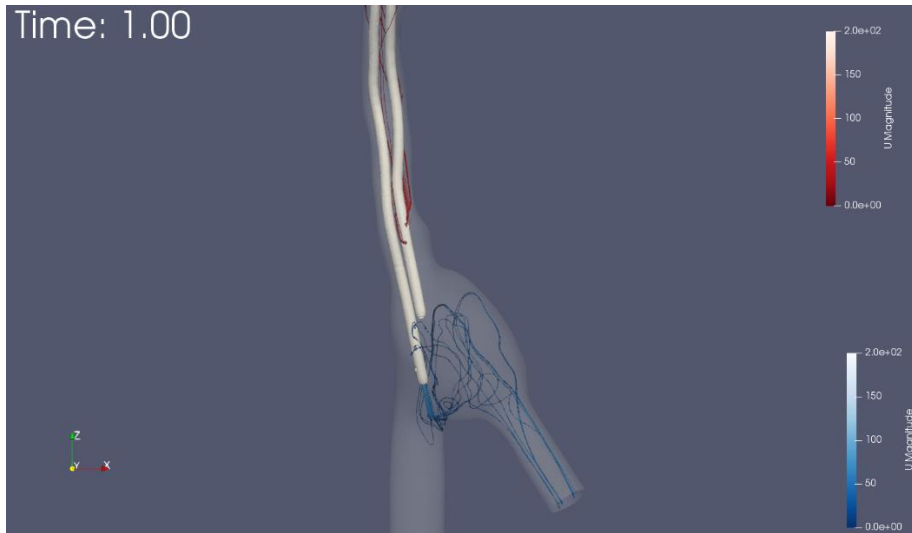


Figure 5.6_Tesio streamlines Time 1.00

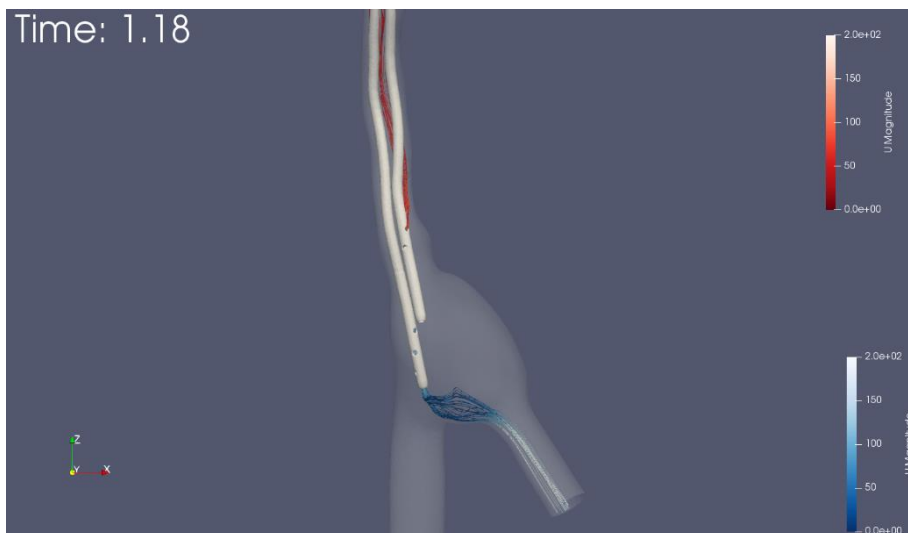


Figure 5.7_Tesio streamlines Time 1.18

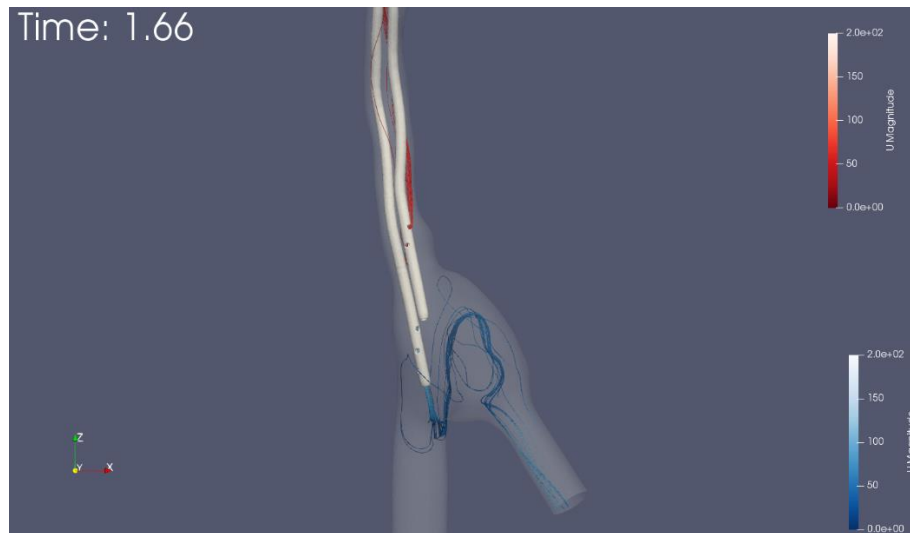


Figure 5.8_ Tesio streamlines Time 1.66

As regards Tesio catheter, Figure 5.6, 5.7, 5.8 show the 3D streamlines in different time steps. 3D streamlines which represent the venous blood flow highlight the fact that the main hole used is the one at the end of the tip, instead side holes are less used. This behaviour is due to the fact that side holes have the function of avoiding the catheter's surface to adhere to the internal vessels wall; they play a fundamental role only in the case of fibrin sheet formation and closing of main hole. Concerning the arterial tube, the mostly used hole is the one side hole further away from the basis tip; the closer we get to the basis tip and the side holes are used less and less to get the blood inside the inner lumen. As in the Palindrome case, also in Tesio case the blood flow from the CVC to the tricuspid valve behave in different way during the cardiac cycle. Figure 5.7 shows that, in the first half of the cycle, blood flows directly from the CVC to the tricuspid valve while, during the second half, blood does not flow directly into the tricuspid valve but it creates eddies in the right atrium. Such as in the Palindrome case, this behaviour is due to the different values of blood flow in veins during the cardiac cycle: higher in the first half and lower in the second one.

5.3 Wall Shear Stress on catheters surface

Figures 5.9, 5.10, 5.11 shows the WSS pattern on the Palindrome surface.

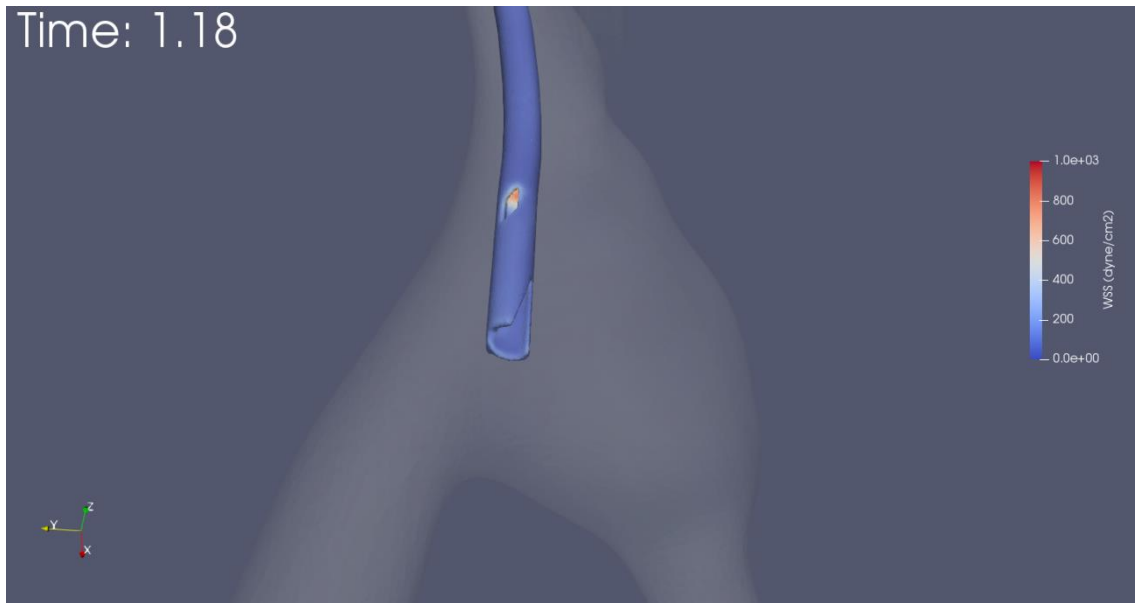


Figure 5.9_Palindrome WSS: arterial side

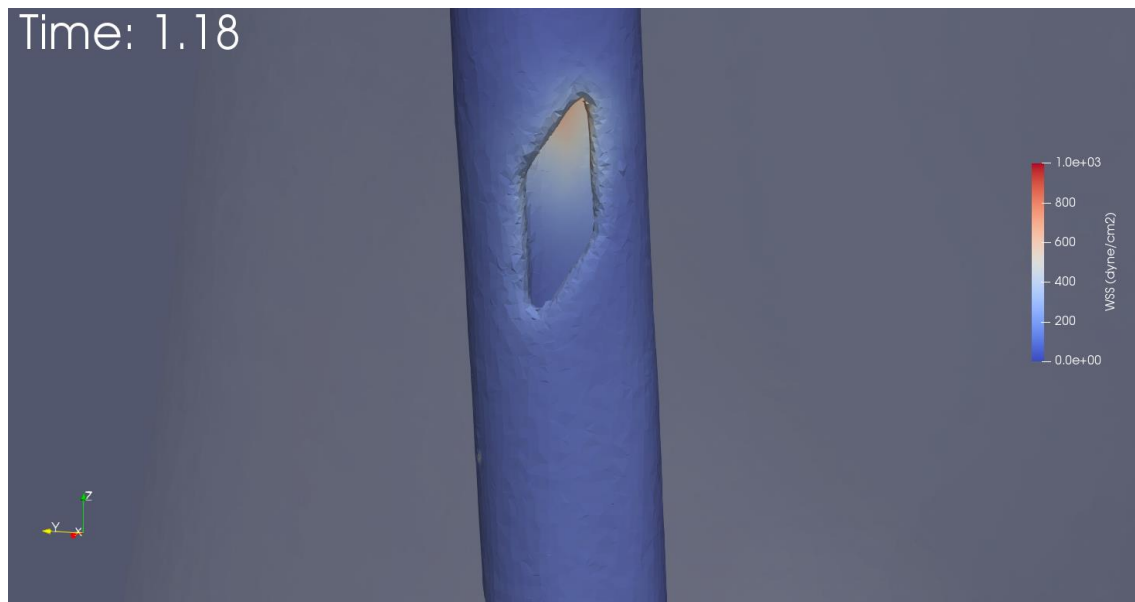


Figure 5.10_Palindrome WSS: focus on arterial side hole

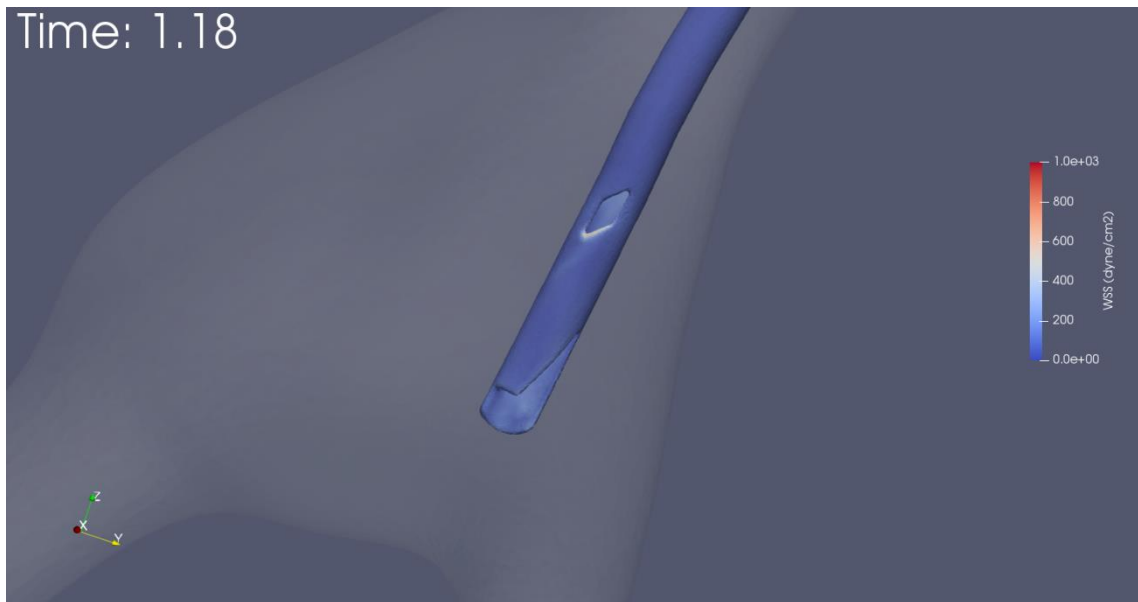


Figure 5.11_Palindrome WSS: venous side

From Figure 5.9 and 5.10 we can observe that, on the external surface, there are not area with altered WSS but high WSS values are present near the side holes. In fact, the area with high WSS (the one with colour tending to red) is the internal surface where is positioned the side hole. This presence of high WSS area is due to the blood flow that, coming into the catheter from the side hole, clashes with the catheter's internal surface and causes this high WSS area. Figure 5.10 shows a focus on the side hole.

Figure 5.11 shows the side hole of the venous part, is subjected to lower WSS values because blood flow comes out prevalently from the principal hole at the basis tip.

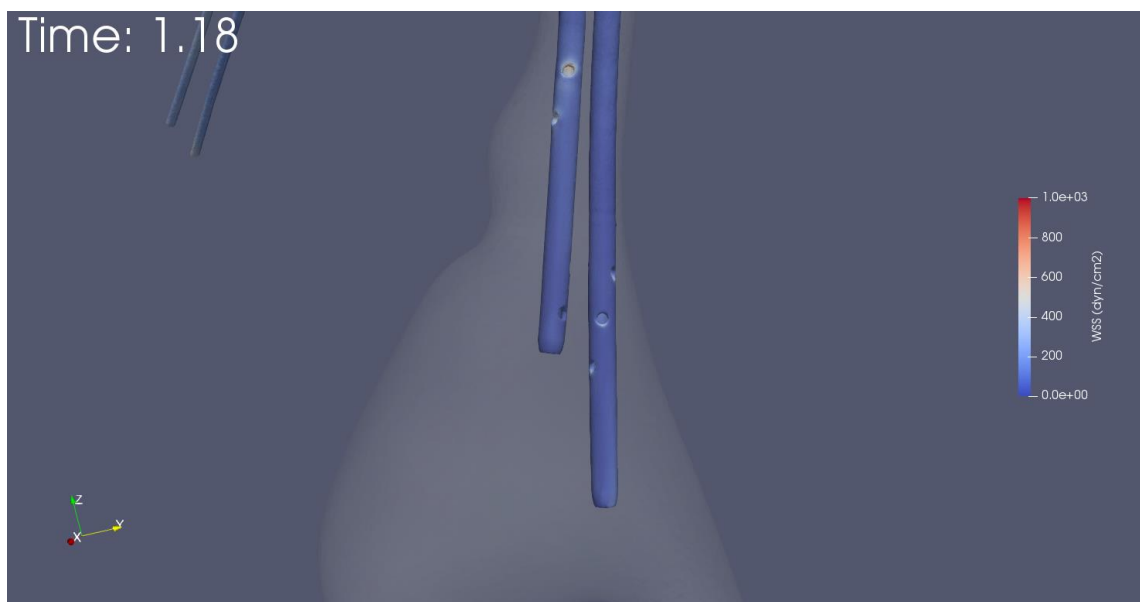


Figure 5.12_Tesio WSS

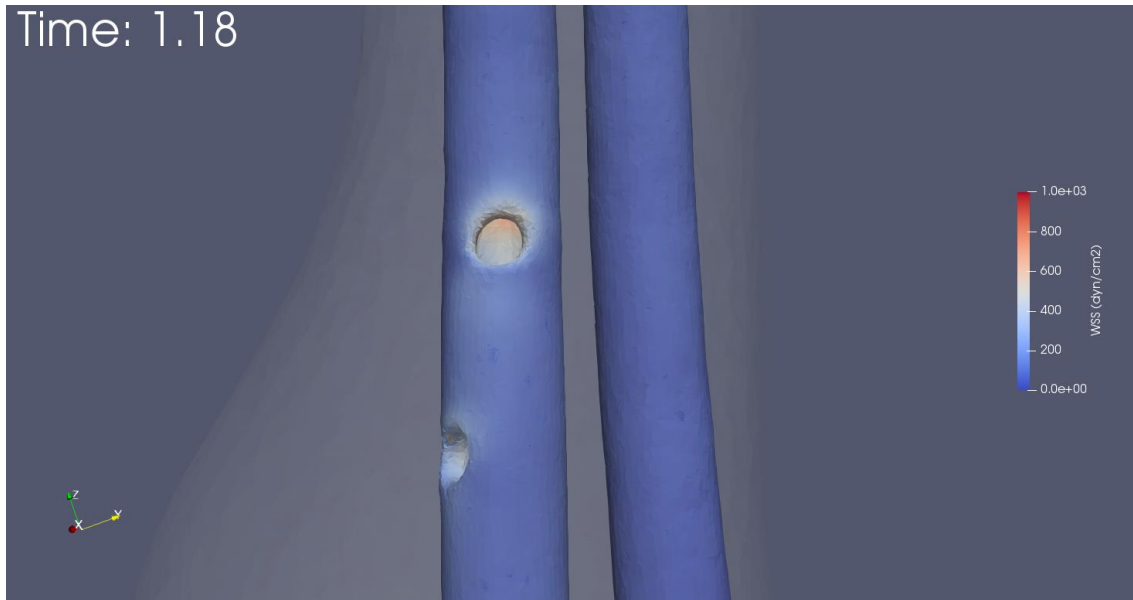


Figure 5.13_Tesio WSS: focus on arterial side holes

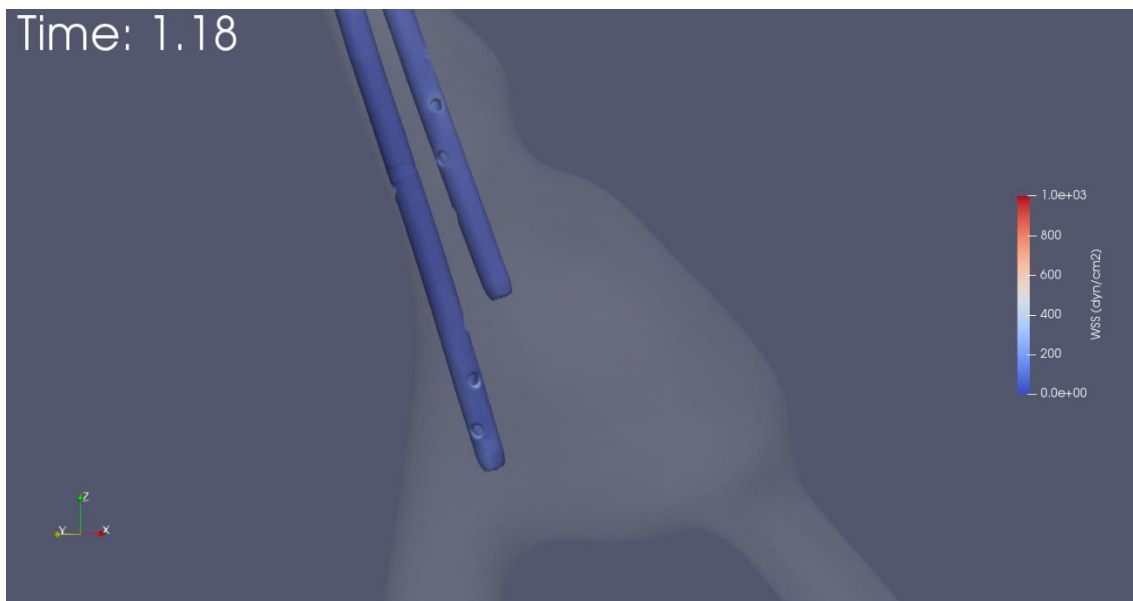


Figure 5.14_Tesio WSS

Figure 5.12, 5.13 and 5.14 show WSS pattern on the Tesio surface. We can notice that, such as in the Palindrome case, even in Tesio the external surface of the tip catheter does not present area with altered WSS values, apart the areas near side holes. From Figure 5.12 and 5.13 we can observe that, concerning arterial needle, the area with high WSS (even in this case, the one with colour tending to red) is the internal surface where is positioned the first side hole. This presence of high WSS area is due to the blood flow that, coming into the catheter from the side hole, clashes with the catheter's internal

surface and causes this high WSS area. From a comparison between Figure 5.11 and 5.14, we can observe that the side hole's area in the Tesio case is subjected to high WSS compared to the Palindrome's side hole. This is due to the different shape and the size of the two side holes.

Instead, the side holes of the venous part, are subjected to lower WSS values because blood flow comes out prevalently from the principal hole at the basis tip.

5.4 Pressure drop inside catheters tube

An additional descriptor of the catheter performance, the pressure drop Δp between the inlet and the outlet sections was used to evaluate the average resistance of the inserted catheter to the flow:

$$R = \frac{TA\Delta p}{Q_{average}}$$

Where Time Average Δp ($TA\Delta p$) and $Q_{average}$ are the cycle values of Δp and of the flow rate at the inflow section of each model, respectively.

In our case, Δp was evaluated such as the difference between the pressure calculated in the venous inner lumen and the pressure calculated in the arterial inner lumen. Then we made a time average because the difference was calculated at each time step. This value of $TA\Delta p$ was divided by the inner lumen area, different in Palindrome and Tesio.

For Palindrome and Tesio, the Δp graph curve are very similar as shown in Figure 5.15 and 5.16; what differed were the $TA\Delta p$ value and the inner lumen area.

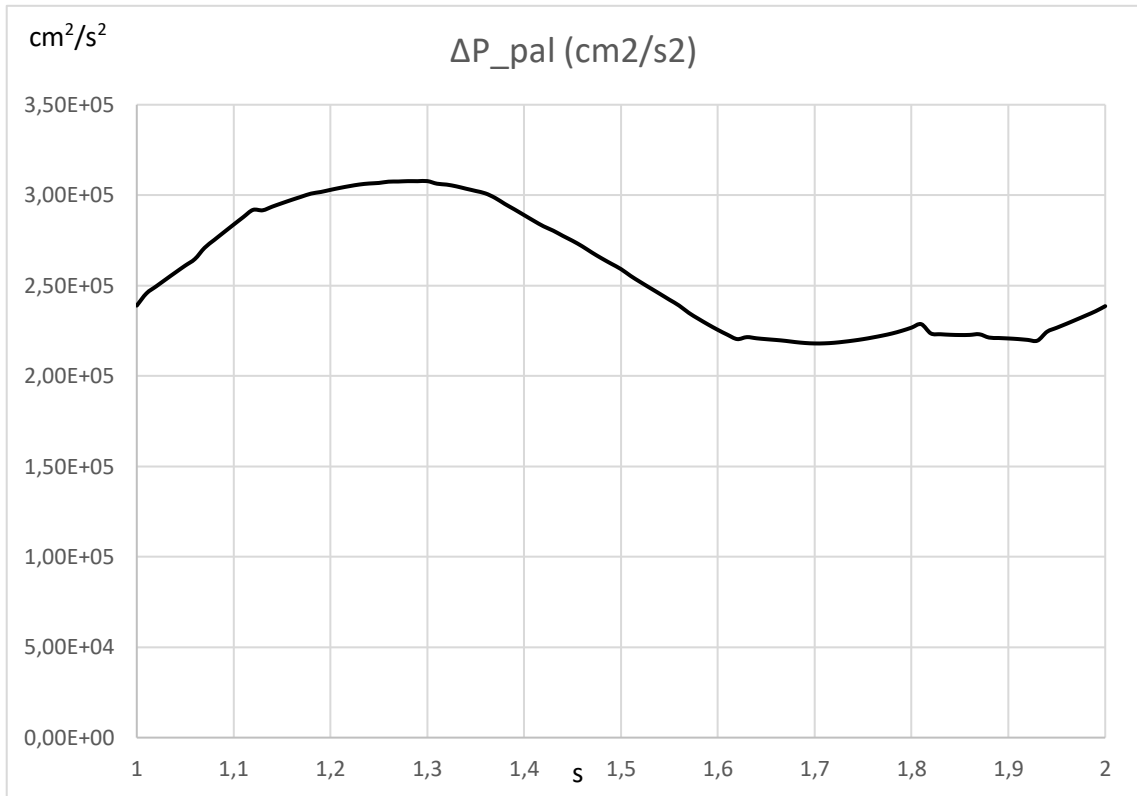


Figure 4.15_Palindrome pressure drop

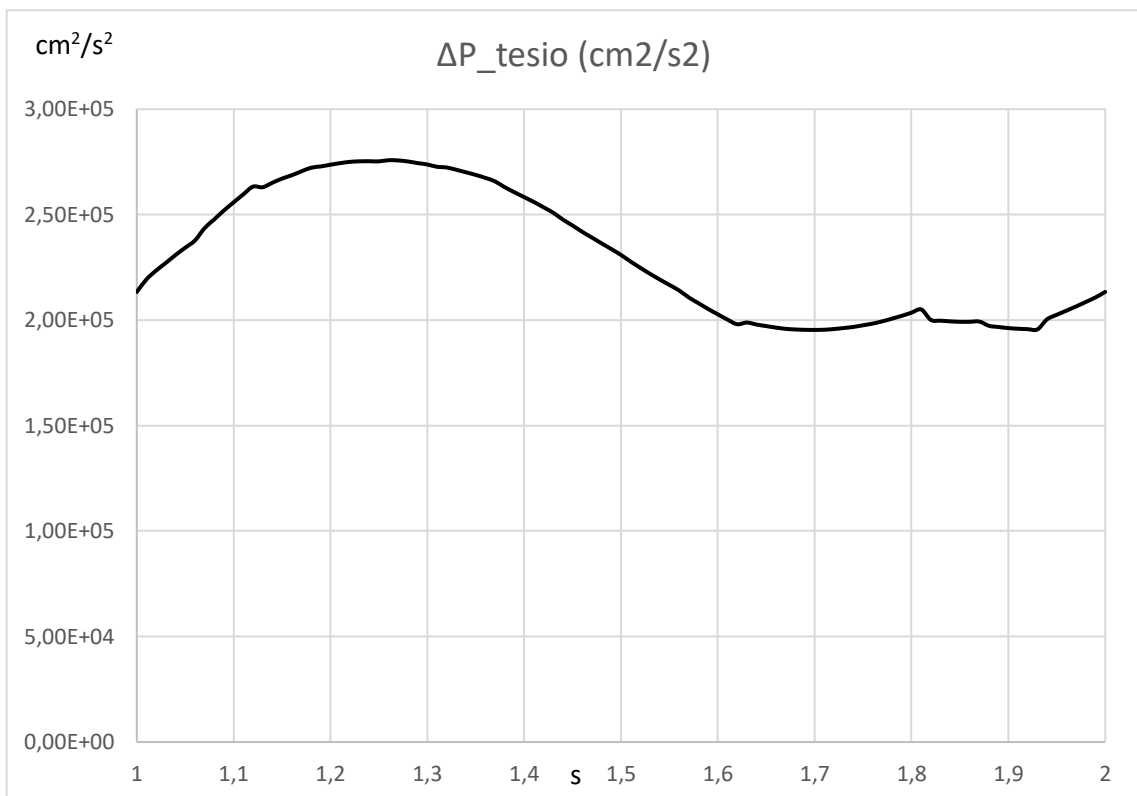


Figure 5.16_Tesio pressure drop

5.5 Turbulent Kinetic energy

Turbulent kinetic energy (TKE) is a parameter which is directly correlated to the intensity of turbulence in the flow. The TKE is defined to be half the sum of the variances (square of standard deviations) of the velocity components:

$$\text{TKE} = \frac{1}{2} * (\overline{u'^2} + \overline{v'^2} + \overline{w'^2})$$

Where $u' = u - u_{\text{average}}$

$$v' = v - v_{\text{average}}$$

$$w' = w - w_{\text{average}}$$

and u is the velocity along the x -axes, v is the velocity along the y -axes and w is the velocity along the z -axes.

This parameter is a helpful tool which allows to evaluate the turbulence produced by each catheter. In our scale, a darker colour indicates a TKE parameter with lower values; instead, a colour which is more like yellow, indicates greater value of TKE.

Figure 5.17, 5.18, 5.19 and 5.20 show that both catheter generates greater values of TKE where the tip is positioned, so in the right atrium; instead, inside the SVC, which is crossed in the whole length by the catheter's tube, there are lower values of TKE.



Figure 5.17_Palindrome TKE

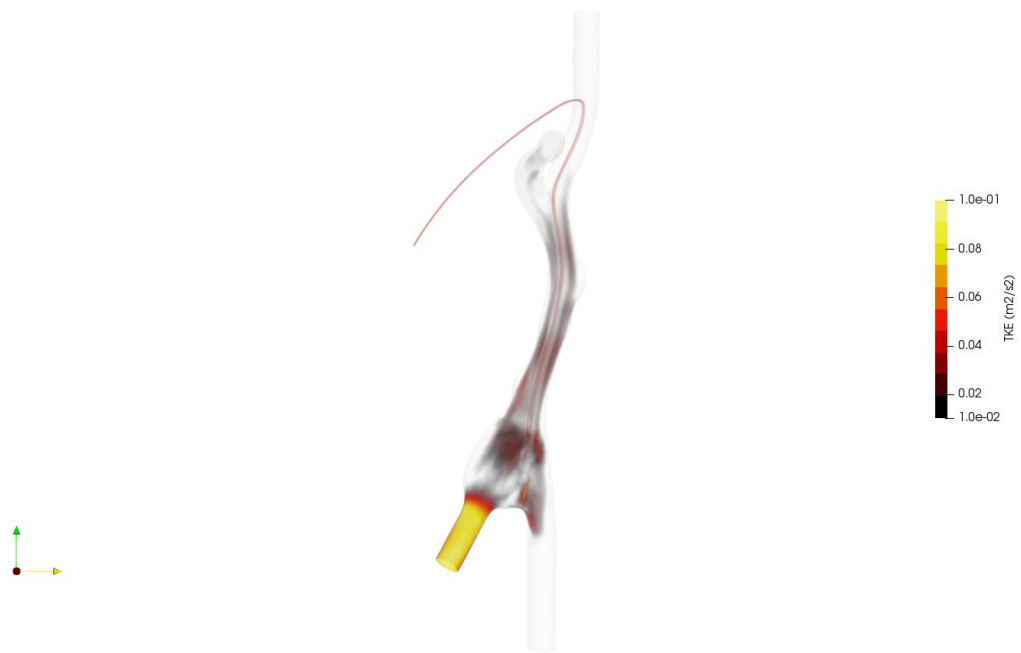


Figure 5.18_Palindrome TKE

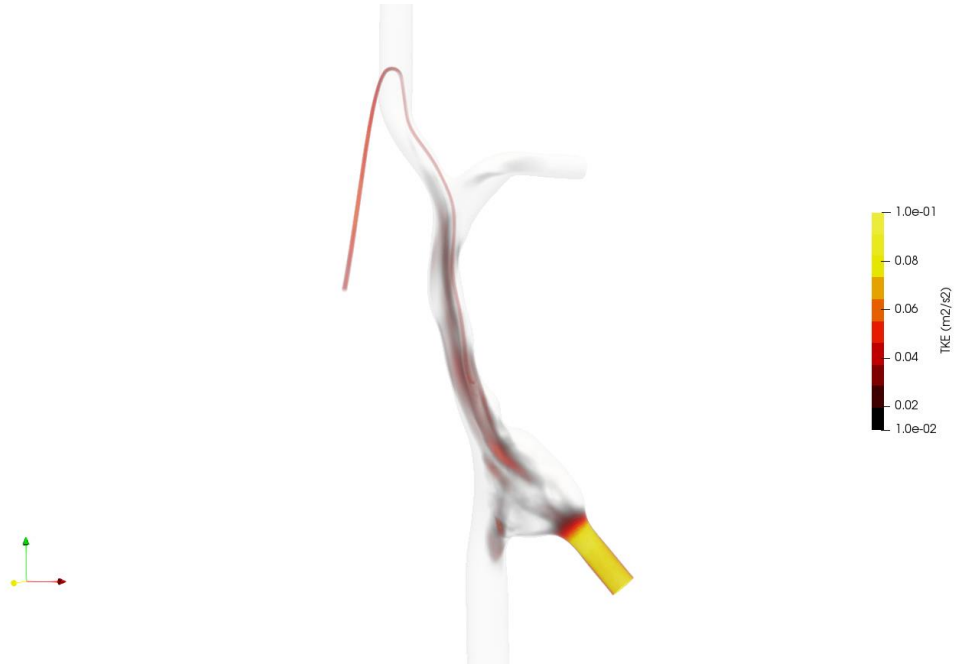


Figure 5.19_Tesio TKE

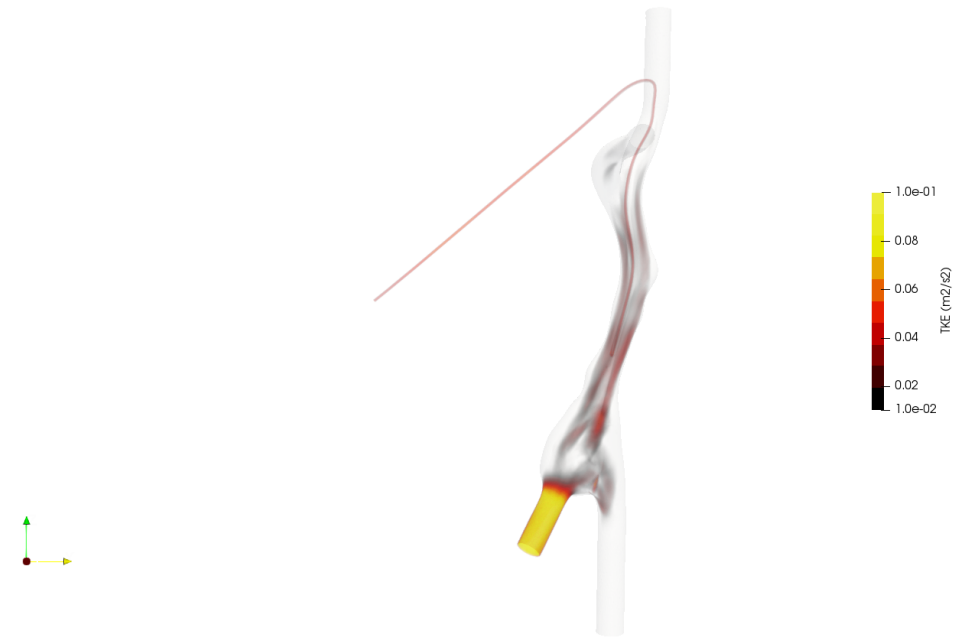


Figure 5.20_TKE in Tesio

5.6 Particle tracking

Thanks to this analysis, we want to evaluate the recirculation of each catheter. Recirculation means that the clean blood which flows from the dialysis machine to the patients could immediately return into the arterial needle. On this basis, we evaluated at the final time step how many particles were going to return inside the atrial needle.

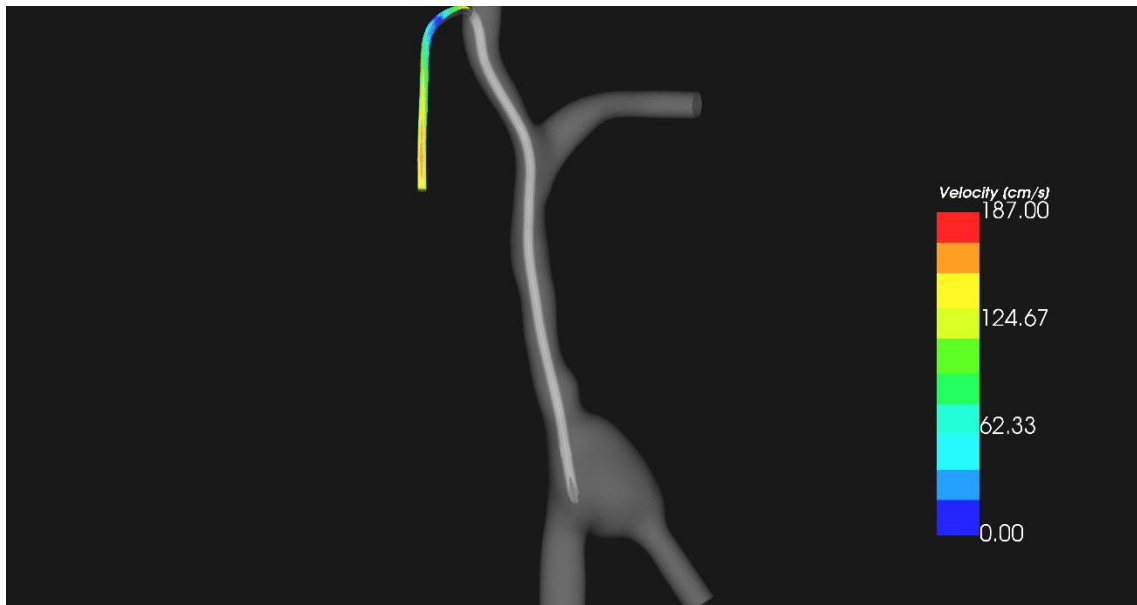


Figure 5.21_Palindrome particle tracking: first time step

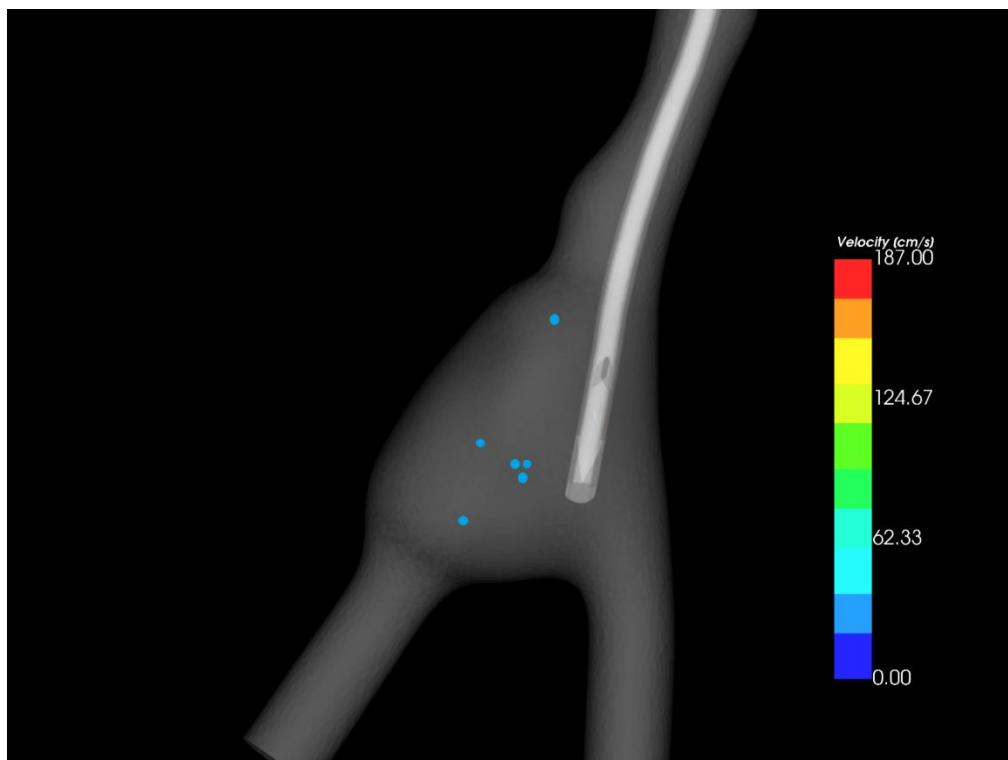


Figure 5.22_Palindrome particle tracking: end step time

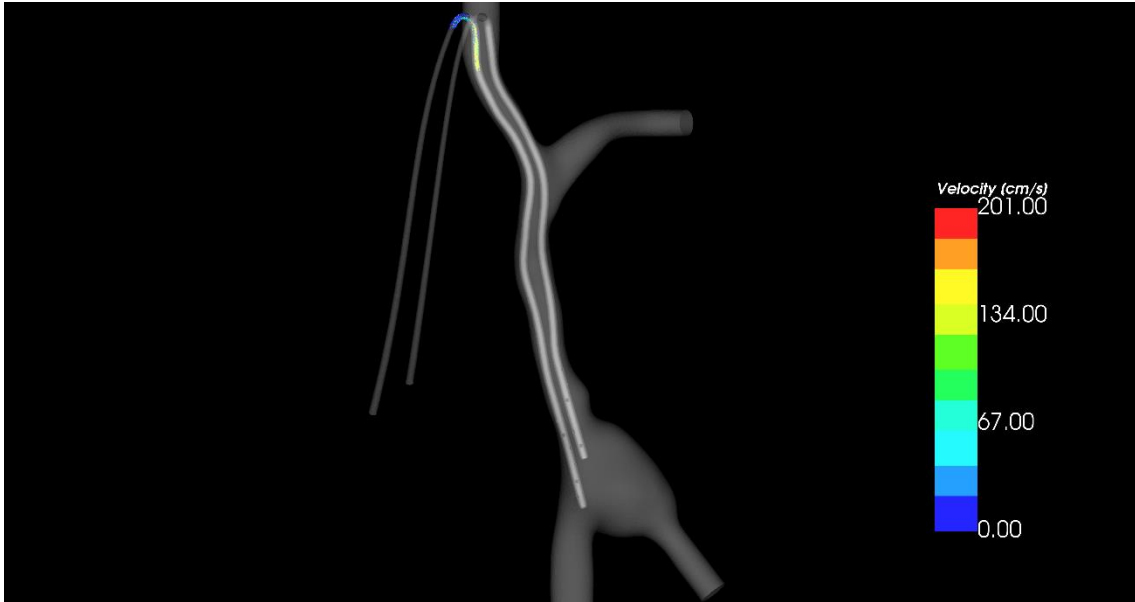


Figure 5.23_Tesio particle tracking: first time step

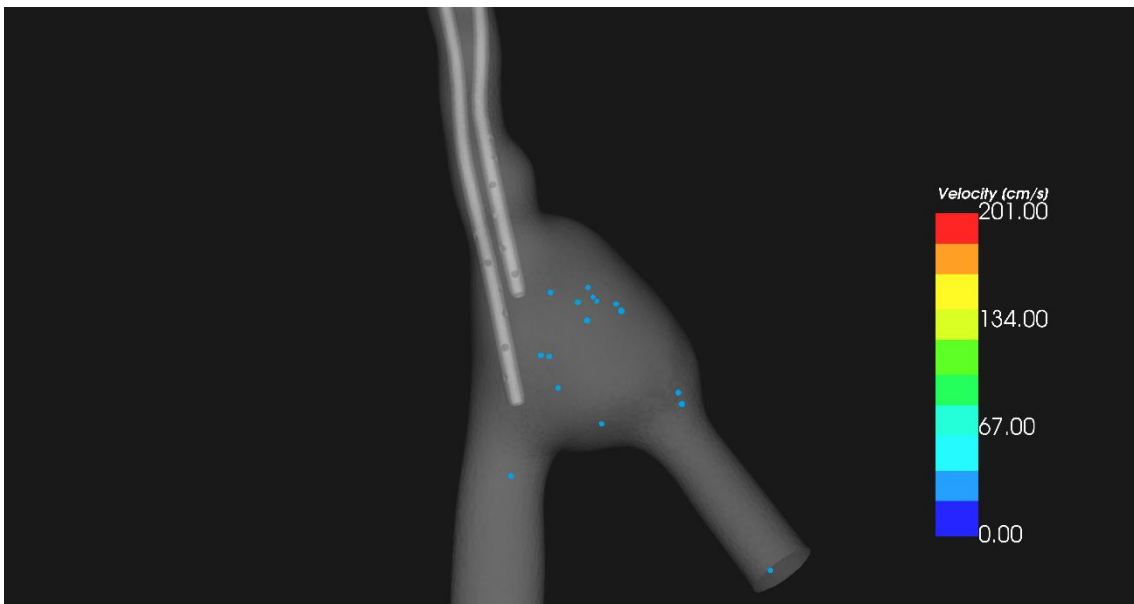


Figure 5.24_Tesio particle tracking: end step time

Figure 5.21 and 5.22 show the particle tracking in the Palindrome case. Figure 5.21 shows the first step time: particles start from the venous lumen because we want to evaluate recirculation. Figure 5.22 shows how many particles remain at the end of the cardiac cycle in the right atrium; the other particles not present are come out from the tricuspid valve.

Figure 5.23 and 5.24 show the particle tracking in the Tesio case. As for Palindrome, Figure 5.23 shows the particles starting from the venous lumen at the first step time. Figure 5.24 shows the situation at the end of the cardiac cycle and the particles still present in the right atrium.

6. Discussion, limitations and future developments

This final chapter contains the discussion of the results of the present thesis, the limits of the computational work and the possible future developments and perspectives of research study field.

6. Discussion, limitations and future developments

6.1 Discussion

In the present thesis, it was possible to describe the nature of the flow inside the veins and the right atrium in the presence of central venous catheter. In particular, the main goal of this work was to identify a methodology for the comparison between the behaviour of two particular catheters, Palindrome and Tesio, once inserted in the patient's body.

In this thesis work we overcame the limitations that previous CFD studies CVC presented. The insertion of the catheter in a geometry directly taken from the patient CT was an improvement, especially in the customization of the simulation. The customization is important in order to compare the behaviour of two different catheters in particular conditions and in specific cases.

From the results that we obtained, the WSS and the streamlines analysis offer a good basis for the evaluation of the flow behaviour inside the right atrium. The WSS colour maps show which area are more subjected to stress during the whole cardiac cycle: catheters are subjected to high WSS in the same area, the internal surface at the level of the arterial side hole. The principle difference is between the distribution of WSS on the side hole's wall: thanks to its particular shape and greater size, Palindrome side hole's wall is subjected to lower WSS compared with the Tesio one.

Thanks to the streamlines, we analysed the development of flow outside and inside the catheters' tip. The results do not show particular difference between the Palindrome and the Tesio cases: for both, during the first half of the cardiac cycle, the blood flows directly from the CVC to the tricuspid valve; during the second half, blood flow present eddies almost equally in both cases; however, TKE offers a further indication for these fluid dynamic conditions.

The Δp analysis offers a tool in order to evaluate the resistance to flow that the presence of catheters inside the vessels. The $TA\Delta p$ in the Tesio catheter was less than in the Palindrome catheter but the section area of Tesio was greater than the Palindrome one. This means that the calculated resistance to flow of the two catheters assumed very similar values.

The TKE as indicator of disturbed flow was important to understand that the turbulence due to the presence of Tesio catheter is greater in the SVC, compared to the Palindrome one. As regard the turbulence in the right atrium, the results show that the Palindrome causes a greater level of turbulence; this is due to the location of the catheter's tip inside the right atrium and the position of the inflow and outflow holes.

As regard the particle tracking analysis, this activity was important to evaluate the recirculation present in the two cases. Results show that the risk of recirculation in Palindrome is lower than in the case of Tesio. We understood this because of the presence of more particles in the right atrium at the end of cardiac cycle in the Tesio case; more particles means a greater possibility that the clean blood returns immediately inside the arterial needle.

6.2 Limitations

Some limitations, inherent to our CFD numerical simulations, require acknowledgement and further examinations:

- *Boundary conditions*: although boundary conditions that we used in our simulation represent an improvement compared to the ones used in previously CFD studies, they are not at all a perfect representation of physiological condition. In this perspective, the main limit of our simulation is the lack in the simulation of the physical behaviour of tricuspid valve. A physiological tricuspid valve remains closed in the first part of cardiac cycle (during the systole phase, about the 40% of the whole cycle) and it is open during the second half (during the diastole phase, the remaining 60% of the cardiac cycle). In our simulation, the tricuspid valve is always open because we did not assign any boundary condition to it, even though we found the curve that represents its trend. We tried to assign the boundary conditions to the tricuspid valve patch but the CFD simulations always crashed.
- *Rigid walls*: the use of rigid walls models, while undoubtedly convenient and justified in many cases, should not overlook the fact that real vessels are influenced by the effect of the compliance. For cases where the compliance and vessel motion are known to have non-negligible quantitative effects, a popular modelling approach is fluid structure interaction (FSI). In our case, the assumption of rigid wall leads to an important simplification because the venous return of blood in the right atrium is mostly due to the pressure variations that the movements of vessels and right atrium wall provoke.

6.3 Future developments

Future developments of this study involve the overcoming of limitations before described in order to research a simulation as physiological as possible.

On this basis, an improvement could be the introduction of the tricuspid valve closing during the systole phase and its aperture during the diastole.

Furthermore, an improvement of the limitations is represent by avoiding the condition of rigid wall by introducing the rhythmic contraction of right atrium and veins.

In conclusion, this work paved the way for future comparison between hemodynamic conditions in different tyoes of CVC.

BIBLIOGRAPHY

- [1] T. M. Vesely and A. Ravenscroft, “Hemodialysis catheter tip design: Observations on fluid flow and recirculation,” *J. Vasc. Access*, vol. 17, no. 1, pp. 29–39, 2016.
- [2] M. Spector *et al.*, “Clinical Outcome of the Tal Palindrome Chronic Hemodialysis Catheter: Single Institution Experience,” *J. Vasc. Interv. Radiol.*, vol. 19, no. 10, pp. 1434–1438, 2008.
- [3] M. G. Tal, “Comparison or recirculation percentage of the palindrome catheter and standard hemodialysis catheters in a swine model,” *J. Vasc. Interv. Radiol.*, vol. 16, no. 9, pp. 1237–1240, 2005.
- [4] Z. J. Twardowski and H. L. Moore, “Side holes at the tip of chronic hemodialysis catheters are harmful,” *J. Vasc. Access*, vol. 2, no. 1, pp. 8–16, 2001.
- [5] G. Mareels, D. S. De Wachter, and P. R. Verdonck, “Dúvida 96: Computational fluid dynamics-analysis of the Niagara hemodialysis catheter in a right heart model,” *Artif. Organs*, vol. 28, no. 7, pp. 639–648, 2004.
- [6] G. Mareels, R. Kaminsky, S. Eloot, and P. R. Verdonck, “Particle Image Velocimetry-validated, computational fluid dynamics-based design to reduce shear stress and residence time in central venous hemodialysis catheters,” *ASAIO J.*, vol. 53, no. 4, pp. 438–446, 2007.
- [7] T. W. I. Clark, K. Van Canneyt, and P. Verdonck, “Computational flow dynamics and preclinical assessment of a novel hemodialysis catheter,” *Semin. Dial.*, vol. 25, no. 5, pp. 574–581, 2012.
- [8] T. W. I. Clark, G. Isu, D. Gallo, P. Verdonck, and U. Morbiducci, “Comparison of symmetric hemodialysis catheters using computational fluid dynamics,” *J. Vasc. Interv. Radiol.*, vol. 26, no. 2, pp. 252–259, 2015.
- [9] T. Reynolds and C. P. Appleton, “Doppler Flow Velocity Patterns of the Superior Vena Cava, Inferior Vena Cava, Hepatic Vein, Coronary Sinus, and Atrial Septal Defect: A Guide for the Echocardiographer,” *J. Am. Soc. Echocardiogr.*, vol. 4, no. 5, pp. 503–512, 1991.

- [10] L. J. M. Kroft, P. Simons, J. M. van Laar, and A. de Roos, "Patients with Pulmonary Fibrosis: Cardiac Function Assessed with MR Imaging," *Radiology*, vol. 216, no. 2, pp. 464–471, 2013.
- [11] D. Fulker, G. Keshavarzi, A. Simmons, D. Pugh, and T. Barber, "Pulsatility produced by the hemodialysis roller pump as measured by doppler ultrasound," *Artif. Organs*, vol. 39, no. 11, pp. 945–950, 2015.
- [12] K. S. Cho, I. K. Ko, and J. J. Yoo, "Bioactive Compounds for the Treatment of Renal Disease," vol. 59, no. 9, pp. 1015–1025, 2018.
- [13] A. Lauder, A. Schieppati, F. Conte, G. Remuzzi, and D. Batlle, "Low mortality and key aspects of delivery of care for end-stage renal disease in Italy," *ScientificWorldJournal.*, vol. 9, pp. 349–359, 2009.
- [14] T. Tuominen *et al.*, *Clinical Practice Guidelines For Chronic Kidney Disease: Evaluation, Classification and Stratification*, vol. 40, no. 1. 2002.
- [15] D. Santoro *et al.*, "Vascular access for hemodialysis: current perspectives.," *Int. J. Nephrol. Renovasc. Dis.*, vol. 7, pp. 281–294, 2014.
- [16] V. Mickley, "Central venous catheters: many questions, few answers," *Nephrol. Dial. Transplant.*, vol. 17, no. 8, pp. 1368–1373, 2002.
- [17] K. W. Gow, D. Tapper, and R. O. Hickman, "The American Journal of Surgery Between the lines : The 50th anniversary of long-term central venous catheters," *Am. J. Surg.*, vol. 213, no. 5, pp. 837–848, 2018.
- [18] M. Vafa Homann, D. Johansson, H. Wallen, and J. Sanchez, "Improved ex vivo blood compatibility of central venous catheter with noble metal alloy coating," *J. Biomed. Mater. Res. - Part B Appl. Biomater.*, vol. 104, no. 7, pp. 1359–1365, 2016.
- [19] S. R. Ash, "Advances in tunneled central venous catheters for dialysis: Design and performance," *Semin. Dial.*, vol. 21, no. 6, pp. 504–515, 2008.
- [20] S. R. Ash, "Fluid mechanics and clinical success of central venous catheters for dialysis-answers to simple but persisting problems," *Semin. Dial.*, vol. 20, no. 3,

pp. 237–256, 2007.

- [21] P. R. Bream, “Update on Insertion and Complications of Central Venous Catheters for Hemodialysis,” *Semin. Intervent. Radiol.*, vol. 33, no. 1, pp. 31–38, 2016.
- [22] S. I. Seldinger and S. I. Seldinger, “Catheter Replacement of the Needle in Percutaneous Arteriography : A new technique,” vol. 6926, 2010.
- [23] J. Adam and A. J. Ash, “Western Journal of Emergency Medicine : Integrating Emergency Care with Population Health Seldinger Technique for Placement of ‘ Peripheral ’ Internal Jugular Line : Novel Approach for Emergent Vascular Access,” 2016.
- [24] A. Graham, C. Ozment, K. Tegtmeyer, S. Lai, and D. Braner, “Central venous catheterization.,” *N Engl. J Med*, vol. 14, no. 7, pp. 26–27, 2006.
- [25] M. G. Tal and N. Ni, “Selecting Optimal Hemodialysis Catheters: Material, Design, Advanced Features, and Preferences,” *Tech. Vasc. Interv. Radiol.*, vol. 11, no. 3, pp. 186–191, 2008.
- [26] D. Frasca, C. Dahyot-fizelier, and O. Mimoz, “Prevention of central venous catheter-related infection in the intensive care unit,” 2010.
- [27] J. C. Keller and G. W. Marshall, “An in vivo method for the biological evaluation of metal implants ”, *Biomed. Mater.*, vol. 18, pp. 829–844, 1984.
- [28] R. J. Sherertz, W. A. Carruth, R. D. Marosok, M. A. Espeland, R. A. Johnson, and D. D. Solomon, “Contribution of vascular catheter material to the pathogenesis of infection: The enhanced risk of silicone in vivo,” *J. Biomed. Mater. Res.*, vol. 29, no. 5, pp. 635–645, 1995.
- [29] S. O. Trerotola *et al.*, “Randomized comparison of split tip versus step tip high-flow hemodialysis catheters,” *Kidney Int.*, vol. 62, no. 1, pp. 282–289, 2002.
- [30] A. B. Cohen *et al.*, “Silicone and polyurethane tunneled infusion catheters: A comparison of durability and breakage rates,” *J. Vasc. Interv. Radiol.*, vol. 22, no. 5, pp. 638–641, 2011.

- [31] M. Gallieni, I. Brenna, F. Brunini, N. Mezzina, S. Pasho, and A. Giordano, "Dialysis central venous catheter types and performance," *J. Vasc. Access*, vol. 15, no. SUPPL. 7, 2014.
- [32] J. Ibeas-Lopez, "New technology: Heparin and antimicrobial-coated catheters," *J. Vasc. Access*, vol. 16, no. Suppl 9, pp. S48–S53, 2015.
- [33] H. A. Cofactor, R. D. Rosenberg, P. S. Damus, and B. Israel, "ARTICLE : The Purification and Mechanism of Action The Purification and Mechanism Cofactor * of Action of Human," pp. 6490–6505, 1973.
- [34] R. D. Rosenberg and G. M. Oosta, "Structure-function relationships of heparin," *Thromb. Haemost.*, vol. 46, no. 1, pp. 3065–3069, 1981.
- [35] T. W. I. Clark *et al.*, "Comparison of heparin-coated and conventional split-tip hemodialysis catheters," *Cardiovasc. Intervent. Radiol.*, vol. 32, no. 4, pp. 703–706, 2009.
- [36] I. Chatzinikolaou *et al.*, "Antibiotic-coated hemodialysis catheters for the prevention of vascular catheter-related infections: A prospective, randomized study," *Am. J. Med.*, vol. 115, no. 5, pp. 352–357, 2003.
- [37] G. Zhao and S. E. Stevens, "Multiple parameters for the comprehensive evaluation of the susceptibility of Escherichia coli to the silver ion," *BioMetals*, vol. 11, no. 1, pp. 27–32, 1998.
- [38] G. E. Kaebnick, "Reasons of the Heart: Emotion, Rationality, and the 'Wisdom of Repugnance,'" *Hastings Cent. Rep.*, vol. 38, no. 4, pp. 36–45, 2008.
- [39] I. Sondi and B. Salopek-Sondi, "Silver nanoparticles as antimicrobial agent: A case study on E. coli as a model for Gram-negative bacteria," *J. Colloid Interface Sci.*, vol. 275, no. 1, pp. 177–182, 2004.
- [40] M. Pollini *et al.*, "Antibacterial coatings on haemodialysis catheters by photochemical deposition of silver nanoparticles," *J. Mater. Sci. Mater. Med.*, vol. 22, no. 9, pp. 2005–2012, 2011.
- [41] S. Trerotola, S. Johnson, and T. Ambrosius, "Tunneled Catheters : Prevention

- Hemodialysis Use of a Catheter of Infection-," pp. 491–496.
- [42] F. Paladini, M. Pollini, D. Deponti, A. Di Giancamillo, G. Peretti, and A. Sannino, "Effect of silver nanocoatings on catheters for haemodialysis in terms of cell viability, proliferation, morphology and antibacterial activity," *J. Mater. Sci. Mater. Med.*, vol. 24, no. 4, pp. 1105–1112, 2013.
- [43] A. K. Agarwal *et al.*, "Maintenance of blood flow rate on dialysis with self-centering CentrosFLO catheter: A multicenter prospective study," *Hemodial. Int.*, vol. 20, no. 4, pp. 501–509, 2016.
- [44] K. Wang, P. Wang, X. Liang, X. Lu, and Z. Liu, "Epidemiology of haemodialysis catheter complications : a survey of 865 dialysis patients from 14 haemodialysis centres in Henan province in China," 2015.
- [45] KDOQI, "I. Clinical Practice Guidelines for Vascular Access Guideline 7. Prevention and Treatment of Catheter and Port Complications," http://www2.kidney.org/professionals/KDOQI/guideline_upHD_PD_VA/va_guideline7.htm, vol. 48, no. 1, 2006.
- [46] M. R. Chan, "Hemodialysis central venous catheter dysfunction," *Semin. Dial.*, vol. 21, no. 6, pp. 516–521, 2008.
- [47] V. D. Niyyar and M. R. Chan, "Interventional nephrology: Catheter dysfunction-prevention and troubleshooting," *Clin. J. Am. Soc. Nephrol.*, vol. 8, no. 7, pp. 1234–1243, 2013.
- [48] L. M. Miller *et al.*, "Hemodialysis tunneled catheter noninfectious complications," *Can. J. Kidney Heal. Dis.*, vol. 3, no. 1, 2016.
- [49] S. Faintuch and G. M. M. Salazar, "Malfunction of Dialysis Catheters: Management of Fibrin Sheath and Related Problems," *Tech. Vasc. Interv. Radiol.*, vol. 11, no. 3, pp. 195–200, 2008.
- [50] C. J. Donlan RM, "Biofilms: survival mechanisms of clinically relevant microorganisms. ; ;," *Clin Microbiol Rev*, vol. 15, no. April, pp. 167–193, 2002.
- [51] M. G. H. Betjes, "Prevention of catheter-related bloodstream infection in patients

- on hemodialysis,” *Nat. Rev. Nephrol.*, vol. 7, no. 5, pp. 257–265, 2011.
- [52] J. E. Silberzweig, D. Sacks, A. S. Khorsandi, and C. W. Bakal, “Reporting standards for central venous access,” *J. Vasc. Interv. Radiol.*, vol. 11, no. 3, pp. 391–400, 2000.
- [53] A. Dwyer, “Surface-treated catheters - A review,” *Semin. Dial.*, vol. 21, no. 6, pp. 542–546, 2008.
- [54] M. Gallieni, A. Giordano, U. Rossi, and M. Cariati, “Optimization of dialysis catheter function,” *J. Vasc. Access*, vol. 17, no. Suppl 1, pp. S42–S46, 2016.
- [55] K. . Yadav, J. S.; Wholey, M. H.; Kuntz, R. E., Fayad, Pierre; Katzen, B. T.; Mishkel, G. J.; Bajwa, T. K.; hitlow, P.; Strickman, N. E.; Jaff, M. R.; Popma, J.J.; Snead, D. B.; Cutlip, D. E.; Firth, B. G.; Ouriel, “New England Journal,” *N. Engl. J. Med.*, vol. 351, no. 15, pp. 1493–1501, 2004.
- [56] I. Raad *et al.*, “Improved antibiotic-impregnated catheters with extended-spectrum activity against resistant bacteria and fungi,” *Antimicrob. Agents Chemother.*, vol. 56, no. 2, pp. 935–941, 2012.
- [57] S. Banerjee, “Dialysis Catheters and Their Common Complications : An Update,” pp. 1294–1299, 2009.
- [58] J. J. Engemann *et al.*, “Clinical Outcomes and Costs Due to Staphylococcus aureus Bacteremia Among Patients Receiving Long-Term Hemodialysis,” *Infect. Control Hosp. Epidemiol.*, vol. 26, no. 06, pp. 534–539, 2005.
- [59] B. Infection, “Review,” *Ann. Intern. Med.*, 2005.
- [60] E. Barre and C. Bosquet, “Complications of Femoral and Subclavian Venous Catheterization in Critically Ill Patients,” vol. 286, no. 6, 2001.
- [61] S. Article, “Complications of central venous catheters: Internal jugular versus subclavian access—A systematic review,” vol. 30, no. 2, 2002.
- [62] A. Manuscript and A. Update, “NIH Public Access,” vol. 54, no. 1, pp. 13–17, 2014.
- [63] J.-F. Timsit *et al.*, “New materials and devices for preventing catheter-related

- infections,” *Ann. Intensive Care*, vol. 1, no. 1, p. 34, 2011.
- [64] H. S. Hwang, S. H. Kang, S. R. Choi, I. O. Sun, H. S. Park, and Y. Kim, “Comparison of the palindrome vs. Step-tip tunneled hemodialysis catheter: A prospective randomized trial,” *Semin. Dial.*, vol. 25, no. 5, pp. 587–591, 2012.
- [65] M. Li *et al.*, “Clinical application of long-term palindrome catheter in hemodialysis patients,” *Iran. J. Kidney Dis.*, vol. 8, no. 2, pp. 123–129, 2014.
- [66] P. Chronic and D. C. Family, “Palindrome™ Precision Chronic Dialysis Catheter Family.”
- [67] C. Ye *et al.*, “A retrospective study of palindrome symmetrical-tip catheters for chronic hemodialysis access in China,” *Ren. Fail.*, vol. 37, no. 6, pp. 941–946, 2015.
- [68] S. Mary, “INTERVISTA A FRANCO TESIO : UN NEFROLOGO PRESTATO ALLA CHIRURGIA O VICEVERSA ? L ’ AFFASCINANTE STORIA DEL SUO CATETERE VENOSO DALL ’ IDEA ALLA REALIZZAZIONE,” vol. 29, no. 1, pp. 104–107, 2012.
- [69] M. Elkhoury, N. Youssef, and C. Issa, “IMECE2010-38048,” pp. 1–8, 2016.
- [70] Cindy L. Stanfield, *Principles of Human Physiology - IV Edition*, IV. 2012.
- [71] L. Antiga, M. Piccinelli, L. Botti, B. Ene-Iordache, A. Remuzzi, and D. A. Steinman, “An image-based modeling framework for patient-specific computational hemodynamics,” *Med. Biol. Eng. Comput.*, vol. 46, no. 11, pp. 1097–1112, 2008.
- [72] J. A. Sethian, F. M. Methods, F. M. Methods, and F. M. Methods, “Level-set method(RooTrack).pdf.”
- [73] W. E. Lorensen and H. E. Cline, “Marching cubes: A high resolution 3D surface construction algorithm,” *ACM SIGGRAPH Comput. Graph.*, vol. 21, no. 4, pp. 163–169, 1987.
- [74] S. Soleimani, G. Dubini, and G. Pennati, “Possible benefits of catheters with lateral holes in coronary thrombus aspiration: A computational study for different

clot viscosities and vacuum pressures,” *Artif. Organs*, vol. 38, no. 10, pp. 845–855, 2014.